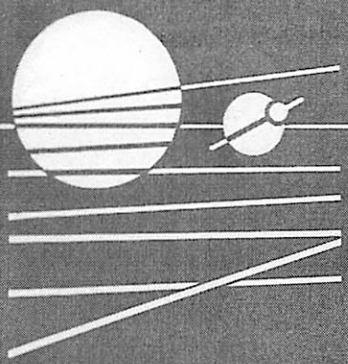

Lunar and Planetary Laboratory
Department of Planetary Sciences

PTYS 594a

PLANETARY FIELD GEOLOGY PRACTICUM

FIELD TRIP 19-21 NOVEMBER 1993

The University of Arizona
Tucson, Arizona

TABLE OF CONTENTS

PTYS 594a,

PLANETARY FIELD GEOLOGY PRACTICUM

Itinerary, Field Trip 19-21 November 1993

H. J. Melosh, 353 Space Sciences, 621-2806

We will assemble at 8:00 am on Friday, 19 November from the LPL loading dock off Warren St. in four 8-passanger Suburban vans. Try to be at LPL by 8:00 am to get the vans loaded. Please be sure that you have had breakfast beforehand, have ice for the coolers, etc. before we are scheduled to leave: breakfast and ice runs just before departure have caused long delays in the past!

Our approximate itinerary, as worked out in the last class meeting is:

Friday, 19 November:

8:30 am	Distribute handouts, Depart LPL, turn right on Cherry to Speedway, then travel East on Speedway to Stone, proceed North on Oracle road.
9:00 am	Take turnoff to La Reserve, proceed on road for overlook of Pusch ridge and view stream terraces of Oro valley, Catalina mountains.-- J. Grier/ B. Cohen
10:00 am	Return to Oracle road, proceed North to town of Catalina, turn left (West) on dirt road, continue 5 miles to quarry, walk 1/4 mile to contact of Catalina granite pluton and sedimentary carapace. -- J. Stansberry
11:00 am	Return to Oracle road, proceed North to Oracle Junction. Take Rte. 77 North to Globe, turn left on Rte. 70 for about 5 miles, then turn right (North) on route 88 to Roosevelt. -- Route geology by D. Dawson
12:30 pm	Stop at abutment of Roosevelt dam on Rte 88, discuss precambrian sedimentary rocks of Apache group. -- C. Steffens
1:00 pm	Lunch Break
2:00 pm	Continue (slowly) on Rte. 88 through Superstition Mountains caldera. Note narrow precipitous dirt road. Several short hikes up side canyons will be made under the direction of B. Bottke and J. Johnson. Discussion of caldera collapse by M. Fischer.
5:00 pm	Camp in vicinity of First Water.
7:00 pm	Campfire history of Salt River Project. -- E. Howell

Saturday, 20 November:

8:00 am	Break Camp, ferry vans to Don's Camp, assemble at trailhead at First Water. Follow Parker pass trail (FS 104), then Peralta trail (FS 102) to Don's Camp, ca. 10.5 miles through heart of Superstition Wilderness. Observe volcanic rocks (Bottke and Johnson), discuss origin of magmas (V. Hillgren) and the "Space Paradox" of igneous intrusions (E. Turtle). Eat lunch on trail.
5:00 pm	Arrive Don's Camp, collect ferry vehicle from First Water,
6:00 pm	Camp in vicinity of Don's Camp
7:00 pm	Campfire description of the eruption of Mt. Pinatubo. -- V. Converse

Sunday, 21 February:

8:00 am Break Camp, return to Rte 88 and proceed West to Apache Junction. Turn right on Ellsworth road to Usery Pass Road (FS 207), drive North to intersection with Bush highway (FS 204), turn right and proceed to Rte. 87.

9:00 am Proceed North on Rte 87 toward Payson. Route geology through transition zone by J. McLarty.

10:30 am Stop at Proterozoic Ophiolite complex south of Payson, stop, and observe pillow basalts and sheeted dikes. -- W. Grundy/ A. Rivkin

11:30 am Return South on Rte. 87, proceed to turnoff of Rte. 188, then follow 188 South through Tonto Basin.

12:00 noon Lunch Break on overlook over Tonto Basin

1:00 pm Continue South on Rte. 188, observe stream terraces of Tonto Basin. -- B. Casavant/ K. Yanow

2:00 pm Join Rte. 88 at Rosevelt Dam, continue South to Globe/Miami. Turn right (West) on Rte 60, proceed to Florence Junction, then turn left (South) on Rte. 77 to Oracle Junction. Continue South on Oracle road.

5:00 pm Arrive Tucson, unpack vans, go home.

Primary Drivers: Vince Converse, W. Grundy, M. Nolan, J. Stansberry

Distribution:

B. Bottke
B. Cohen
S. Croft
M. Fischer
W. Grundy
E. Howell
D. Kring
J. Mclarty
A. Rivkin
E. Turtle
C. Steffens
B. Casavant
V. Converse
D. Dawson
J. Grier
V. Hillgren
J. Johnson
G. Komatsu
M. Nolan
T. Ruzimaika
J. Stansberry
K. Yanow

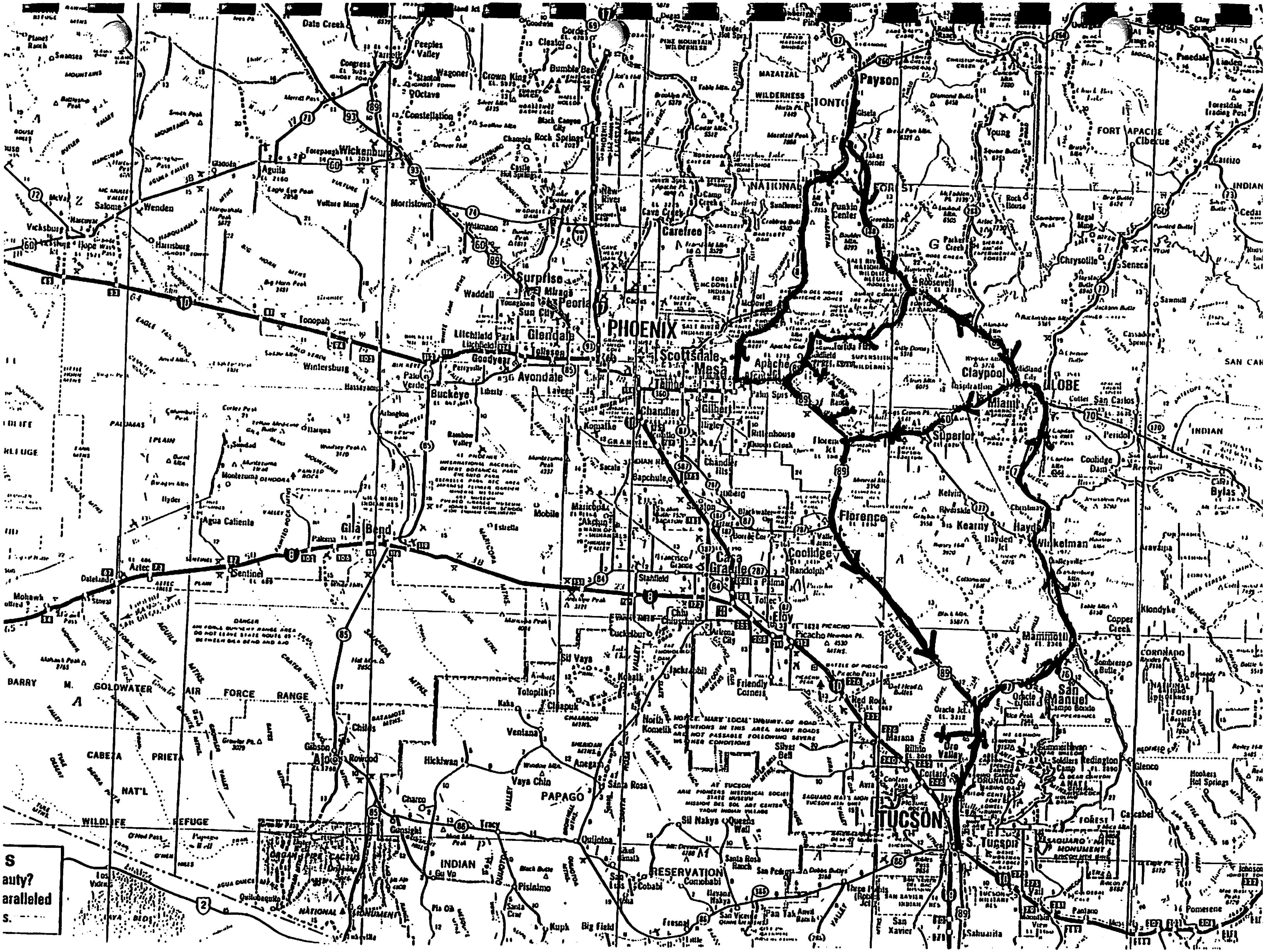

PHOENIX
Scottsdale
Mesa
Tempe
Chandler
Gilbert
Glendale
Peoria
Sun City
Surprise
Tolleson
Goodyear
Avondale
Buckeye
Litchfield Park
Waddell
Wickenburg
Congress
Yarnell
Peoples Valley
Wagoner
Crown King
Constellation
Aguila
Wenden
Salome
Vicksburg
Hope
Harrisburg
Tonopah
Wintersburg
Hassayampa
Palo Verde
Morristown
Wittmann
Carefree
Cave Creek
New River
Cordes
Cleator
Bumble Bee
Black Canyon City
Rock Springs
Payson
Gisela
Young
Punkin Center
Roosevelt
Tortilla Flat
Apache Jct
Globe
Claypool
Miami
Superior
Florence
Coolidge
Casa Grande
Eloy
Picacho
Red Rock
Marana
Tucson
S. Tucson
Oracle
San Manuel
Mammoth
Winkelman
Hayden
Kearny
Kelvin
Riverside
Coolidge Dam
Peridot
San Carlos
Bylas
Copper Creek
Klondyke
Redington
Sahuarita
Vail
Pantano
Pomerene
Cascabel
Hookers Hot Springs
Gila Bend
Paloma
Sentinel
Aztec
Dateland
Mohawk
Ajo
Gibson
Rowood
Why
Sells
Santa Rosa
Quijotoa
Ventana
Hickiwan
Vaya Chin
Charco
Gunsight
Tracy
Pisinimo
Komatke
Maricopa
Mobile
Stanfield
Sacaton
Randolph
Toltec
Friendly Corners
Silver Bell
Three Points (Robles Jct)
San Xavier
Fresnal
Agua Caliente
Hyder
Chiules
MAZATZAL WILDERNESS
TONTO NATIONAL FOREST
FORT APACHE
INDIAN
PAPAGO
INDIAN RESERVATION
BARRY M. GOLDWATER AIR FORCE RANGE
CABEZA PRIETA NAT'L WILDLIFE REFUGE
ORGAN PIPE CACTUS NATIONAL MONUMENT
SAGUARO NAT'L MONUMENT

HIKING TRAIL: FIRST WATER TO DON'S CAMP

START

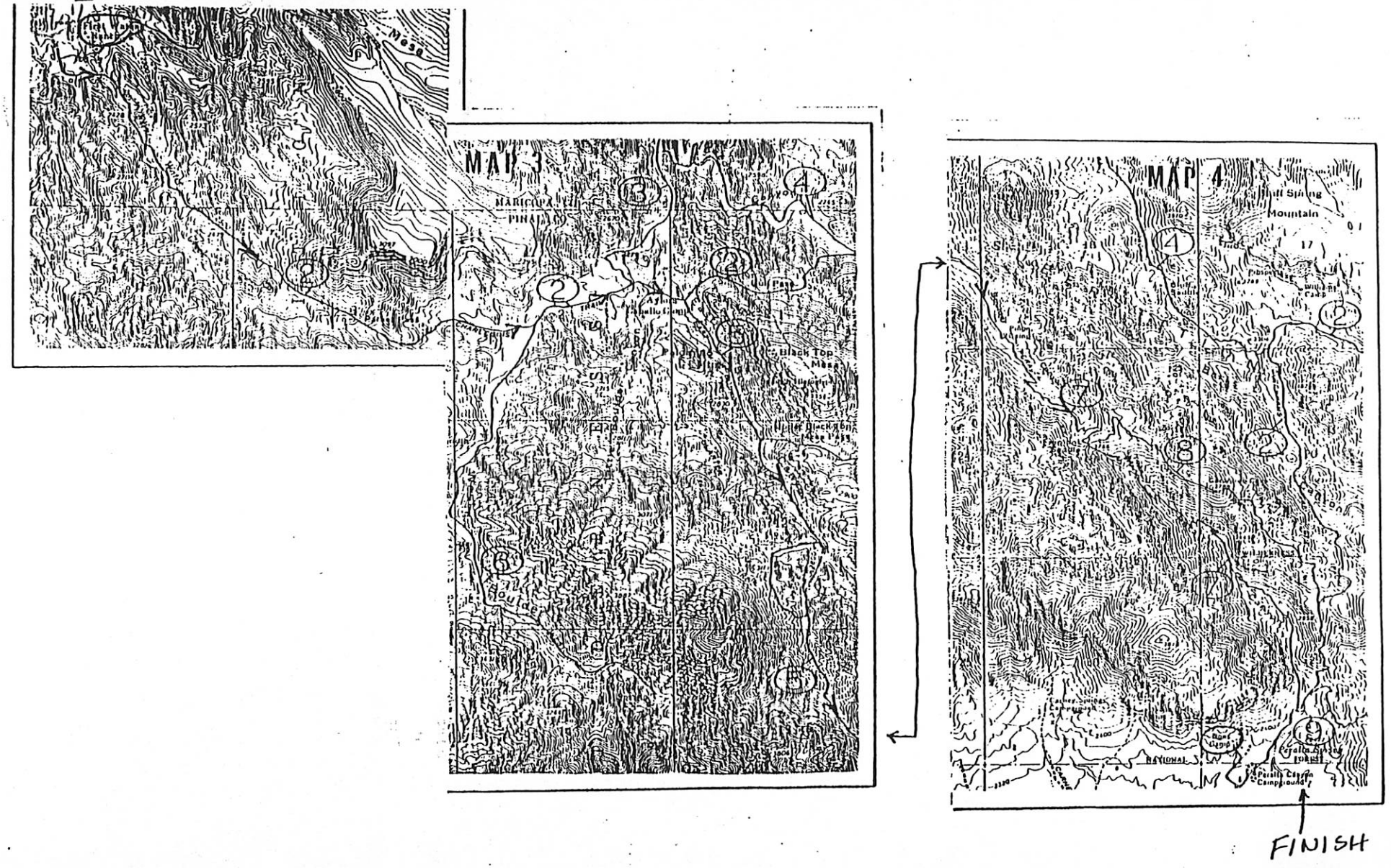

FINISH

TABLE 4-1. Geologic Time Scale

Era	Period	Epoch	Millions of Years Ago
Cenozoic	Quaternary	Holocene	0.02
		Pleistocene	1.8
	Tertiary	Pliocene	5
		Miocene	25
		Oligocene	37
		Eocene	55
		Paleocene	65
Mesozoic	Cretaceous		135
	Jurassic		180
	Triassic		230
Paleozoic	Permian		275
	Pennsylvanian		330
	Mississippian		355
	Devonian		410
	Silurian		430
	Ordovician		500
	Cambrian		600
PRECAMBRIAN Proterozoic			1000
			1500
			2000
Archeozoic			3000
			4500

Stratigraphic Ranges of Selected Fossils

Fusulinids
Tetracorals
Hexacorals
Archaeocyathids
Productid Brachiopods
Ammonoid Cephalopods
Trilobites
Ostracoderm Fishes
Placoderm Fishes
Sharks and Bony Fishes
Amphibians
Reptiles
Dinosaurs
Graptolites
Birds
Mammals
Conodonts
Horses
Elephants
Whales
Humans
Terrestrial Plants
Flowering Plants

Oldest Rocks in Arizona

Earliest Record of Bacteria

Age of Meteorites, Moon and Probably Earth

Tectonic Events in Arizona

Basin and Range Crustal Extension and Volcanism
Mid-Tertiary Orogeny

Laramide Orogeny and Regression
Marine Transgression

Plutonism and Volcanism in Southern Arizona

Marine Regression
Marine Transgression
Marine Regression
Marine Transgression
Marine Regression

Marine Transgression

Regional Uplift and Erosion, Regression

Marine Transgression

Grand Canyon Disturbance

Mazatzal Orogeny and Plutonism

Data Compiled from Several Sources

TABLE 1–3. Some Common Minerals and Their Physical Properties

Mineral	*Chemical Composition*	*Common Colors*	*Luster*	*Hardness*	*Cleavage*
Quartz	SiO_2	Clear colorless, milky white, pink, gray, etc.	Glassy	7	None, concoidal fracture
Plagioclase	$NaAlSi_3O_8$ $CaAl_2Si_2O_8$	White, gray, colorless	Glassy to Pearly	6	Two directions, intersect at about 90°
Orthoclase (K-feldspar)	$KAlSi_3O_8$	Pink, white, gray, colorless	Glassy	6	Two directions, about 90°
Muscovite (white mica)	$KAl_3Si_3O_{10}(OH)_2$	Clear to silvery green, or yellow	Silky or Pearly	2–2.5	One direction, cleaves to thin sheets
Biotite (black mica)	$K(Mg,Fe)_3AlSi_3O_{10}(OH)_2$	Dark brown to black	Silky or Pearly	2.5–3	One direction, cleaves to thin sheets
Hornblende (Amphibole Group)	$Ca_2Na(Mg,Fe)_4(Al,Fe)(Al,Si)_8O_{22}(OH)_2$	Dark green to black	Glassy	5–6	Two directions, intersect at 56° and 124°
Augite (Pyroxene Group)	$Ca(Mg,Fe,Al)(Si,Al)_2O_6$	Dark green to black	Glassy	5–6	Two directions, intersect at 90°
Olivine	$(Mg,Fe)_2SiO_4$	Green to brown	Glassy	6.5–7	None, conchoidal fracture
Calcite	$CaCO_3$	Colorless to white	Glassy to Earthy	3	Three directions, intersecting at 75° and 105°
Pyrite	FeS_2	Pale brass-yellow	Metallic	6–6.5	none
Chalcopyrite	$CaFeS_2$	Brass yellow	Metallic	3.5–4	none

TABLE 1–4. Moh's Hardness Scale.

10	Diamond
9	Corundum
8	Topaz
7	Quartz
6	Orthoclase feldspar
5	Apatite
4	Fluorite
3	Calcite
2	Gypsum
1	Talc

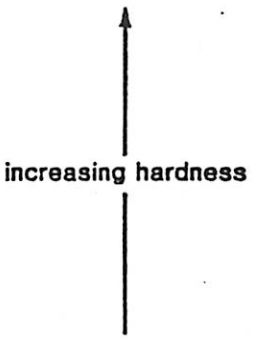

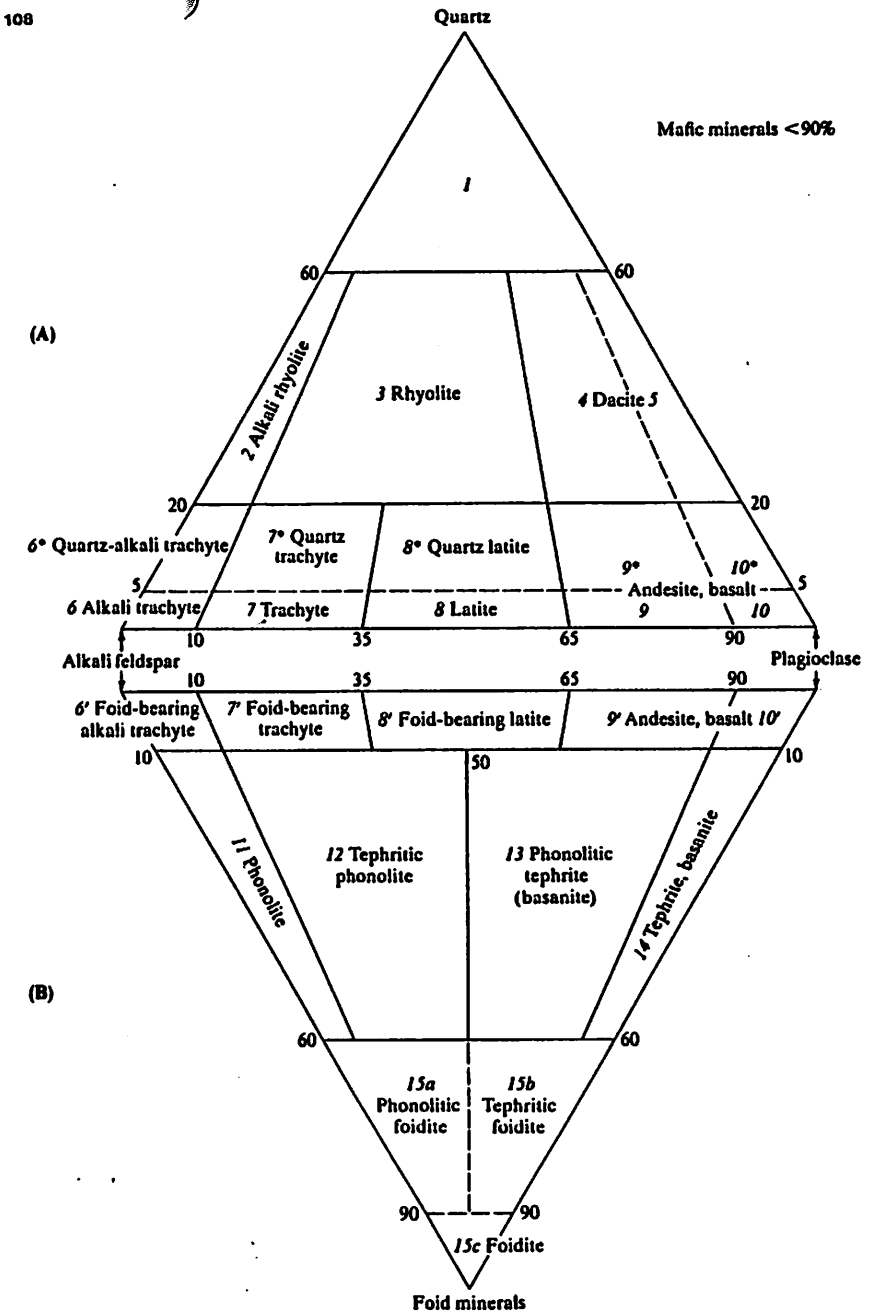

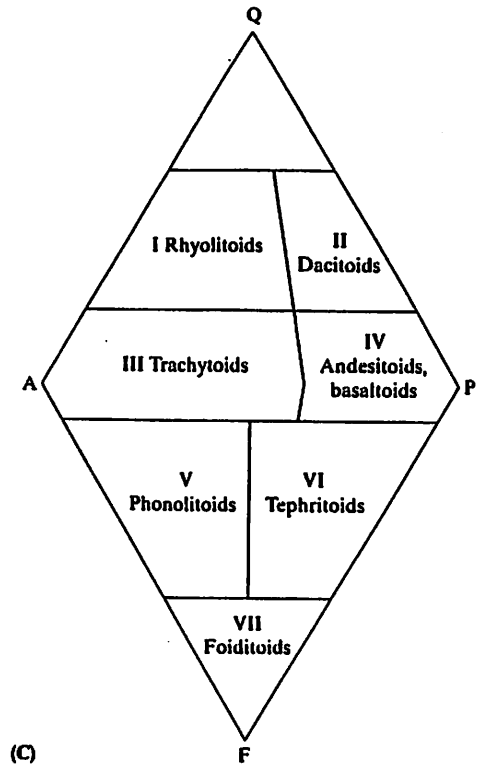

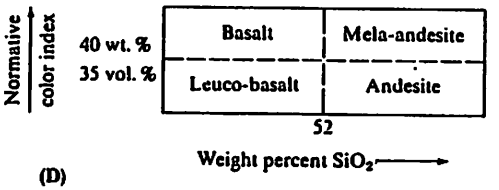

Figure 4–3
(A, B) The classification of volcanic igneous rocks. In order to be included within the triangles an igneous rock must be aphanitic. The rock must contain at least 10% plagioclase, alkali feldspar, and either quartz or feldspathoid (foid). The relative amounts of these three minerals are recalculated to 100% and plotted within the appropriate triangle, as shown in Figure 4–2. Appropriate modifying terms are used based upon mafic mineral composition or distinctive texture. In the case of those rocks whose matrix is too fine for determination, a tentative classification can be based upon minerals present in phenocrysts. (C) Generalized group names (for field use). (D) Distinction between basalt and andesite is based on color index (volume percentage of mafic minerals) and silica content. [From A. L. Streckeisen, 1979, *Geology, 7,* Figs. 1, 2; and A. Streckeisen, 1979, personal communication.]

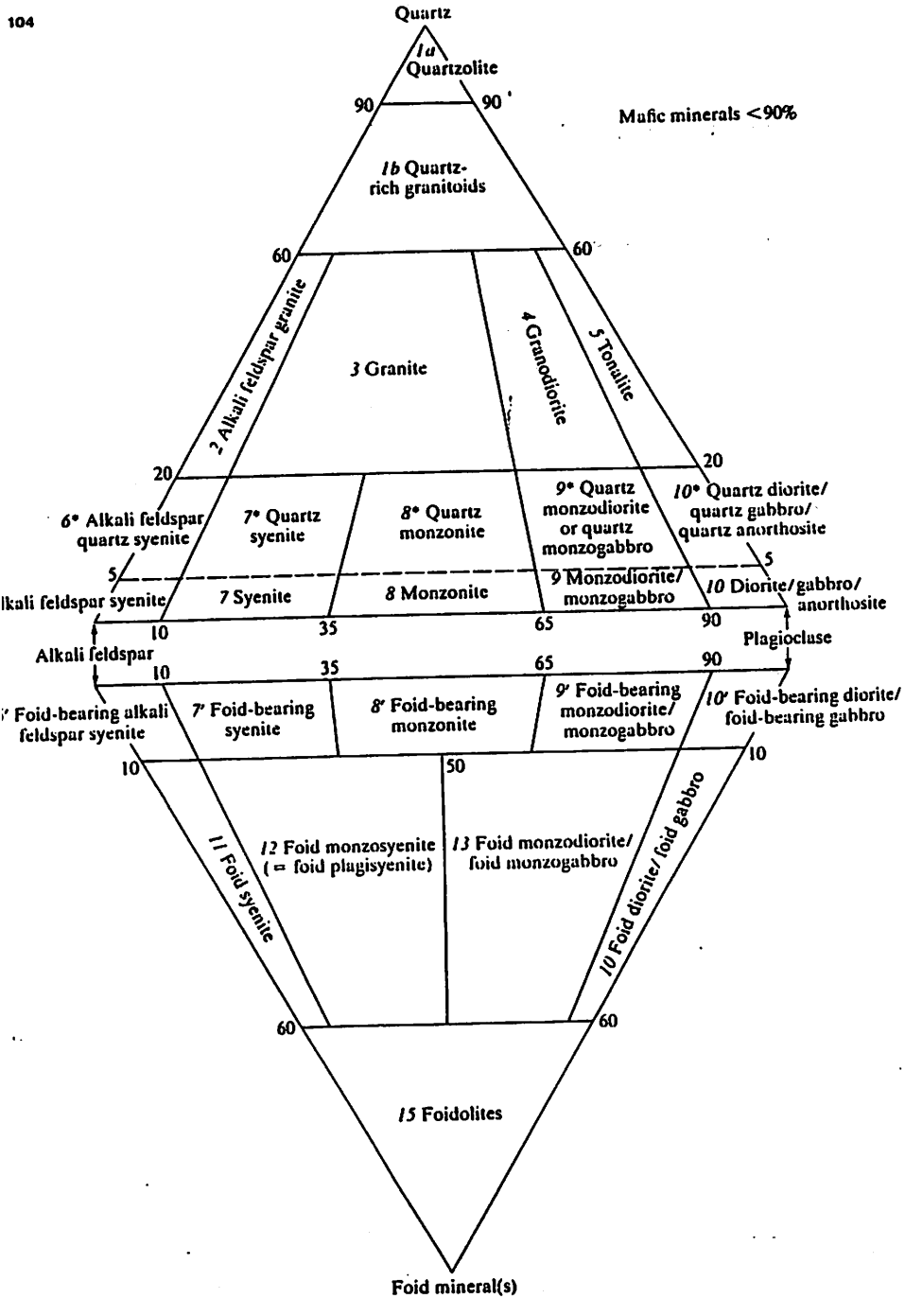

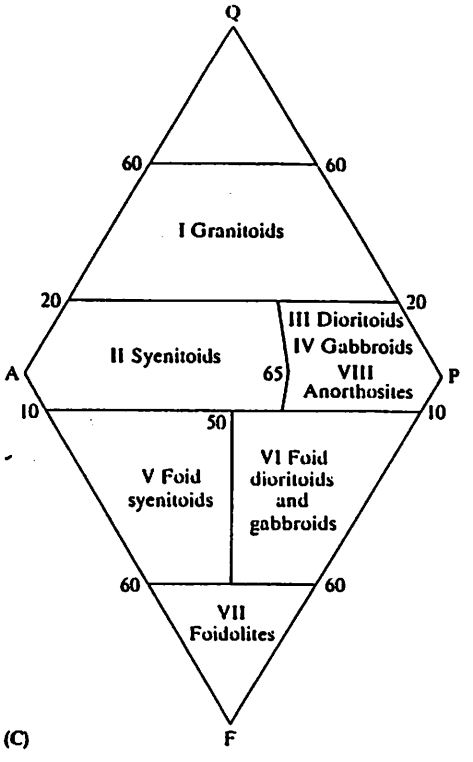

Figure 4–1
(A, B) The classification of plutonic rocks. In order to be included in these triangles, the igneous rock must be phaneritic. The rock must contain at least 10% plagioclase, alkali feldspar, and either quartz (triangle A) or feldspathoid (triangle B). The relative amounts of these minerals are recalculated to 100% and plotted within the appropriate triangle by the technique shown in Figure 4–2. Appropriate modifying terms are based upon mafic mineral composition or distinctive texture. (C) Generalized group names (for field use) when mineral percentages cannot be determined with precision. In fields II, III, and IV the qualifier "foid-bearing" should be used when feldspathoids are present. [From A. L. Streckeisen, 1976, *Earth Sci. Rev., 12,* Fig. 1a.]

(see Figure 4–1B). A rock cannot appear on both triangles, because quartz and feldspathoid are chemically incompatible; when mixed they will react to form a compound (feldspar) of intermediate silica content.

The volcanic igneous rocks are named on the basis of a similar triangular arrangement (see Figure 4–3). Distinction between basalt and andesite is made mainly on the basis of silica content (a rock with more than 52% SiO_2 is andesite, and a rock with less than 52% SiO_2 is basalt, as shown in part D), or less accurately on plagioclase composition (a rock with a plagioclase composition more sodic than An_{50} is andesite).

PTYS 594a

PLANETARY FIELD GEOLOGY PRACTICUM

FIELD TRIP 19-21 NOVEMBER 1993

RIVER TERRACES - RILLITO WASH

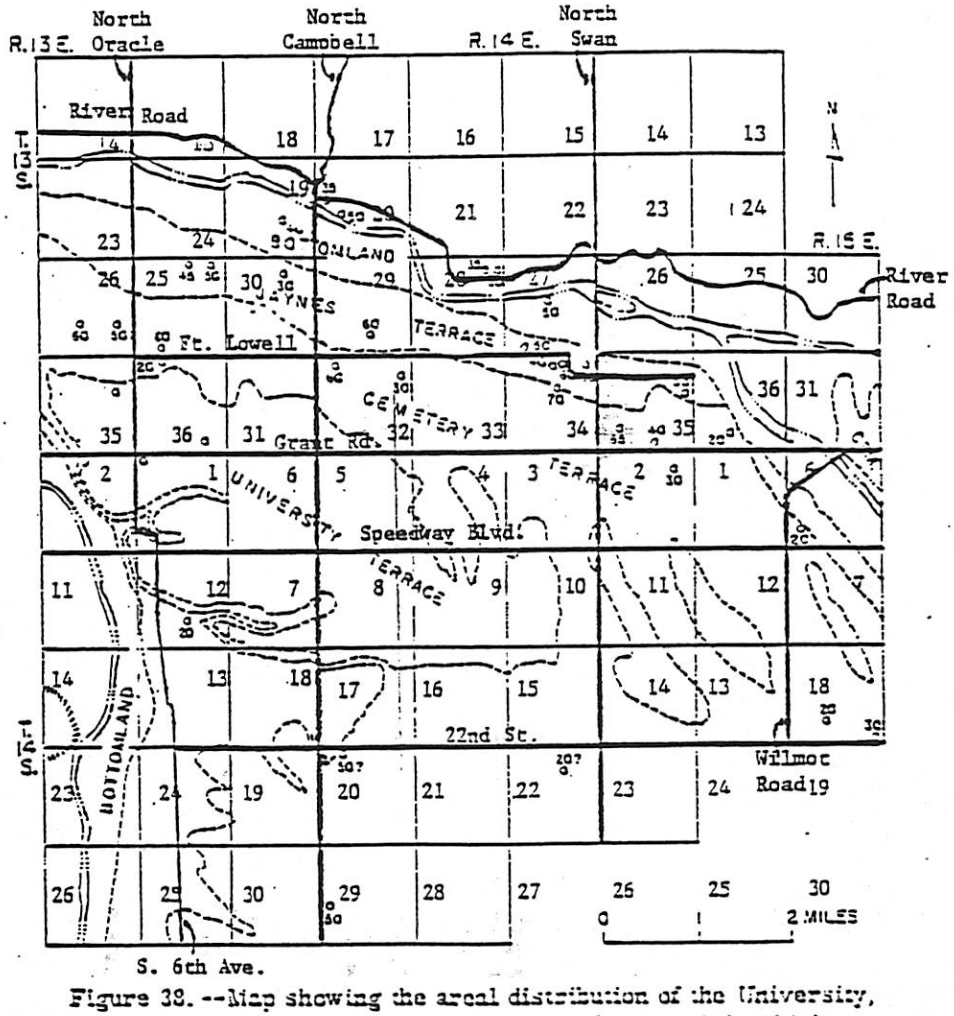

Figure 38. --Map showing the areal distribution of the University, Cemetery, and Jaynes terraces, bottom land, and the thicknesses of terrace deposits and Quaternary alluvium at well sites. (Revised from Smith, 1938, pl. V.)

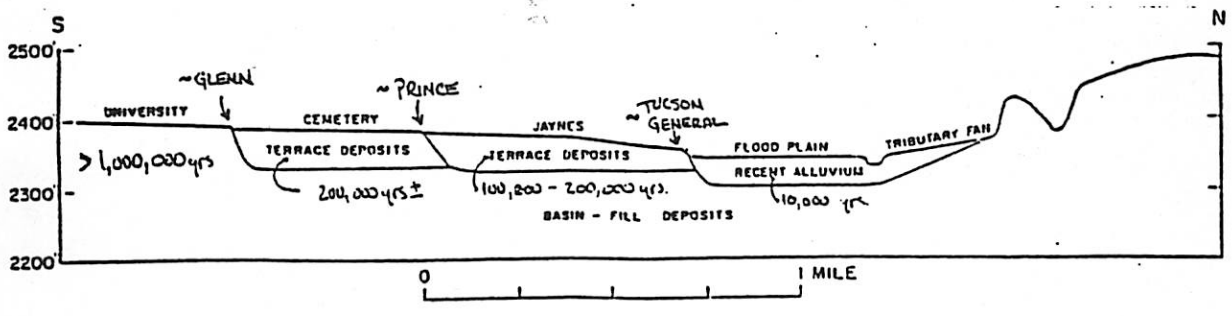

Figure 40. --Geologic cross section across Rillito Creek along Campbell Avenue showing the relation of physiography to the underlying deposits.

RIVER TERRACES - FORMATION

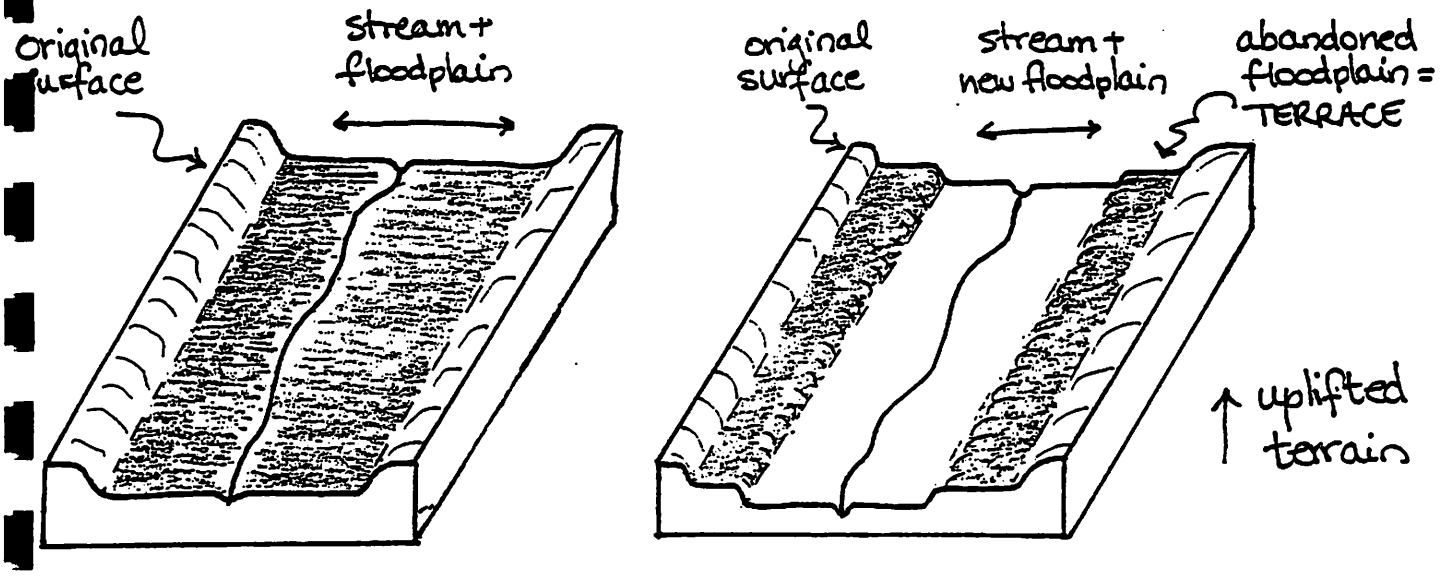

Table 2. March 1979 Pima County Flood Control District estimates (Reich, 1979) of damage to buildings and personal property by dam breach or 100-yr floods. The estimated damage figures are based upon using 30% of the 100% destroyed figures of dam breach estimate for each property within the 100-yr flood plain except for bridges which are assumed to be capable of passing Q_{100} without damage.

	In path of dam break flood		In 100-yr flood plain	
Sub-Area	Estimated No. Lives Endangered	Estimated Damage	Estimated No. Lives Endangered	Estimated Damage
County line to Golder Ranch Road	21	$ 827,500	21	$ 248,000
Golder Ranch Road to Wilds Drive	39	552,000	39	165,000
Wilds Drive to end of Bowman Road at Lago del Oro Parkway	90	1,433,000	90	430,000
Bowman Road at Lago del Oro Parkway to Sutherland Wash intersection with U.S. 89	53	629,000	28	141,000
Sutherland Wash at U.S. 89 to First Avenue	20	1,641,000	20	192,500
First Avenue to La Cañada Drive	577	13,918,000	523	3,689,500
La Cañada Drive to La Cholla Boulevard	164	2,842,000	164	852,500
La Cholla Boulevard to Magee Road	1,076	29,638,000	68	58,500
Magee Road to Ina Road	1,207	33,555,000	0	0
Ina Road to I-10	870	38,540,000	24	117,000
TOTALS	4,117	$123,575,500	977	$5,894,500

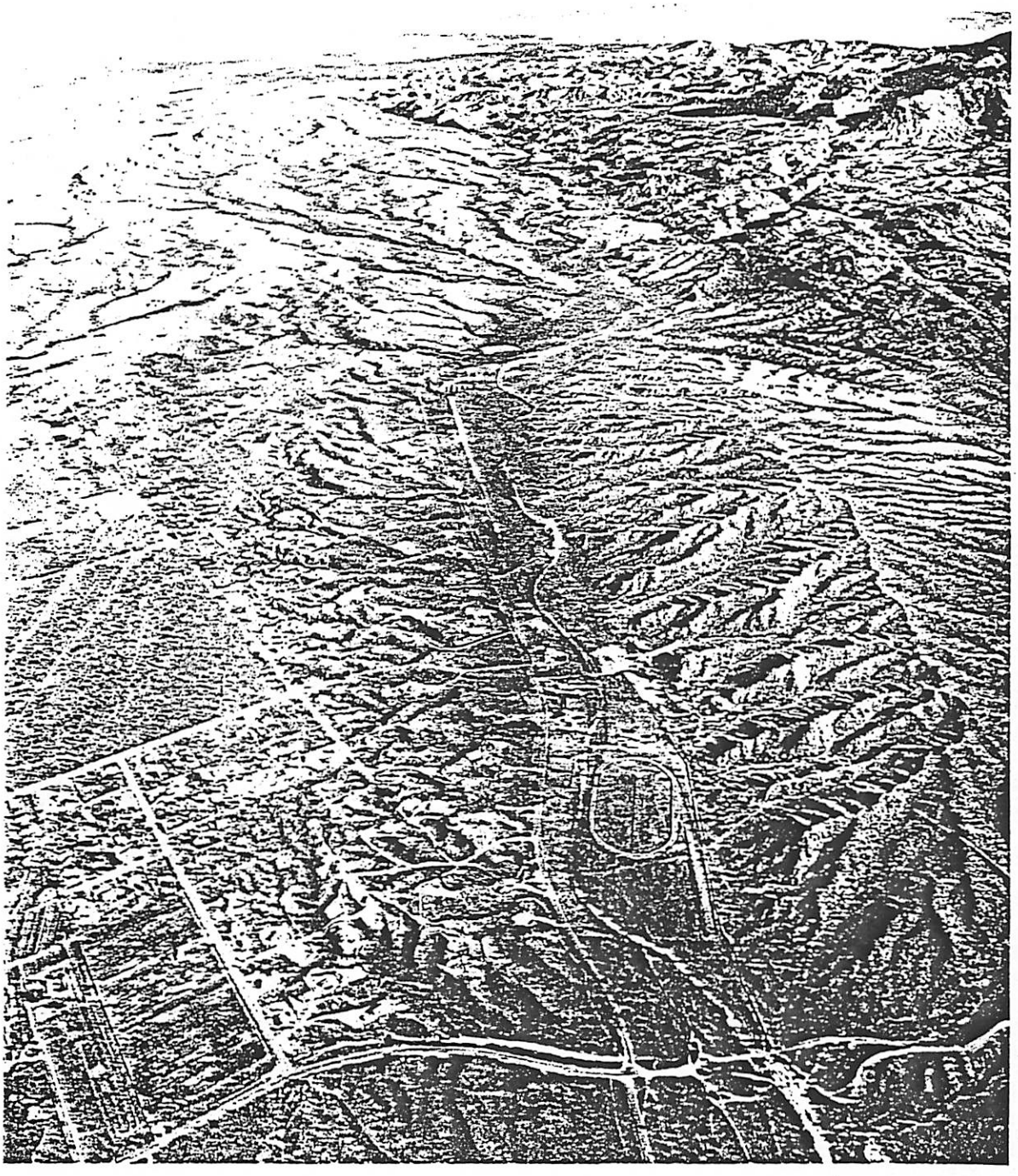

FIGURE 2. View up the Canada del Oro Valley depicting the different stream terraces and the exhumed bedrock pediment of the Santa Catalina Mountains.

RIVER TERRACES - CANADA DEL ORO WASH

Subsequent to the extensive pedimentation of the western margin of the Santa Catalina Mountains, a vast complex of alluvial fans was deposited, burying much of this pediment and basin deposits. This period was followed by four phases of valley downcutting during which alluvial drainage basins were developed. Each downcutting phase was followed by deposition of inset, fill terraces. Progressively older geomorphic surfaces are more dissected and are present at higher elevations.

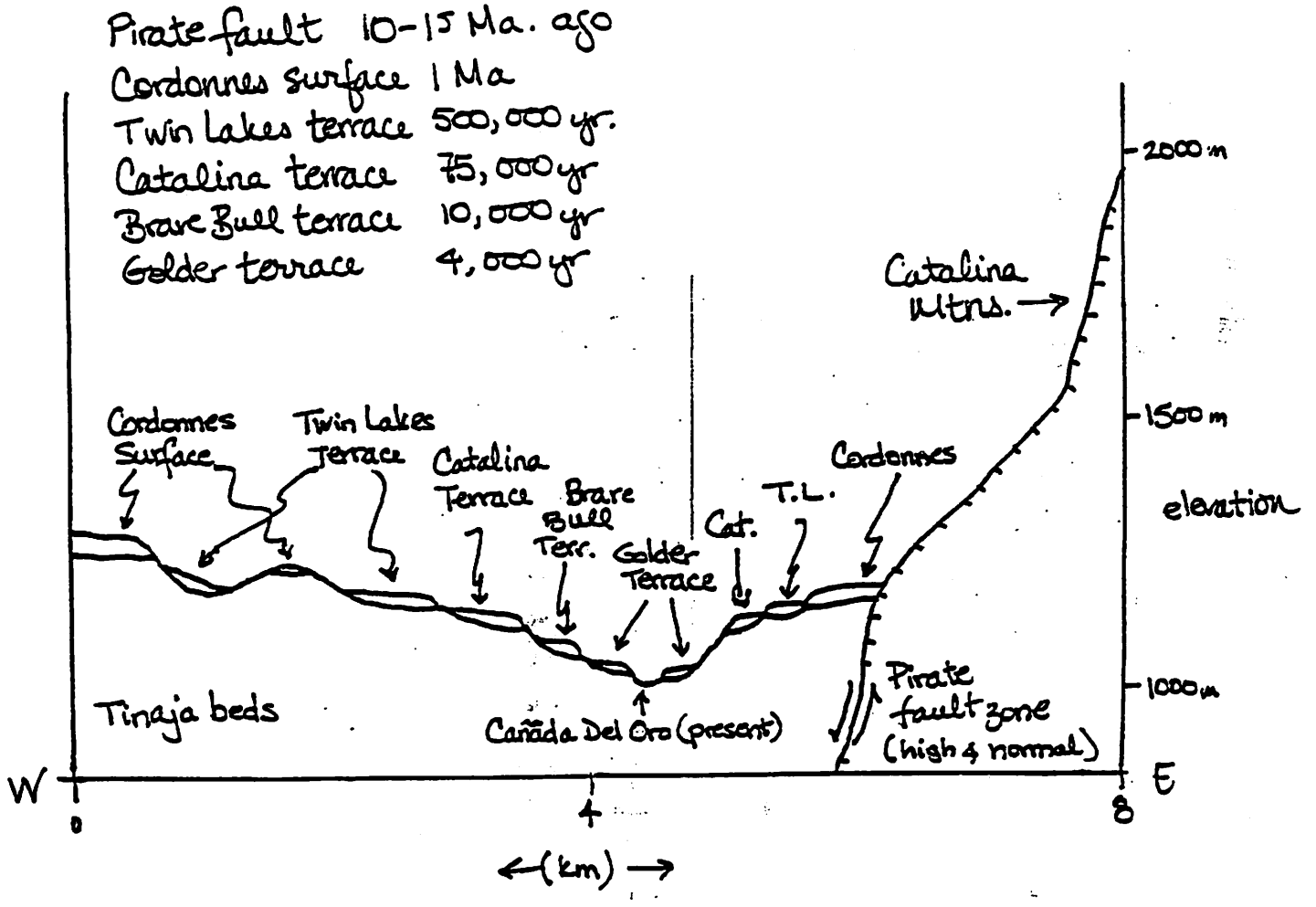

SOURCES:

Pashley. MS Thesis 1966. University of Arizona

Geomorphic Surfaces in the Tucson Basin, Arizona. Complied by Lisa Ely and Victor Baker.

Quaternary Geology and Geologic Hazards Near Canada del Oro, Tucson AZ. Bull W.B. et al. Geologic Excursions Through the Sonoran Desert Region, Arizona and Sonora. Ed. by George Gehrels and John Spencer. AGS SP-7. 1990.

Stop #2 On highway 89 go north through 3 stop lights in Catalina, 1 mile past (K) (on right), 1 more mile to <u>Rail X Ranch</u> sign (on left). Turn left & go ~6 miles, taking no turns, to the White Rock Mine gate.

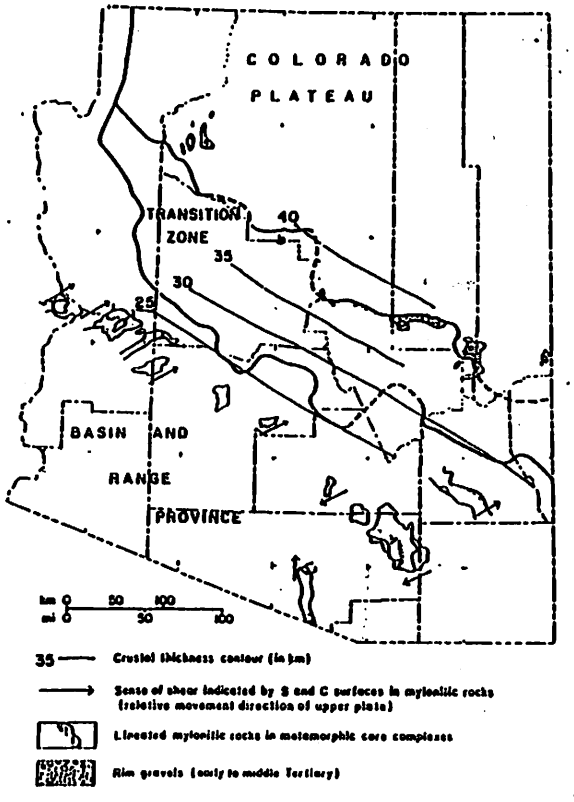

Figure 7. Map of Arizona showing crustal thickness changes associated with the Transition Zone and location of metamorphic core complexes and early to middle Tertiary rim gravels. The rim gravels are located along the presently topographically high margin of the Colorado Plateau and were deposited by northeast-flowing streams that drained the presently topographically lower Transition Zone and Basin and Range Provinces. The arrow next to each metamorphic core complex indicates the direction the upper plate moved based on sense-of-shear indicators in mylonitic rocks.

From Spencer & Reynolds, AGS Digest 17, 539-574, 1989.

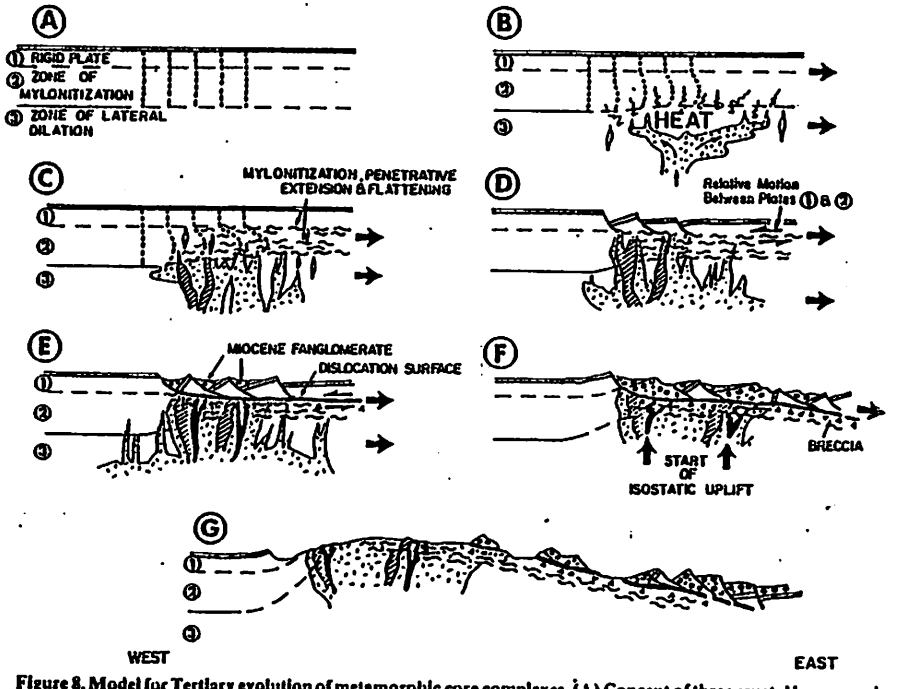

Figure 8. Model for Tertiary evolution of metamorphic core complexes. (A) Concept of three crustal layers, each responding distinctly to Tertiary heating and tensional stress. (B) Magma emplacement and east-northeast–directed extension initiate necking (stretching) in zone 2. (C) Continued extension in zone 3 leads to tensional separation and intrusive dilation; mylonitization develops in more ductile zone 2. (D) Differences in response to crustal extension between zones 1 and 2 create differential strain and fragmentation of rigid plate. (E) Continued differential strain between zones 1 and 2 and dissipation of heat creates the dislocation of surface and further rotational faulting of upper-plate blocks; rapid fanglomerate-breccia accumulation within fault-bounded troughs; clasts mainly from nonmylonitic plate 1, but exposure and erosion of mylonite zone may occur locally. (F) As tectonic denudation proceeds, area of maximum thinning responds to removal of zone 1 by isostatic uplift and deformational thinning in zone 2. (G) Present configuration of complex.

From Rehrig & Reynolds, GSA Memoir 153, 131-157, 1980

Starsberry, page 2

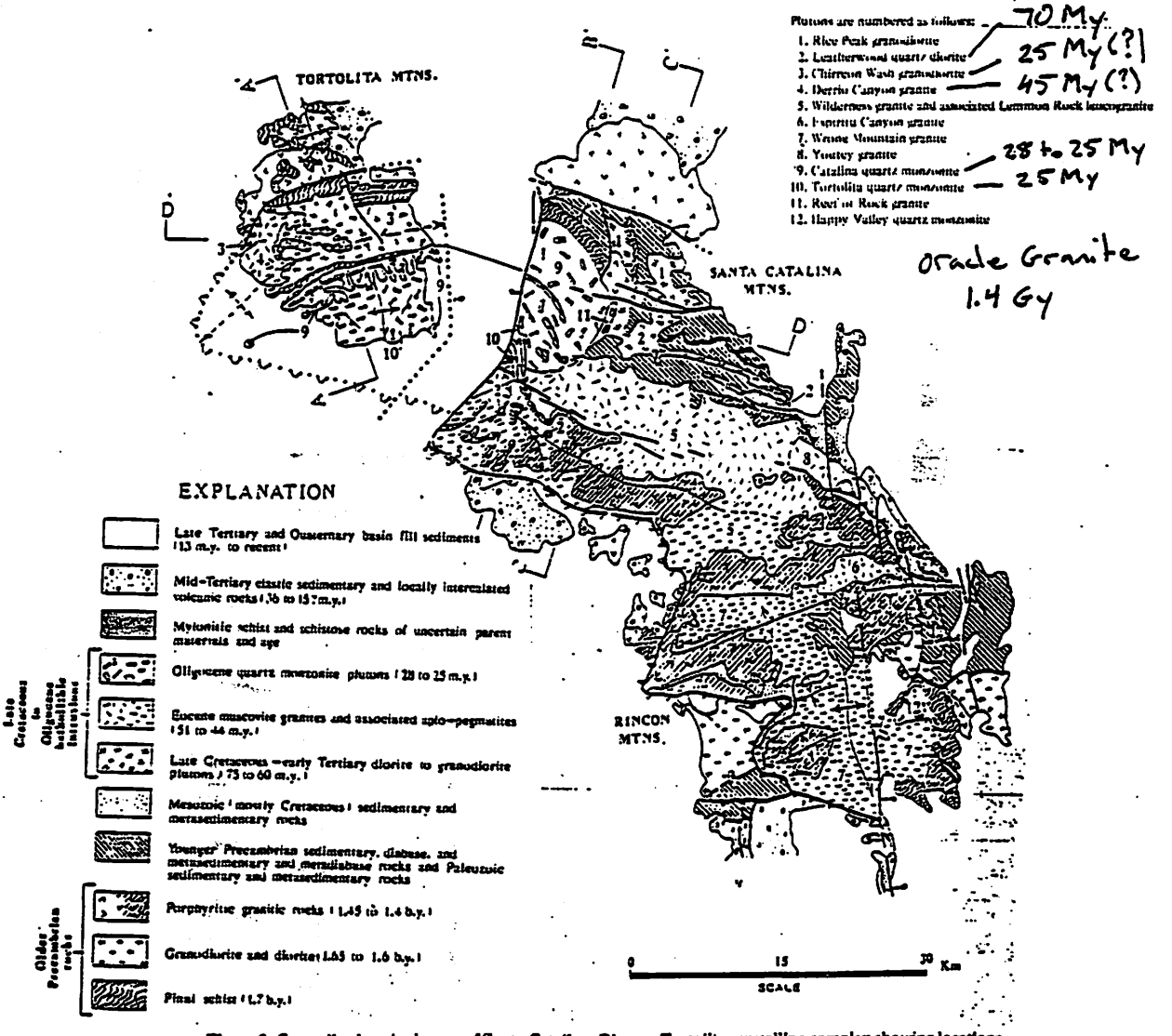

Figure 3. Generalized geologic map of Santa Catalina–Rincon–Tortolita crystalline complex showing locations of cross sections and plutons discussed in text. Sources of map data are as follows: for Tortolita Mountains—Budden (1975), Banks and others (1977), and Keith (unpub. mapping); for Santa Catalina Mountains—Tolman (1914, unpub. mapping as presented in Wilson and others, 1969), Creasey (1967), Shakel (1974), Creasey and Theodore (1975), Banks (1976), Hoelle (1976), Suemnicht (1977), Wilson (1977), and Keith (unpub. mapping); for Rincon Mountains—Drewes (1974, 1977) and Thorman and Drewes (1978). Aligned patterns in Late Cretaceous through Oligocene intrusions show deformed areas of mylonitic gneiss, and random patterns show undeformed areas. East-northeast–trending ruled lines show areas of mylonitically deformed porphyritic mesocratic gneiss believed to have been previously undeformed 1,400- to 1,450-m.y.-old biotite granitic rocks (shown by random pattern). Barbed heavy lines are low-angle faults with barbs in upper plate. Heavy lines are high-angle normal faults with bar and ball on downthrown side.

From Keith et al., GSA Memoir 153, 217-267, 1980.

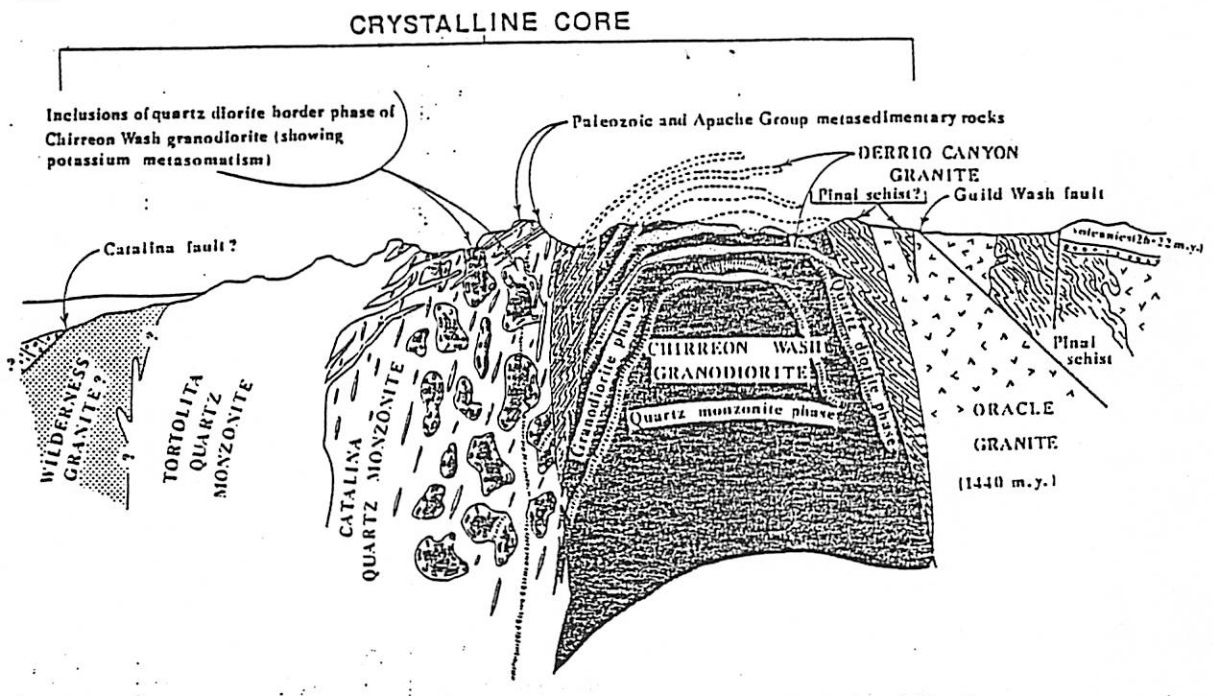

Figure 4. Diagrammatic cross section A–A' through Tortolita Mountains. Location of section shown in Figure 3.

From Keith et al., GSA Memoir 153, 217-267, 1980.

Geologic Map, Vicinity White Rock Mine, Tortolita Mountains

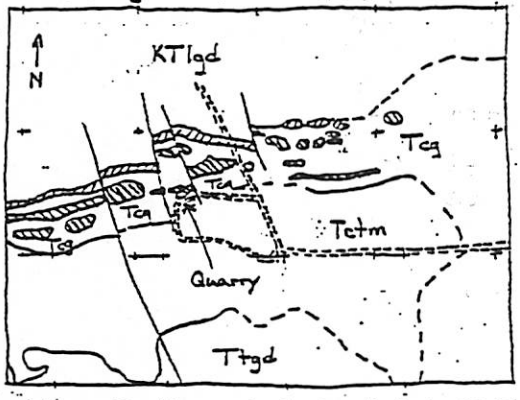

Ttgd - tertiary tortolita granodiorite
Tctm - tertiary catalina/tortolita migmatite
Tcg - tertiary catalina granite
KTlgd - cretaceous/tertiary Leatherwood granodiorite
▨ - precambrian Pinal schist
▨ - paleozoic metamorphics
contact
fault
==== dirt road

After Budden, Thesis, U of A, 1975 and AGS MM87-A, Dickinson 1987

Precambrian Sedimentary Rocks

Steffens

from Wrucke, in Jenney & Reynolds, 1989 AZGS Digest 17.

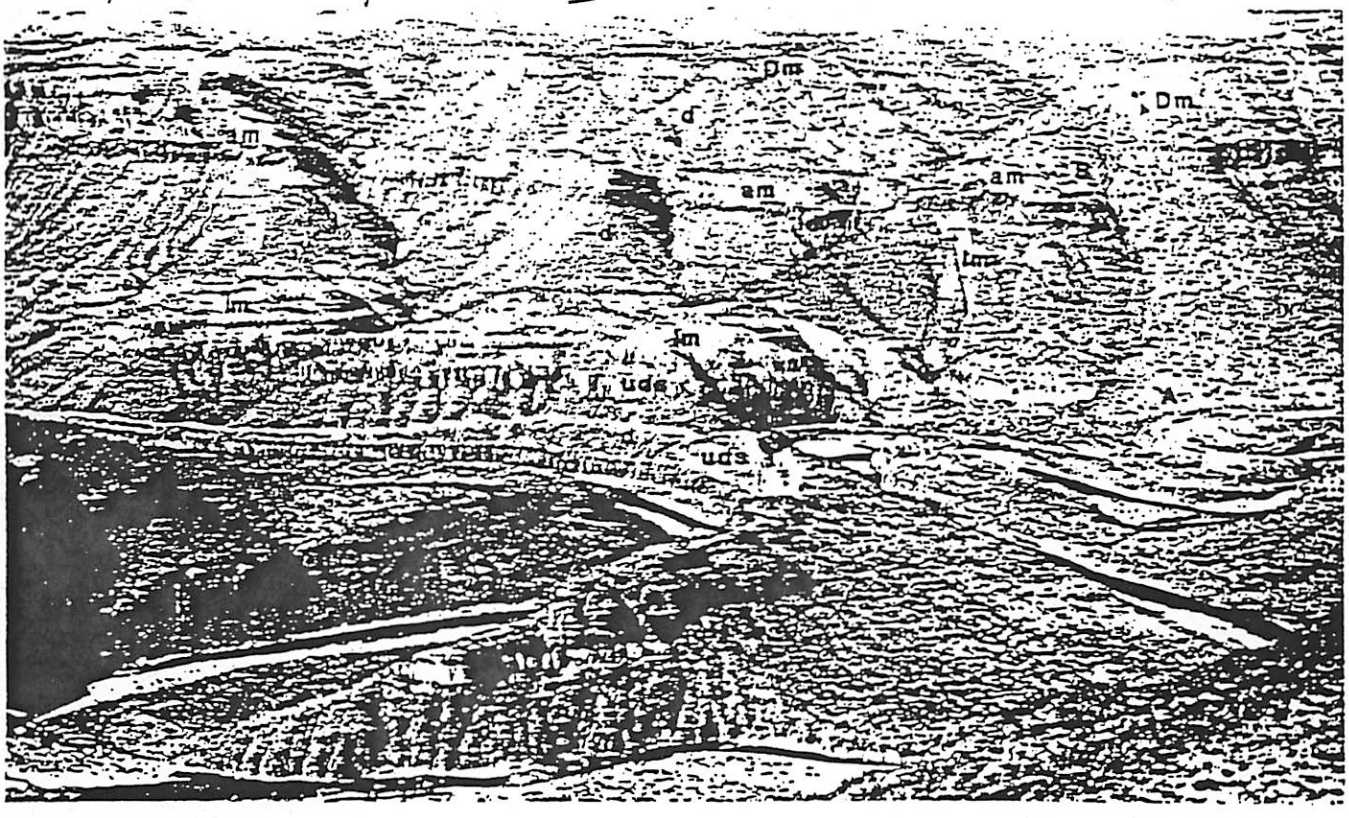

Figure 2. Photo showing outcrops characteristic of Middle Proterozoic rocks near the southern margin of the Colorado Plateau. View north across the Salt River Canyon downstream from Highway 60 (visible at right center) (A). For several square kilometers in this vicinity, in common with many other localities, the slope-forming diabase sills and the cliff-forming strata dilated by diabase are exposed in about equal aggregate thicknesses. Diabase (d) at river level inflated the upper (siltstone) member of the Dripping Spring Quartzite (uds). In mid-view, beyond the river and above the Dripping Spring cliffs, the white-weathering, bench-forming strata constitute all but the upper 3-10 m of the lower member of the Mescal Limestone (lm). The broad concave slope next above, typical of diabase-sill topography, is capped by cliff-forming limestone largely of the algal (stromatolite-bearing) member of the Mescal (am). The cliffs above these strata at the left (west) edge of the view are Troy Quartzite (tr); on to the east at the same level another slope-forming sill has split uppermost strata of the Mescal. This diabase and the Troy are overlain along an erosional unconformity by the even-layered Devonian Martin Formation (Dm). The thin dark cliff at the top of the diabase sheet below the stromatolite strata outlines a separate intrusion. Locally beneath this dark layer near the west edge of the view and in the right center, thin seams of limestone mark the contact between this sill and the thicker sill below. At the right center of the view, above and to the right of the thin seam of limestone beneath the dark cliff, a thin sill (B) is markedly discordant to underlying sills. On close inspection, the Dripping Spring on the north side of the river proves to be cut by a second sill traced by a road. Distance across the field of view at road level is about 2.5 km. From A. F. Shride (written commun., 1986).

ERA	PERIOD	UNIT		THICKNESS (METERS)	
PALEOZOIC	DEVONIAN	Martin Formation		10–120	
	CAMBRIAN	Abrigo Formation		0–255	
		Bolsa Quartzite		0–145	
		Unconformity			
MIDDLE PROTEROZOIC		Diabase			
		Intrusive contact			
		Troy Quartzite	Quartzite member	0–150	0–365
			Chediski Sandstone Member	0–210	
			Arkose member	0–140	
		Unconformity			
	APACHE GROUP	Basalt			0–115
		Unconformity			
		Mescal Limestone	Argillite member	0–30	75–130
			Unconformity		
			Basalt	0–35	
			Unconformity		
			Algal member	12–40	
			Lower member	45–82	
		Unconformity			
		Dripping Spring Quartzite	Upper member	55–130	140–215
			Middle member	40–110	
			Barnes Conglomerate Member	0–18	
		Unconformity			
		Pioneer Shale			45–155
			Scanlan Conglomerate Member	0–15	
		Unconformity			
		Granitic rocks			
		Intrusive contact			
EARLY PROTEROZOIC		Sedimentary and volcanic rocks, locally foliated			

Figure 3. Stratigraphic column of the Apache Group and associated rocks. Modified from Shride (1967).

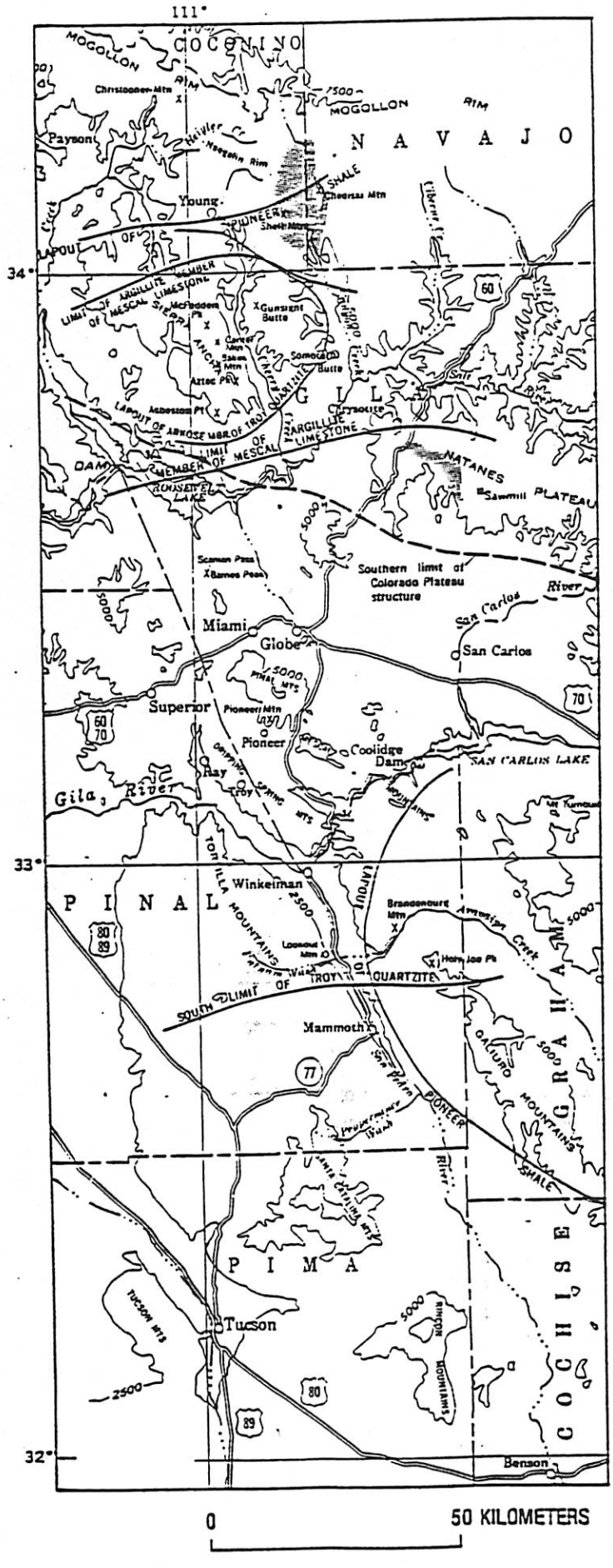

Figure 4. Geographic limits of the Apache Group and Troy Quartzite in central and southern Arizona. The area of karst in the Mescal Limestone is shown by stippling. Formations are present on the side of the line with

PTYS 594a Fall 1993 Superstition Volcanic Field Jeff Johnson and Bill Bottke

Geology and Stratigraphy Overview (see Figure 10 also):

- *~ 35 Ma:* Whitetail Conglomerates/sandstones/arkoses (feldspar-rich fragments) → possibly correlated to "rim gravels" deposited by north-flowing rivers before uplift of Colorado Plateau.

- *> 29 Ma*: Weekes Wash basalt lavas and cinder deposits (near Government Well) → heavily weathered (epidote, calcite) and jointed.

Saddle Rock Rhyolite Tuffs show base surge beds from hydroclastic eruptions (Figure 8): cross-bedding ⇒ proximal, turbulent deposition; while planar texture ⇒ distal, laminar deposition.

- *29-20 Ma.* Government Well Latites (Figure 11) → actually composed of 7 sub-units, from andesite latites to rhyodacite tuffs and lavas to basalts; form domes ringing the Superstition Caldera (Figures 2,3,4,5)

- *25-20 Ma.* Superstition Caldera collapses (Figures 4,5), allowing extrusion of welded ash flow tuffs (e.g., Siphon Draw member of Superstition Tuff); cliff-former, with evident columnar jointing. Different colors represent varying cooling units (strongly welded ⇒ hot deposition vs. loosely welded ⇒ cooler deposition).

- *21-18 Ma.* Apache Gap Rhyodacite erupted after collapse of Superstition caldera. Mostly tuff breccias, distinguished from latites by lack of hornblende but greater phenocryst content in rhyodacites (plus small scale flow banding and needle-like crystals ("*pilotaxitic*" texture)).

- *16-15 Ma.* Begin rhyolite eruptions (Figure 11), with Geronimo Head and First Water Tuffs associated with Goldfield Caldera formation and collapse. Basin and Range faulting begins around this time as well.

- *15-14 Ma.* Canyon Lake welded tuffs (± basalts) associated with a strongly zoned magma chamber (wide range of SiO_2 in samples) responsible for formation of Tortilla caldera. Probably related to:

Peters Canyon dome complex: composed of rhyolite to rhyodacite domes related to formation and eventual collapse of Tortilla Caldera (domes would be on rims of caldera), or possibly with resurgence of Superstition Caldera (domes would be in center of caldera). NW-SE Basin and Range extension plays a role also (Figure 3).

< 15 Ma. Tortilla Caldera collapse generates lahars and breccias of Mesquite Flat Breccia; composed of debris flows interbedded with lahars, ash-flow tuffs and other water-laid sediments.

REFS: (1) Sheridan, M.F., 1971. Superstition Wilderness Guidebook, QE 86 S83 S47. (2) Fisher, R.V., and Schmincke, H.-U., 1984. Pyroclastic Rocks, 472 pp. (3) Kilbey, T.R., Geology and structure of the Goldfield mining district, central Arizona, M.S. Thesis, ASU, Tempe, 1986. (4) Prowell, S.E., Stratigraphic and structural relations of the north-central Superstition volcanic field, M.S. Thesis, ASU, Tempe, 1984. (5) Sheridan, M.F., 1987, Caldera structures along the Apache Trail in the Superstition Mountains, Arizona, in Geological Diversity of Arizona and its Margins: Excursions to Choice Areas, G.H. Davis and E.M. VandenDolder, eds., Ariz. Bur. Geol. Min. Tech. Geol. Surv. Br., Spec. Pap. 5, 238-243.

Eruption Mechanics and Volatiles

- Explosive eruptions are controlled by the physical and chemical properties of the magma:

a) Viscosity, which depends on chemical composition (basaltic to latitic to rhyolitic), volatile content, temperature, and the amount of bubbles and crystals.

b) Type and amount of volatiles

c) Rate of ascent and depth of vesiculation

d) Water availability to magma chamber

e) Other: Periodic removal of upper level compositions by eruption

- Most common trigger for eruption of a magma chamber is vesiculation, which is controlled by the volatile distribution in the magma column: (FIG. 5)

a) Volatiles become concentrated in the upper part of the magma column (H_2O, CO_2, SO_2 most abundant), where they lower the liquidous temperature (fewer phenocrysts). The volatiles go into melt during differentiation, where they rise to find lower temperatures, higher solubility in the upper magma column.

b) Buoyant bubbles rise into unsaturated parts of magma column and increase vesiculation.

c) Since the volatiles (H_2O) cannot move out of the top magma, pressures must rise. With these higher pressures, more volatiles become soluble and diffuse into bubbles. However, they cannot increase their size because the incompressible magma cannot increase its volume in the enclosed chamber.

d) Oversaturation of volatiles in magmas decreases the viscosity of magma, producing explosive eruptions and high discharge rates once the overburden pressure of the magma chamber is met. Later eruptions are less voluminous and slower, indicating depletion of volatiles compared to former magmas.

e) Depressurization occurs near the disruption surface as the magma breaks the surface and causes large bubbles to burst, creating particles of pumice and ash explosively. The rate of disruption of the bubbles is controlled by the rheology of magma, size of vent, gas content, gas escape velocity, and degree of magma fragmentation. Different disruption rates create different eruptive styles (number of bubbles vs. volume of magma determines amount and size of ash particles): (a) Rapid disruption of vesicles produces an explosive eruption (pressure may play a role in viscous magmas), (b) Slow disruption of vesicles produces a more quiescent eruption.

Pyroclastic Fragments, Fallout, and Flow Deposits

- Pyroclastic fragment transport can be grouped into two categories: (FIG. 7, 8)

a) Abrupt transport through the air, falling back as a fallout deposit (ash clouds)

b) Pyroclastic flow deposits from flow along the surface (ash flows, pyroclastic surges, lahars, ignimbrite)

- Origin: (FIG. 6)

Produced by (a) inclined blast from the base of an emerging spine or dome, (b) collapse of a growing dome, (c) boiling-over of a highly gas-charged magma from an open vent, (d) gravitational collapse of an overloaded vertical eruption column, (e) explosive eruption from the front of a lava flow.

- Composition and Structure (FIG. 9)

Pyroclastic flow and surge units composed of crystals, glass shards, and pumice, lithic fragments. Ash-flow tuff is composed of > 50% material ~ 2mm. Layering within an idealized flow unit consists of (bottom to top): (a) pyroclastic ground surge, (b) pyroclastic (ash) flow, a massive, poorly sorted, coarse-grained breccia; flow processes cause it to segregate into vertically stratified sections (c) separation of pumice from ash cloud from washing or settling, (d) ash cloud settling from atmosphere to form tuff; cross-bedding results from further flow processes.

- Transport and Mobility of Pyroclastic Flows:

Flows typically move at high velocity, travel long distances (> 100 km) and can move around barriers (> 600 m). Their great mobility has been traced to (a) exsolution of gas from glassy particles which can buoy up and reduce friction, (b) release of gas from hot magma fragments within the lithic material, (c) heating and expansion of air engulfed at the front of the flow.

$J^2 + B^2$ (1)

KILBEY, 1986

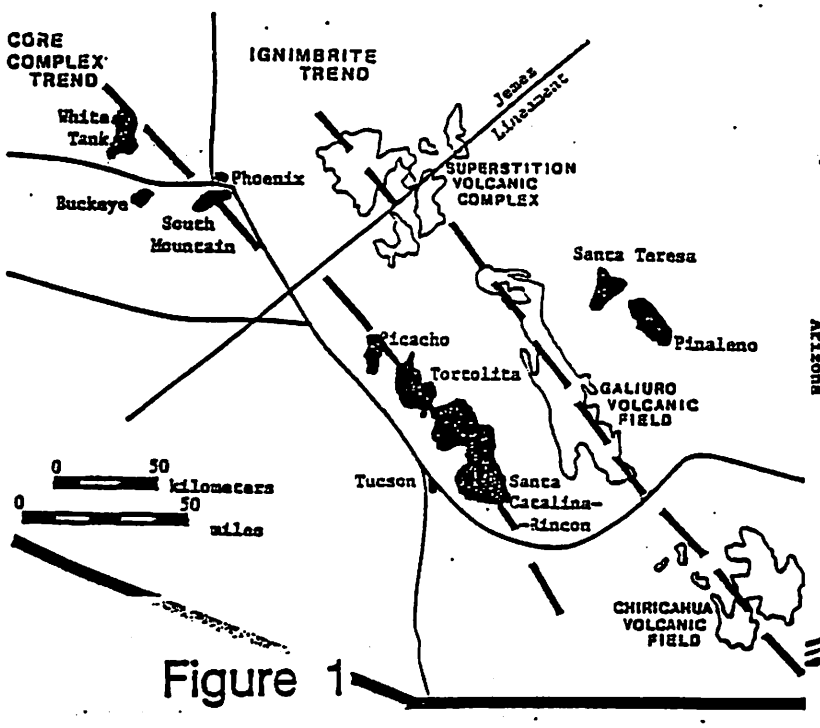

Figure 1

Figure 2.

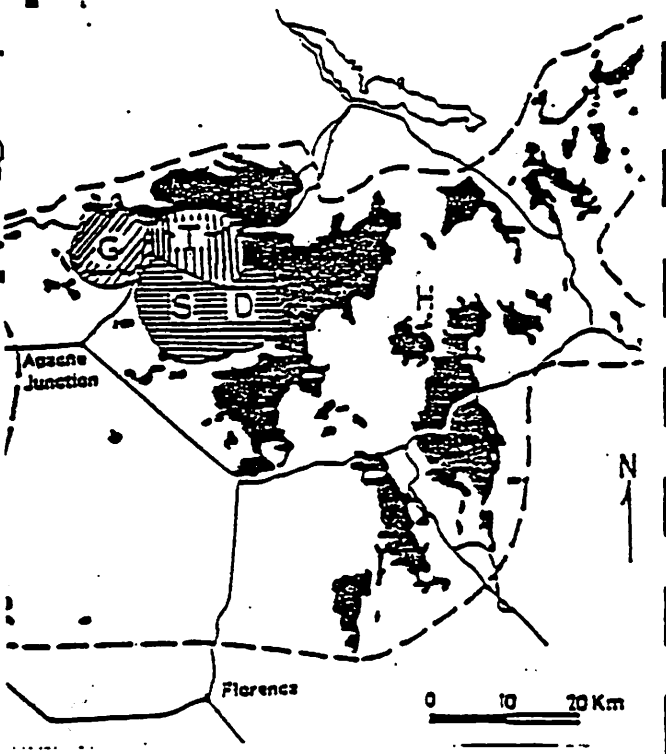

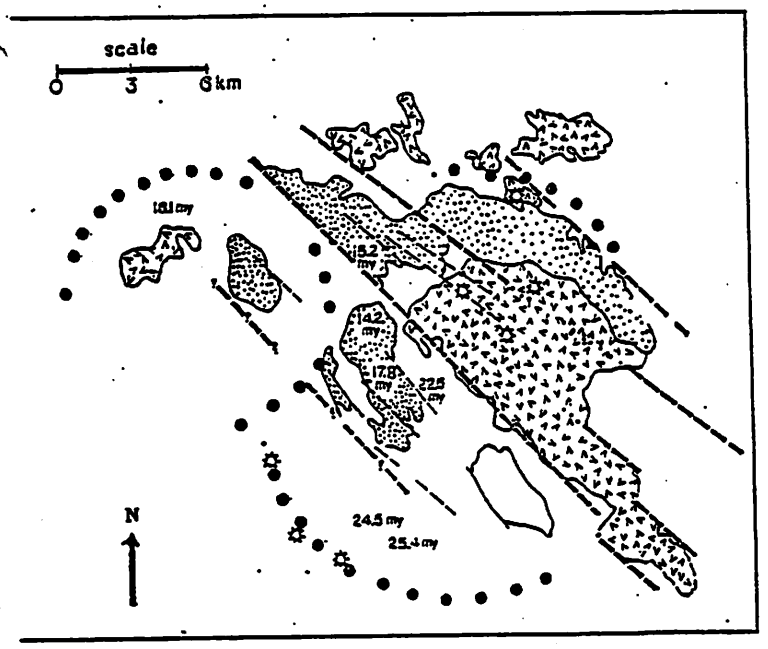

Figure 25. Generalized Caldera-Related and Basin-Range Related Structures. The Goldfield (upper left), Superstition (bottom center) and proposed Tortilla (upper right) caldera boundaries are shown in solid dots. NW-trending faults and lineations are shown in dashed lines. These relations may suggest resurgent activity of the Superstition caldera with synchronous basin-range influence over the eruption and distribution of late-stage volcanic units.

Figure 3.

PROWELL, 1984

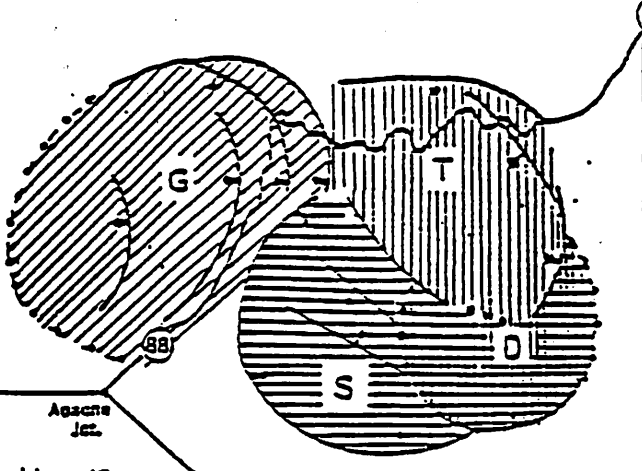

Figure 4.

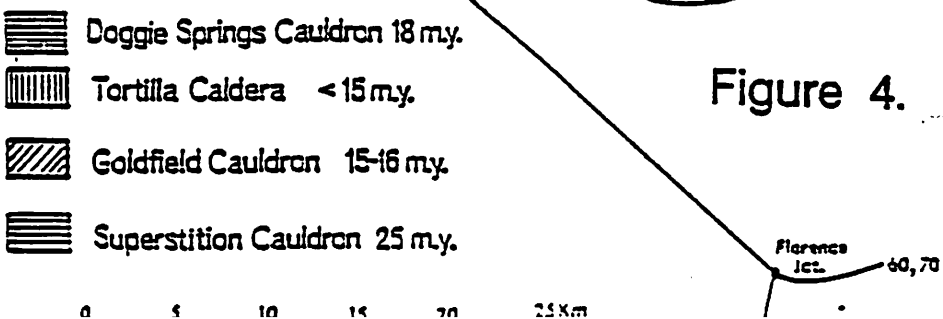

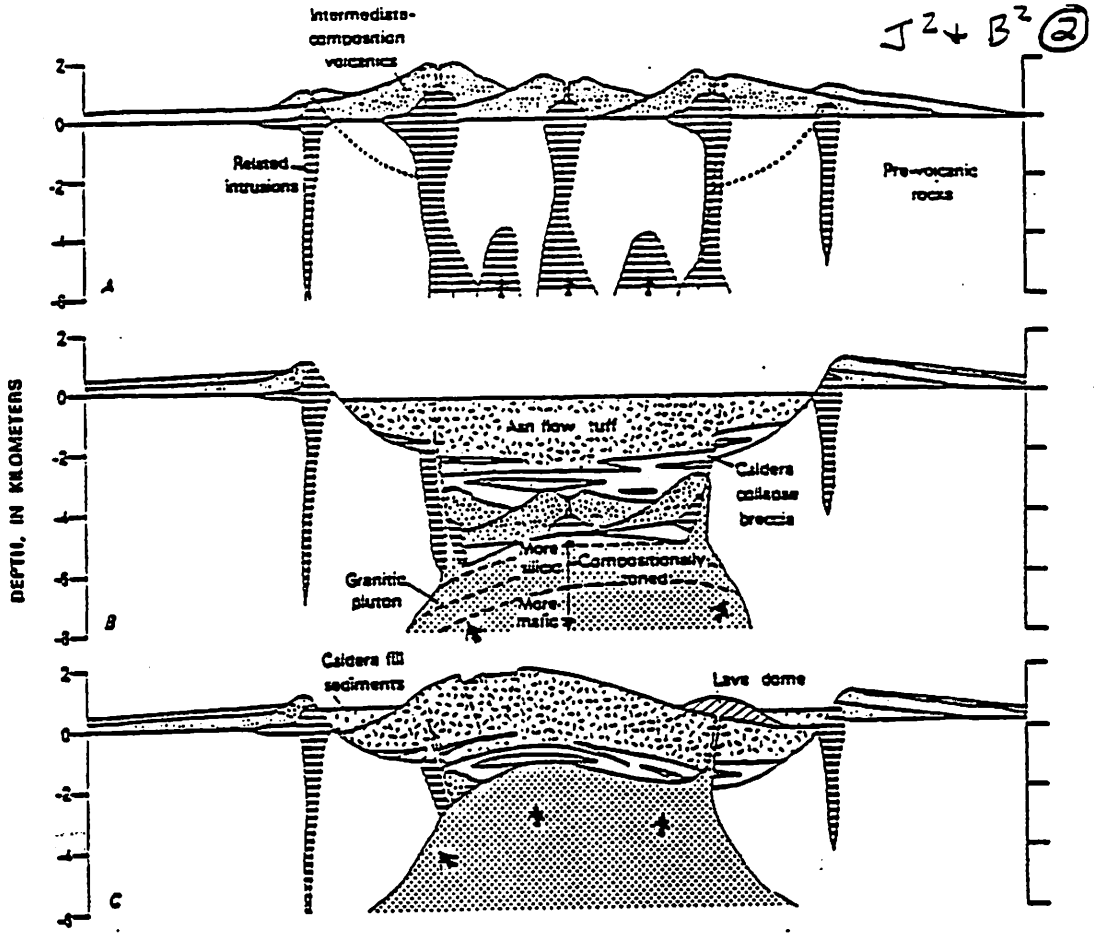

Figure 5.

KILBEY, 1986

A generalized ash flow caldera cycle. These diagrams incorporate many common elements of ash flow calderas; complex possible alternative scenarios are discussed in the text. (*a*) Precollapse volcanism. Clustered intermediate-composition stratovolcanoes grow over isolated small high-level plutons that mark beginning of accumulation of batholithic size silicic magma body that will feed ash flow eruptions. Uplift related to emplacement of plutons leads to development of arcuate ring fractures; site of subsequent caldera collapse indicated by dotted lines. Heavy arrows indicate upward movement of magma. (*b*) Caldera geometry just after ash flow eruptions and concurrent caldera collapse. Central area of clustered earlier volcanoes caves into collapsed area. Intracaldera tuff ponds during subsidence and is an order of magnitude thicker than cogenetic outflow ash flow sheet. Initial collapse along ring faults is followed by slumping of oversteepened caldera walls and accumulation of voluminous collapse breccias that interfinger with ash flow tuff in the caldera fill sequence. Caldera floor subsides asymmetrically and is tilted to the left side of diagram. Main magma body underlies entire caldera area and is compositionally zoned (or was prior to eruptions), becoming more mafic downward. (*c*) Resurgence and postcaldera deposition. Resurgence is asymmetrical, with greatest uplift in area of greatest prior collapse. Extensional graben faults form over crest of the dome. Some resurgent uplift is accommodated by movement along the ring faults in the sense oppposite that during caldera subsidence. Magma body has risen into volcanic pile and intrudes cogenetic intracaldera welded tuff. Original caldera floor has been almost entirely obliterated by rise of the magma chamber to near the level of prevolcanic land surface. Caldera moat is partly filled by lava domes and volcaniclastic sediments. Hydrothermal activity and mineralization become dominant late in cycle.

Fig. 8-40 A–C. Some ways that pyroclastic flows can originate. (After Macdonald, 1972)

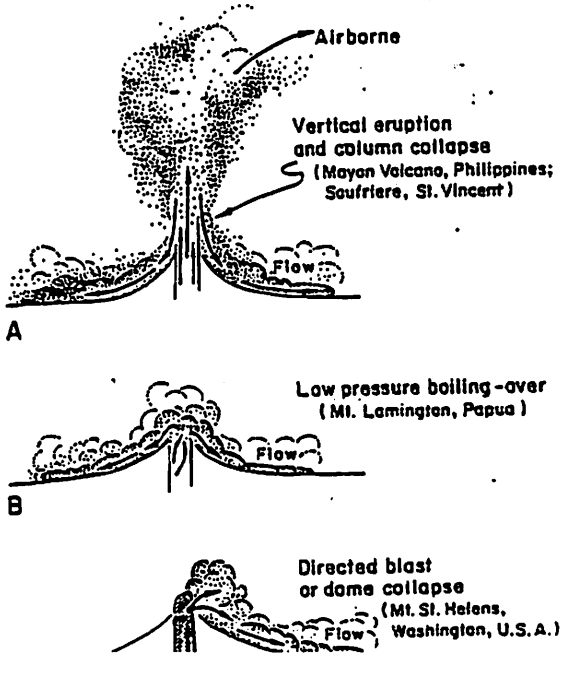

Figure 6.

FISHER + SCHMINCKE, 1984

FISHER AND SCHMINCKE, 1984

$J^2 + B^2$ (3)

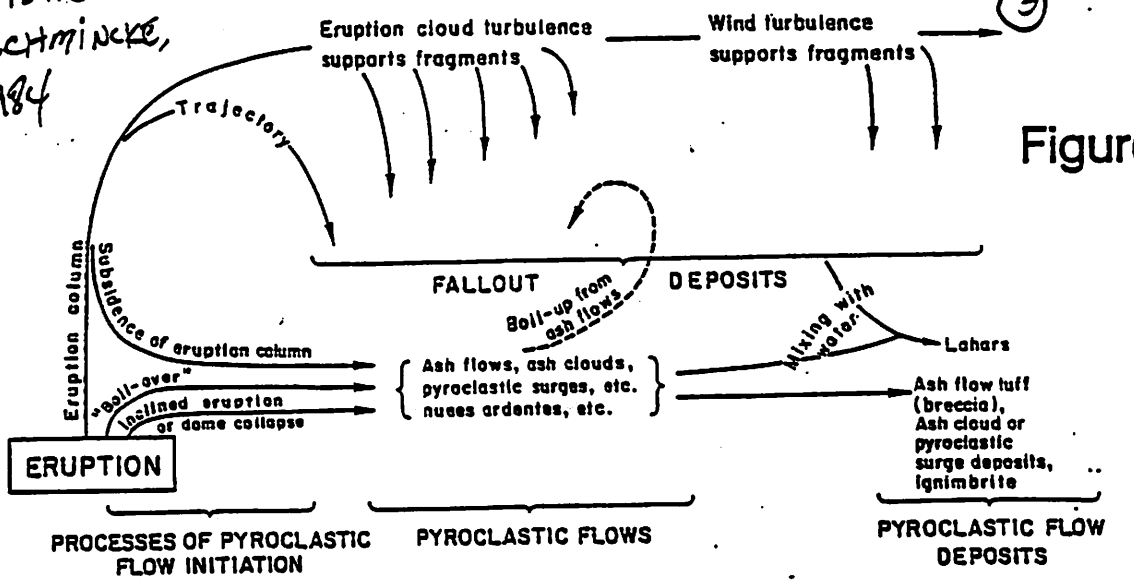

Figure 7.

Fig. 1-3. Processes by which subaerial pyroclastic flow and fallout deposits originate

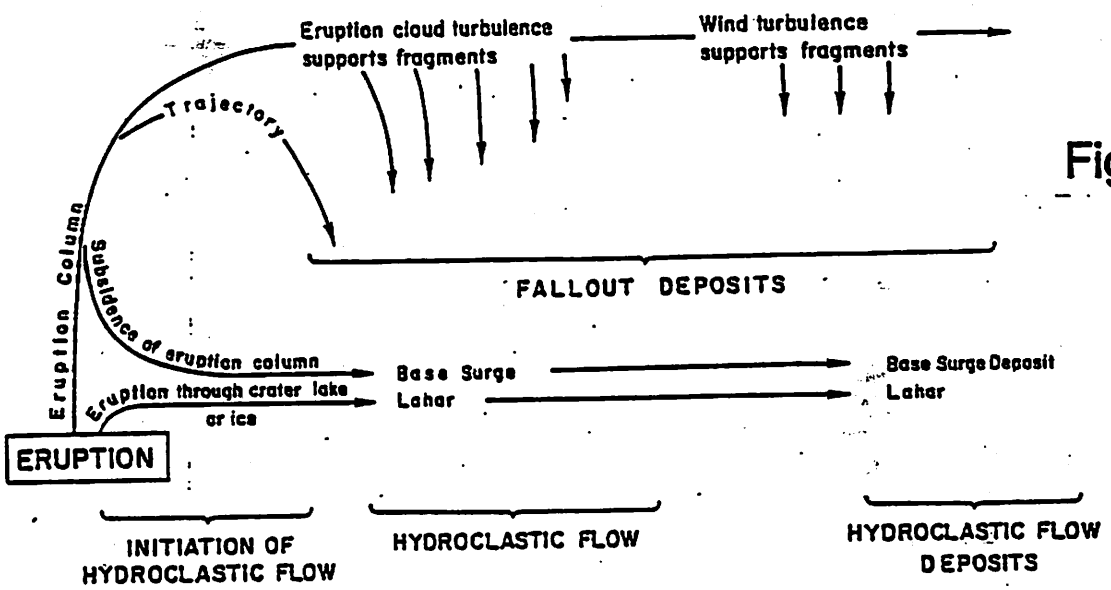

Figure 8.

Fig. 1-5. Processes by which subaerial hydroclastic flow and fallout deposits originate

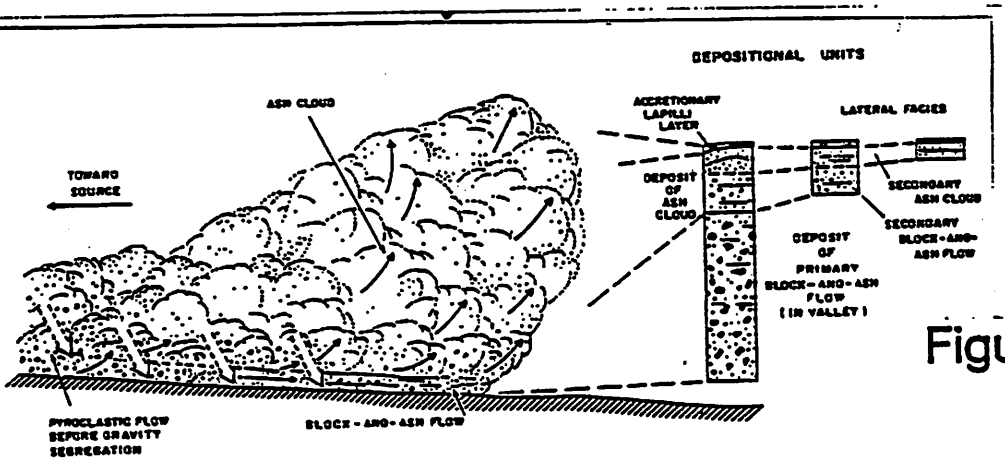

Figure 9.

Fig. 8-41. Diagram showing development of block-and-ash flow and ash cloud surge by gravity segregation from turbulent flow from source. Wide downward arrows show trends of bulk movement of greatest volume of fragments. Lateral facies illustrate continued gravity segregation of ash cloud surge

Figure 10.

Generalized Stratigraphy of the Superstition Volcanic Field PROWELL, 1984

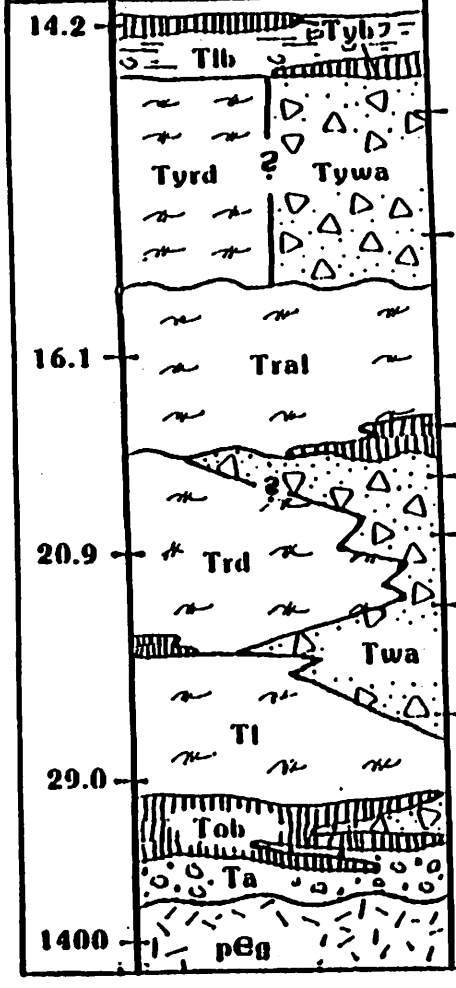

AGE (m.y.)	SYMBOL	GENERALIZED UNIT	DESCRIPTION	VOL. Km^3
14.2	Tyb	Young Basalts	Localized Basaltic Flows	1
14.9	Tlb	Laharic Breccias (MESQUITE FLAT)	Coarse, Poorly-Sorted Laharic Breccia	10
15.4	Tyrd	Young Rhyolite to Rhyodacite Domes (PETERS CANYON)	Aphyric, Alkali-Rhyolite Domes and Crystal-Rich, Rhyodacite to Rhyolite Domes	20
	Tywa	Young Welded Ash (CANYON LAKE)	Crystal-Rich, Rhyodacite to Rhyolite Welded Tuff	50
16.1	Tral	Rhyolite Ash and Lava (FIRST WATER) (BERON/MD HEAD)	Crystal-Poor Rhyolite Lavas and Non-Welded Tuffs	75
17.7	Trd	Rhyodacite Ash and Lava (APACHE GAP)	Crystal-Rich Rhyodacite Lava, Tuff and Surge Deposit	65
18.4	Twa	Welded Ash (SIPHON DRAW) (S.S. TUFF)	Crystal-Rich Rhyodacite Welded Tuff	75
19.9	Tl	Latite Lava and Breccia (GOV'T WELL)	Crystal-Rich Latite Lavas and Breccias (GOV'T WELL)	60
22.6	Tob	Older Basalts (WEEKES WASH)	Alkali-Olivine Basalt and Rhyolite Lava and Non-Welded Tuff (SAPPLE ROCK?)	4
25.4	Ta	Arkosic Sediments	Coarse Arkosic Conglomerate (WHITETAIL CONGLOMERATE)	
29.0	pEg	Ruin Granite	Coarse-Grained Granite	
1400				

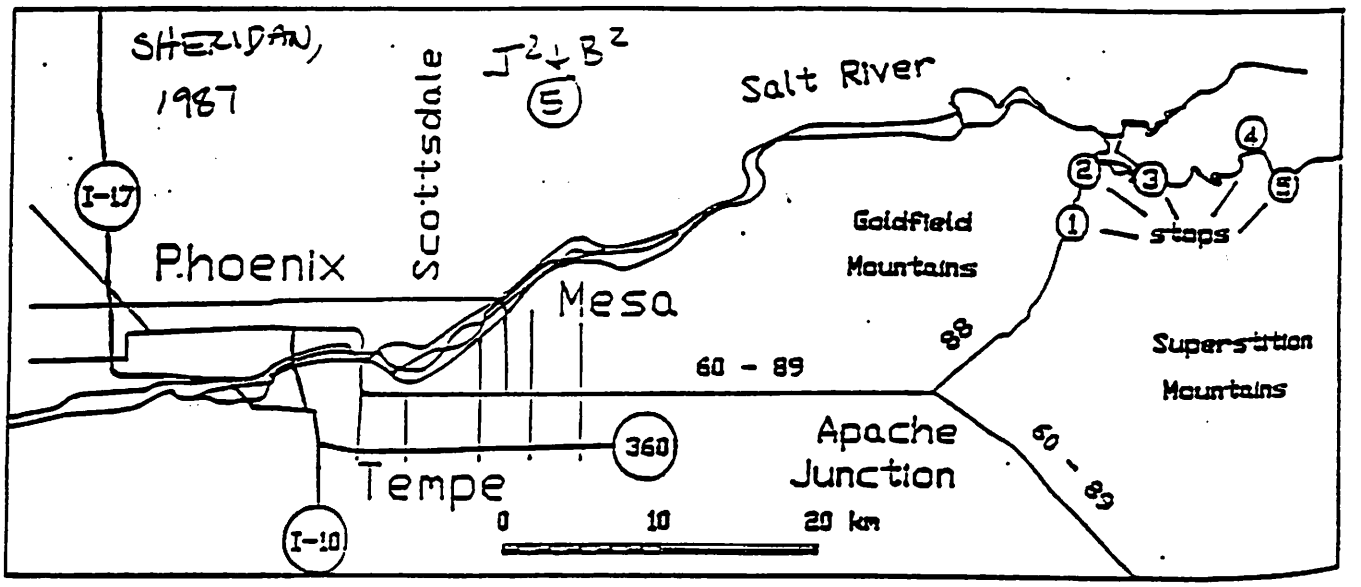

Figure 1. Index map showing the location of the Superstition and Goldfield Mountains relative to Phoenix and other valley cities. The five stops for this field trip are located along the Apache Trail (highway 88).

Figure 12.

Figure 13.

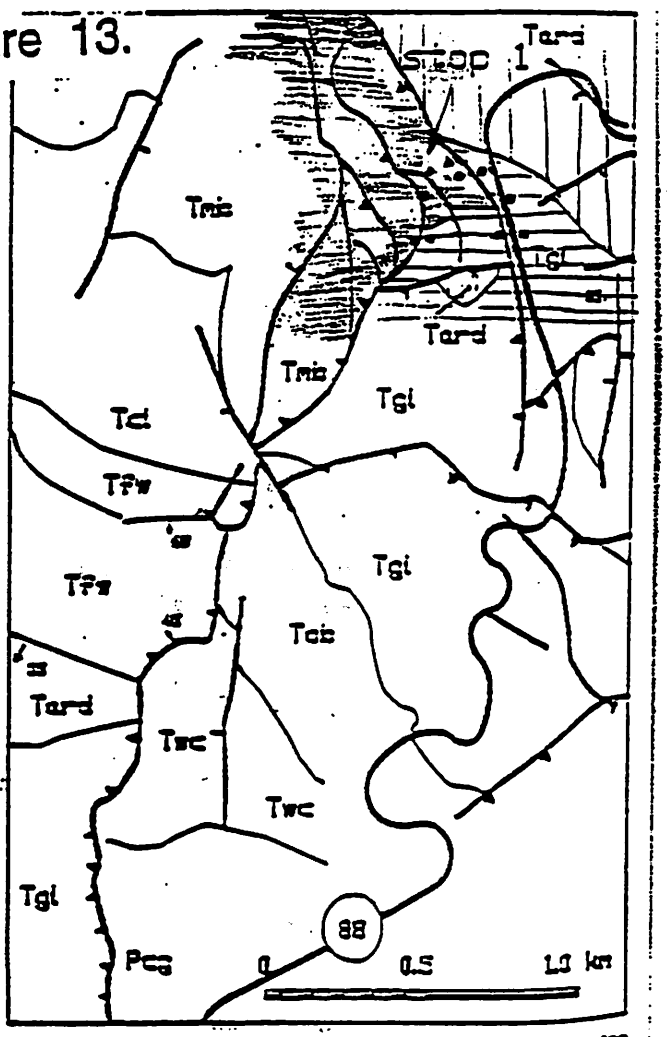

Figure 3. Geologic map of the Apache Gap area. At stop 1 we will examine low-angle faults (shown with teeth on hanging wall) along eastern margin of the Goldfield caldera. Dots indicate the path that we will hike.

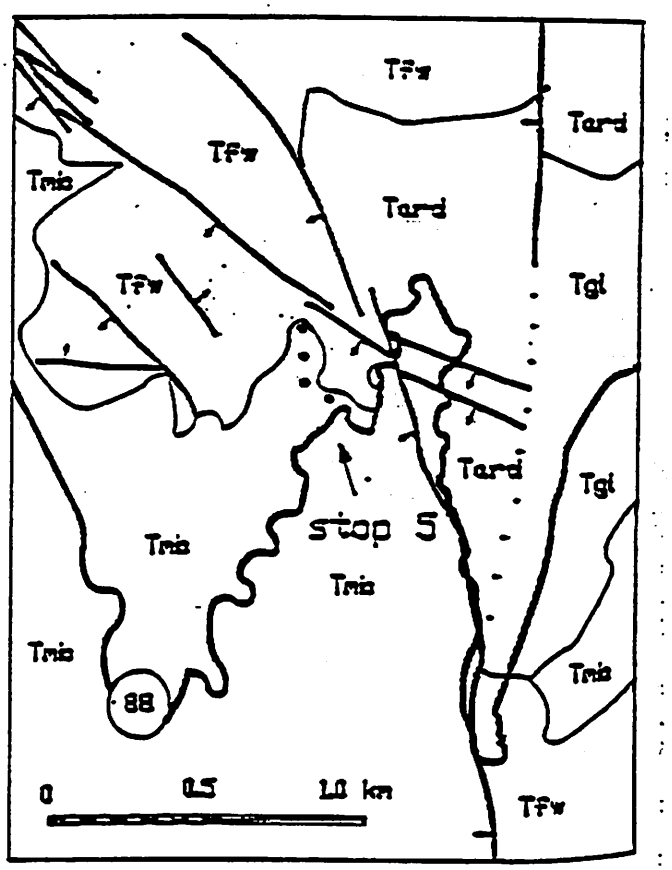

Figure 7. Geologic map of the Fish Creek overlook. At stop 5 we will inspect the faulting at the northeast margin of the Tortilla caldera.

Figure 14.

Tgl - Gov't WELL LATITES Tard - Apache Gap Rhyodacite

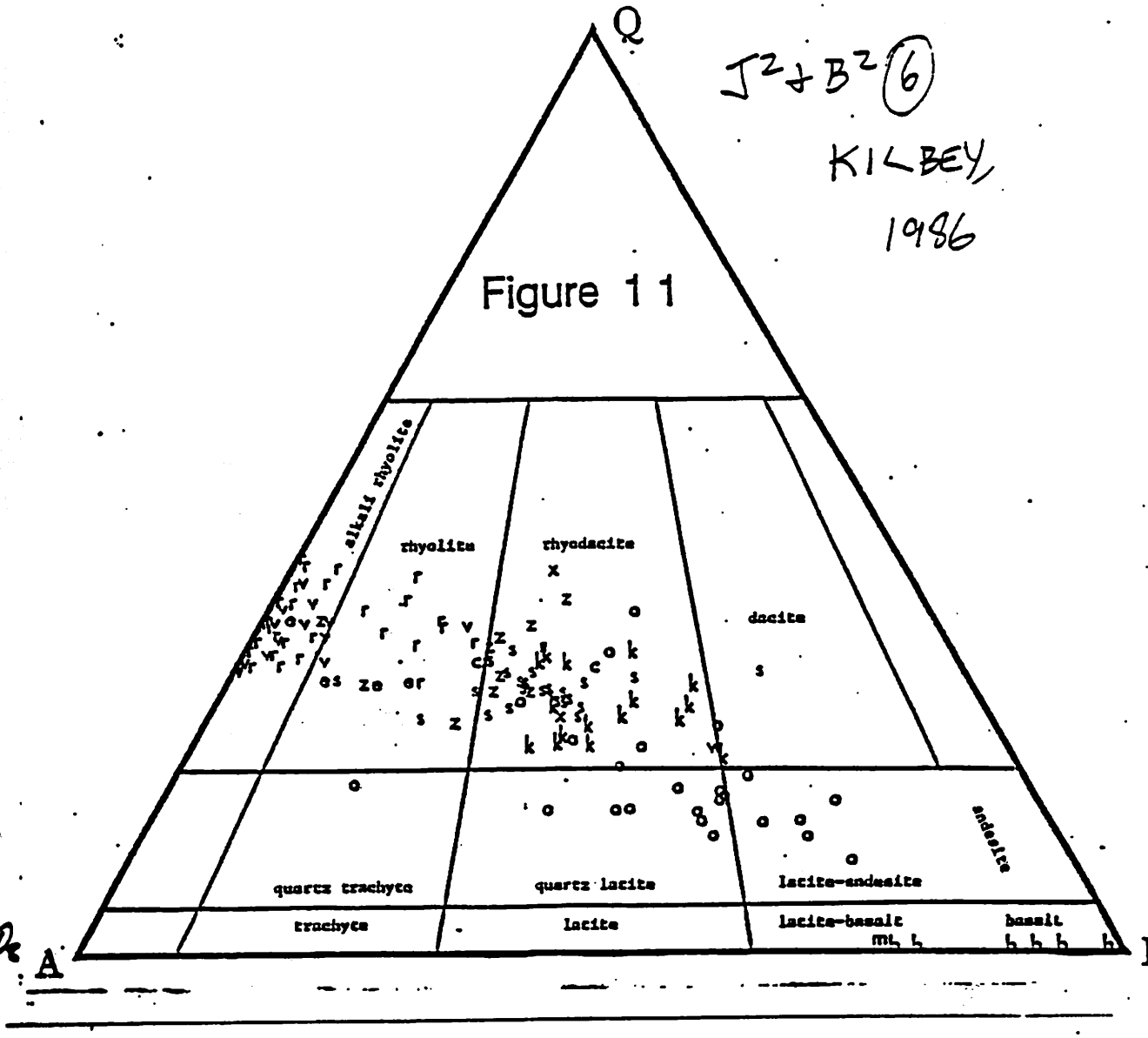

FIG. 64. QAP Streckeisen (1979) classification diagram for rocks of the Superstition Volcanic Complex. The A and P Rittmann norms were calculated from the bulk normative compositions using the feldspar geochemical relationships developed by Gottini (1973). Q is Rittmann Normative Quartz, A is Rittmann Normative Alkali Feldspar, and P is Rittmann Normative Plagioclase. All the samples plotted on this diagram and diagrams of this section are taken from this study, Prowell (1984), Rettenmaier (1984), Isagholian (1983), Suneson (1976), Fodor (1969), Hillier (1978), Stuckless (1969), and D.W. Peterson (1961). These samples are calculated 100% water-free.

Symbols; b = all basalts; m = Weekes Wash basaltic-andesite; x = Saddle Rock Rhyolite; o = Government Well Latites; s = All Superstition Tuffs; v = First Water Rhyolites; z = Government Well Rhyodacites; c = Blue Ridge Rhyolite Tuff; k = Apache Gap Rhyodacites; r = undifferentiated younger Rhyolites; w = Government Well welded tuff; e = older rhyolites reported by Suneson (1976). These symbols are for all the Figures of this section.

MECHANICS OF C E
A S
LDERA COLLAP

by
Mark Fischer

As defined by Williams and McBirney [1979], calderas are large, volcanic collapse depressions, the diameters of which are much larger than the diameters of any included vents. Two calderas are located in the vacinity of the Apache Trail: Willow Springs caldera, a 4-by-3 mile collapse structure, and Black Mesa caldera, a 7-by-5 mile structure (figures 1 & 2).

Collapses that produce calderas may be triggered by the following mechanisms:

1. magma chamber evacuation - withdrawal of support from the roof of the magma chamber;

2. cauldron subsidence - passive sinking of a piston-like block, along steep ring faults, into the underlying magma reservoir.

Figure 3 contains a representative diagram of caldera formation and evolution.

MAGMA CHAMBER EVACUATION

Support may be withdrawn from the roof of the magma chamber in several ways. The primary methods of withdrawal appear to be [Williams and McBirney, 1968]:

1. rapid, voluminous eruptions of ash, pumice, and scoria,

2. eruption of fluid lavas from rifts on the flanks of shield volcanoes,

3. subterranean injection of magma into rift zones.

Subsurface movements of magma are probably more important causes of caldera collapse than are eruptions, especially for shield volcanoes. Eruptions may accompany collapse, but they are not necessarily the cause of it. Rather, it may be the collapse that has triggered the eruption [Williams and McBirney, 1979].

CAULDRON SUBSIDENCE

This mechanism is probably most prevalent where the magma is less dense than its roof-rocks, as was the case at Glen Coe. Subsidence may, however, occur where the magma is more dense than the roof-rocks. In this case, the subsiding block would only subside to an appropriate level in the magma reservoir, as dictated by Archimedes' Principle.

Most cauldrons are larger than most calderas, which suggests that cauldron subsidence is more relevant to larger collapse depressions. In addition, most known ring dikes occur in Precambrian crust, indicating that this mechanism may operate best where the crust is sufficienctly rigid and strong [Walker, 1984].

PLANETARY COMPARISON

In addition to the Earth, calderas have been indentified on Mars, Venus, and Jupiter's satellite, Io. A comparison of these bodies yields several interesting observations:

1. The existence of shield volcanoes and calderas on four solar system bodies suggests that hot spot volcanism and associated summit collapse are basic processes in planetary geology.

2. Shield volcanoes and calderas are considerably larger on Mars, Venus, and Io than they are on Earth. Olympus Mons on Mars is an order of magnitude larger than Mauna Loa, the largest shield volcano on Earth. These differences are presumedly due to plate tectonics on Earth (and lack thereof on the other bodies).

3. Provided that caldera diameters are related to magma chamber diameters and depths, magma chambers on Mars, Venus, and Io are significantly larger than terrestrial ones.

4. Calderas on Io appear to lie on flat plains rather than on mountains. This is probably due to the very low viscosity of sulphur-rich lava flows.

REFERENCES

Lipman, P. W., S. Self, and G. Heiken, Introduction to Calderas Special Issue, *J. Geophys. Res.*, *89*, 8219-8221, 1984.

Sheridan, M. F., *Volcanic Geology along the Western Part of the Apache Trail, Arizona* (field guide).

Walker, G. P. L., Downsag Calderas, Ring Faults, Caldera Sizes, and Incremental Caldera Growth, *J. Geophys. Res.*, *89*, 8407-8416, 1984.

Williams, H., and A. R. McBirney, *Geologic and Geophysical Features of Calderas*, 87 pp., Center for Volcanology, University of Oregon, Eugene, 1968.

Williams, H., and A. R. McBirney, *Volcanology*, 397 pp., Freeman, Cooper, San Francisco, Calif., 1979.

Wood, C. A., Calderas: A Planetary Perspective, *J. Geophys. Res.*, *89*, 8391-8406, 1984.

FISCHER: MECHANICS OF CALDERA COLLAPSE [from Sheridan]

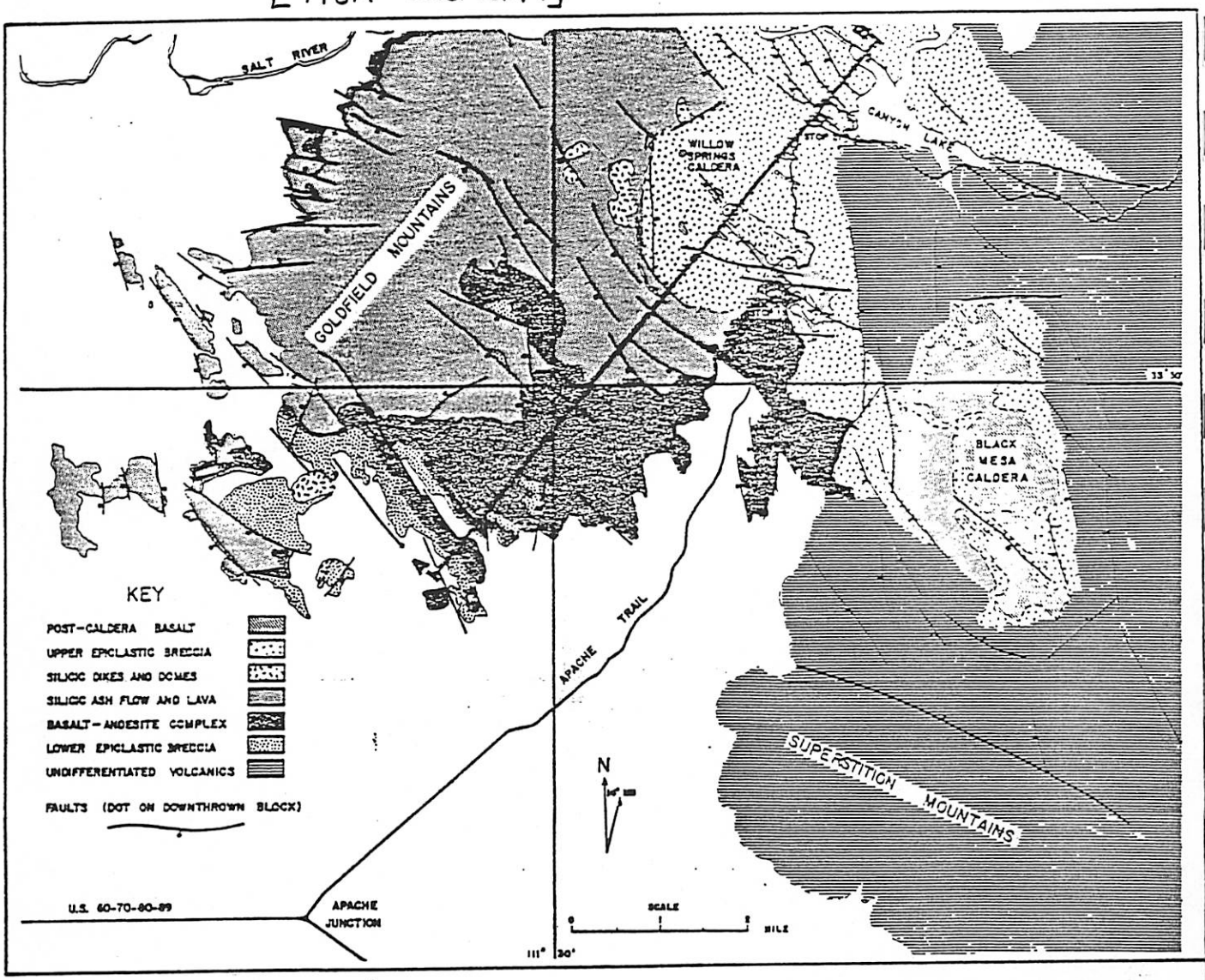

Figure 1 – Surficial geology of a portion of the Goldfield and Superstition Mountains

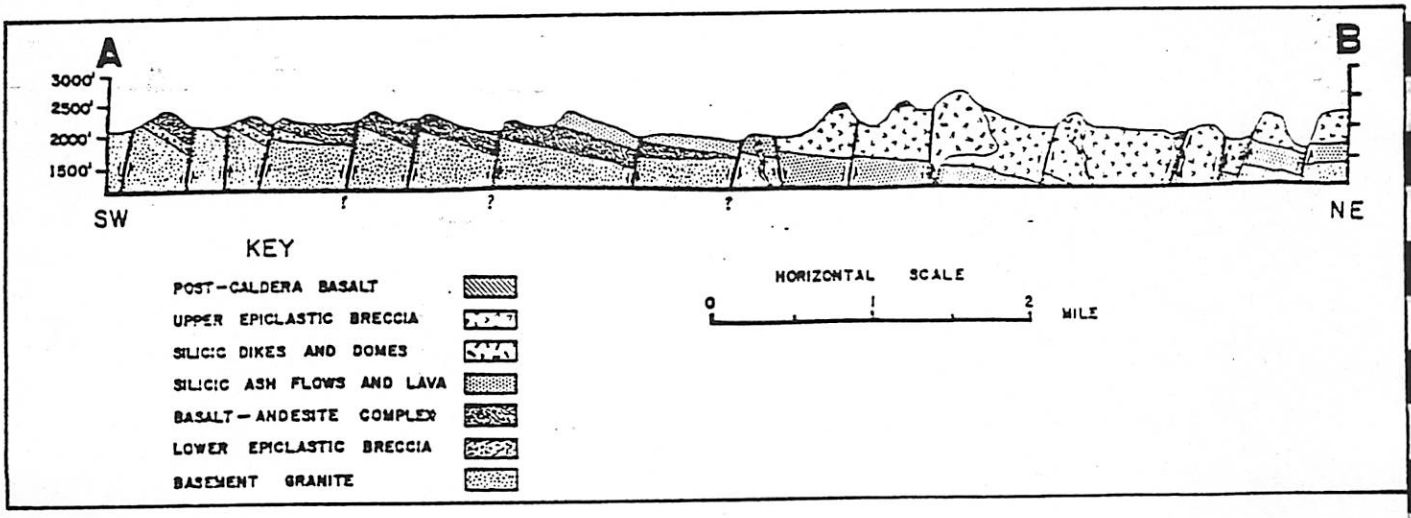

Figure 2 – Cross Section A–B Showing the Willow Springs Caldera

FISCHER: MECHANICS OF CALDERA COLLAPSE

Figure 3. [From Williams & McBirney, 1979]

~~Fig. 9-6~~7. The origin of the Toba volcano-tectonic depression. *1*, Tertiary sediments; *2*, pre-Tertiary crust; *3*, basic and intermediate magma and volcanic rocks; *4*, siliceous lavas; *5*, siliceous tuffs; *6*, granitic batholith. Vertical exaggeration 5 times, elevations in meters. Compare with *Fig. 9-5*. (Redrawn from Bemmelen, 1939.)

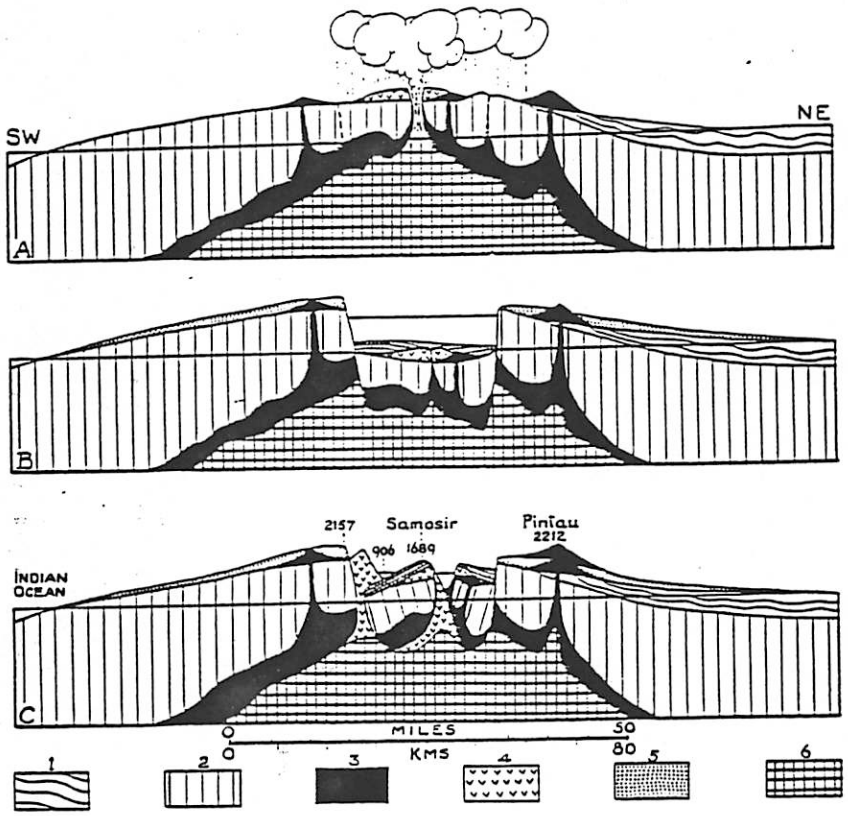

Silicic Volcanism in the Superstition Complex

with Valerie, your cruise director

Age: 30-15 Ma
Type: Calc-Alkaline Suite (That means subduction zone!!!)
I-Type (That means igneous precursors)

Other Burning Questions:
Where do subduction zone magmas come from?
How many parent magmas?
Most likely only two: A basalt magma and a quartz latite magma. Almost all the silicic magmas can be derived by differentiating the latite magma.

General Sequence of Events
1) Formation and early differentiation of a latitic magma leading to the eruption of rhyolites (Saddle Rock Tuff and Blue Ridge Tuff)
2) Continued eruption of lavas from latite magma chamber producing the Government Wells sequence
3) Explosive eruption of the Siphon Draw Tuff (Siphon Draw magma evolved from original latitic magma)
4) Mixing in the magma chamber between remaining Siphon Draw magma and invading basalt to form Apache Gap Rhyodacite (9 to 1 mix)
5) Evolution of Apache Gap magma to form later rhyodacites and rhyolites

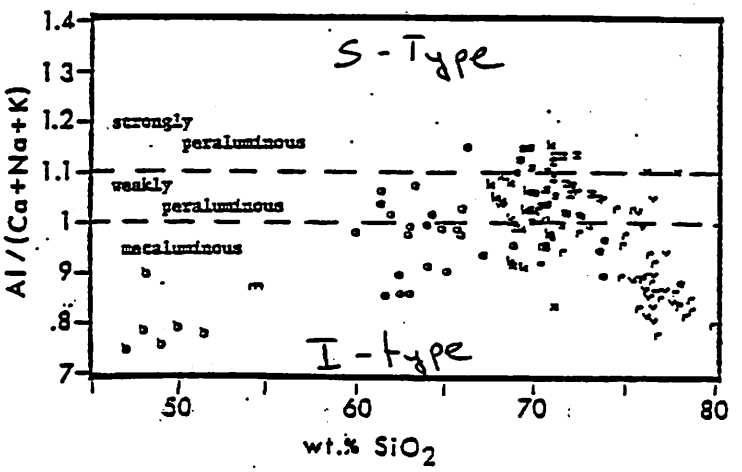

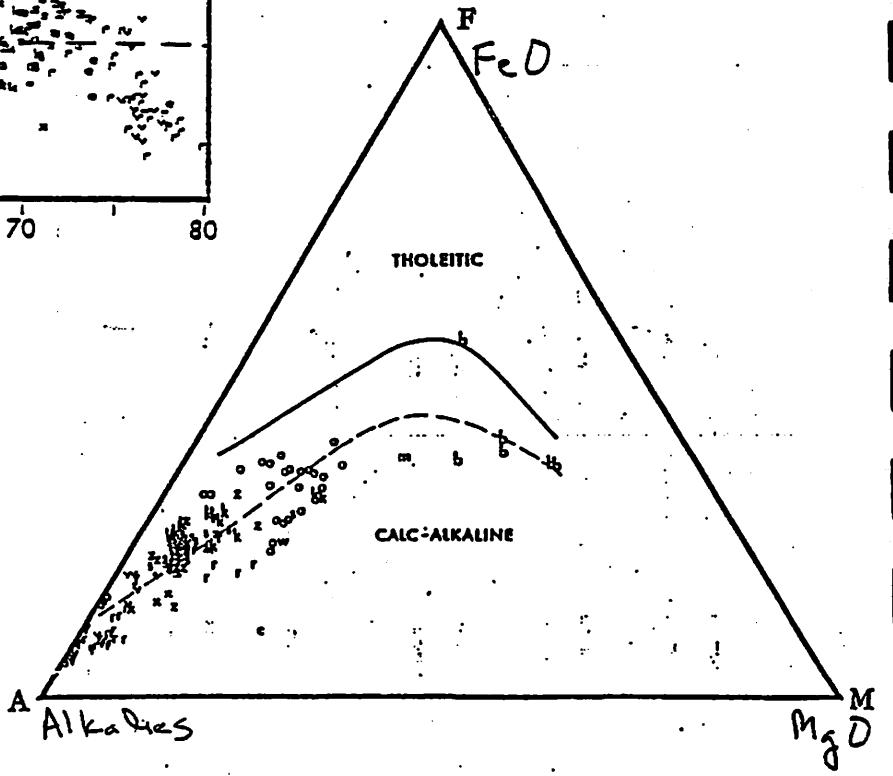

Helpful Mineral Formulas:
Quartz - SiO_2
Feldspar group
Plagioclase:
$CaAl_2Si_2O_8$ - Anorthite
$NaAlSi_3O_8$ - Albite
K-Feldspar
$KAlSi_3O_8$

TABLE 1. Generalized stratigraphy of the western Superstition Complex.
(from Prowell, 1984)

AGE (m.y.)	LITHOGRAPHY	AGE (m.y.)	SYMBOL	GENERALIZED UNIT	DESCRIPTION	VOL. Km³
14.2			Tyb	Young Basalts	Localized Basaltic Flows	1
	Tlb	14.9	Tlb	Laharic Breccias	Coarse, Poorly-Sorted Laharic Breccia	10
	Tyrd ? Tywa	15.4	Tyrd	Young Rhyolite to Rhyodacite Domes	Aphyric, Alkali-Rhyolite Domes and Crystal-Rich, Rhyodacite to Rhyolite Domes	20
			Tywa	Young Welded Ash	Crystal-Rich, Rhyodacite to Rhyolite Welded Tuff	50
16.1	Trai		Trai	Rhyolite Ash and Lava	Crystal-Poor Rhyolite Lavas and Non-Welded Tuffs	75
		17.7				
		18.4	Trd	Rhyodacite Ash and Lava	Crystal-Rich Rhyodacite Lava, Tuff and Surge Deposit	65
20.9	Trd	19.9				
		22.6	Twa	Welded Ash	Crystal-Rich Rhyodacite Welded Tuff	75
	Twa		Tl	Latite Lava and Breccia	Crystal-Rich Latite Lavas and Breccias	60
		25.4				
29.0	Tl		Tob	Older Basalts	Alkali-Olivine Basalt and Rhyolite Lava and Non-Welded Tuff	4
	Tob		Ta	Arkosic Sediments	Coarse Arkosic Conglomerate	-
	Ta		pEg	Ruin Granite	Coarse-Grained Granite	
1400	pEg					

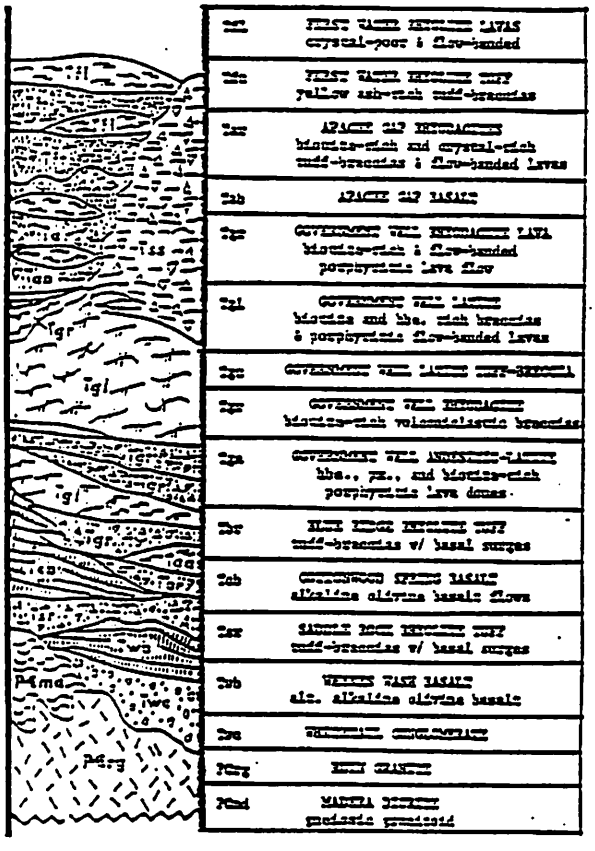

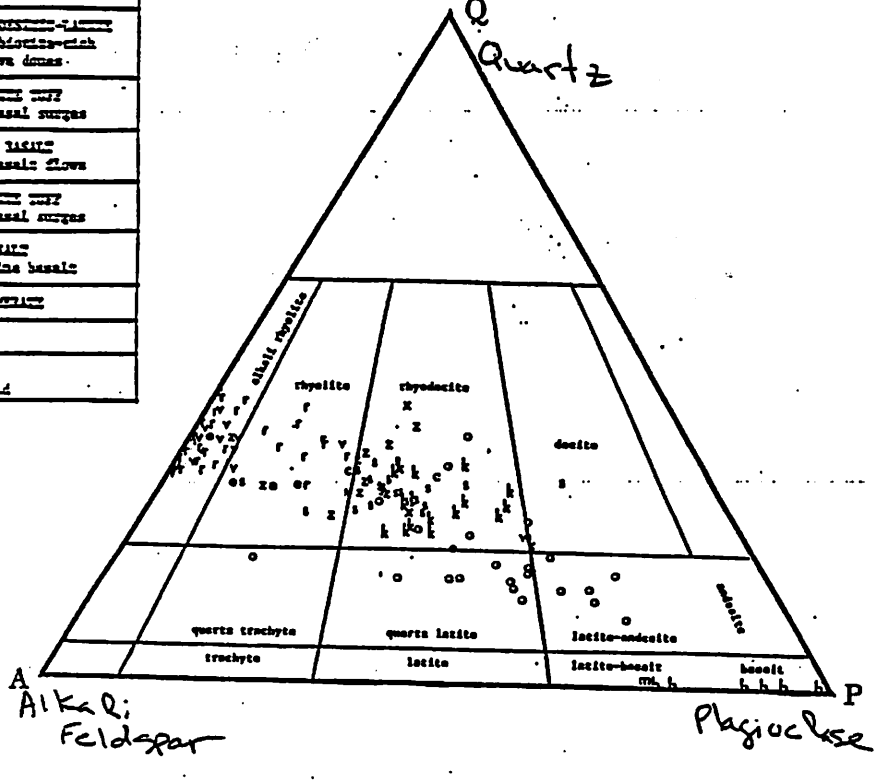

Source of Arc Magmas

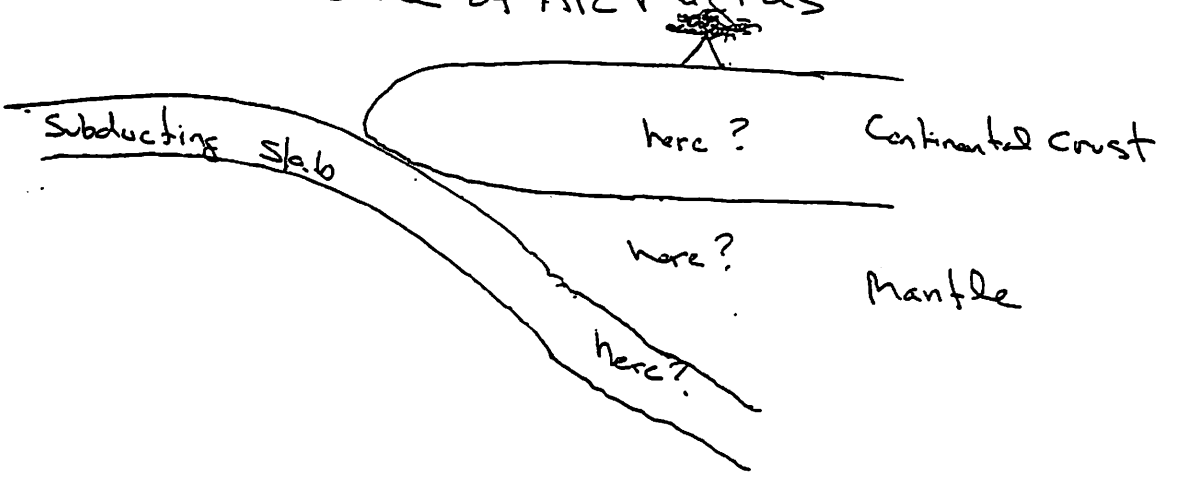

Nature Vol. 270 1 December 1977

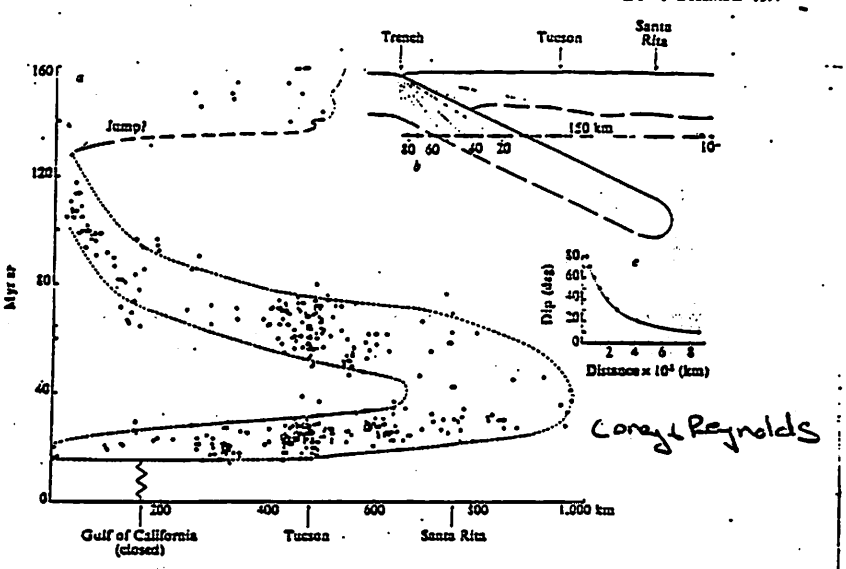

Fig. 2 *a*, Distribution of radiometric ages from Fig. 1 plotted as a function of time. Dates projected into a line passing through Tucson, Arizona, and Santa Rita, New Mexico after closure of Gulf of California. ○, single mineral K/Ar ages on plutons in southeastern California. *b*, Hypothetical arc-trench system scaled to southwestern North America. Various dip-angles of Benioff zones shown with points of intersection with 150 km depth line. *c*, Graphical representation of function controlling distance from trench to magmatic arc with varying Benioff zone dip angles.

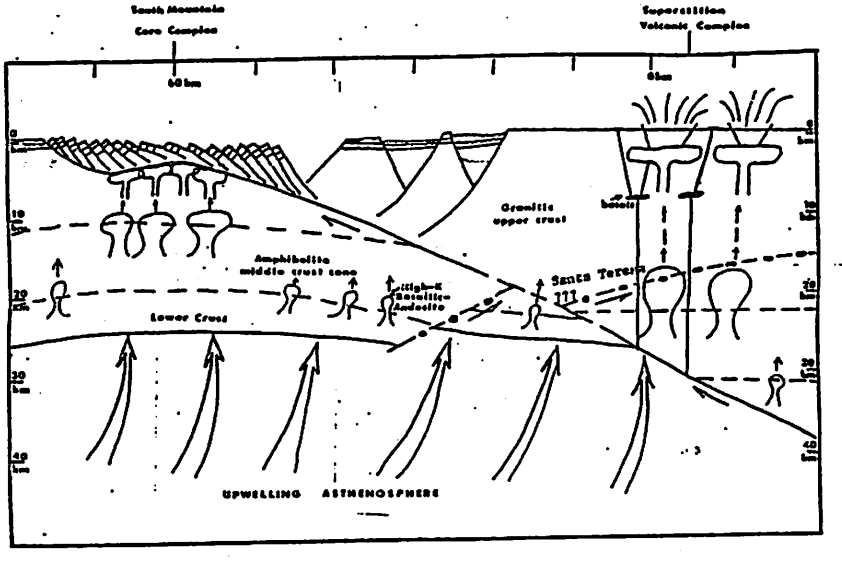

Emplacement mechanisms: The space problem

Elizabeth Turtle

The problem:

– Geochemical and petrological studies of plutons indicate that the magmas have moved significantly from their source regions and that they do not incorporate large volumes of wall rock material.

– Crustal extension rates are slow and often plutons are emplaced into wall-rock with temperatures significantly below magma emplacement temperatures.

So, how are huge volumes of magma emplaced in the crust?

Over-simplified version: Emplacement mechanisms are traditionally divided into two types:

Forceful: magma pushes wall rocks aside
rate of buoyant uprise exceeds the rate of tectonic cavity opening
includes: doming, diapirism, ballooning

Passive: fractures opened by regional stresses
rate of cavity opening greater than rate of buoyant uprise
includes: stoping, cauldron subsidence, and sheeting

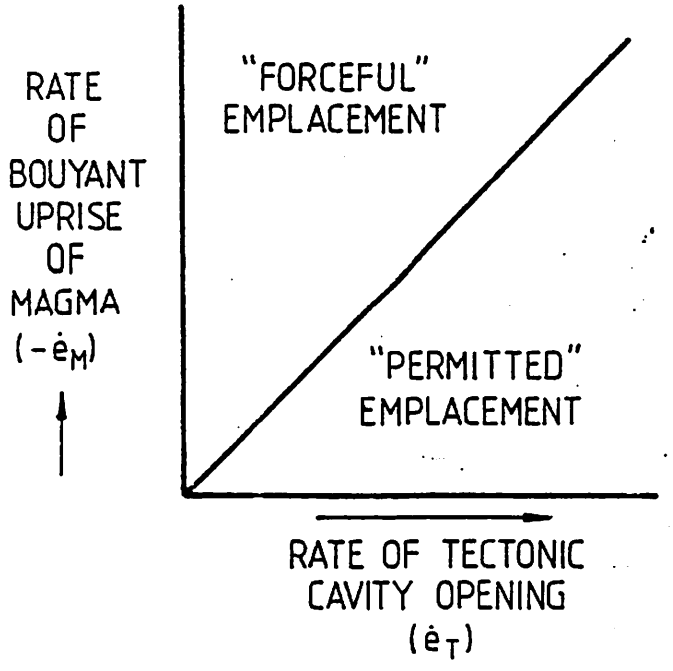

Hutton 1988

Figure 6 Simplified view of the relationship between magma related buoyancy forces and strain rates and tectonic 'cavity creating' rates leading to a spectrum of emplacement types with two basic end members.

Some possible mechanisms:

Extension

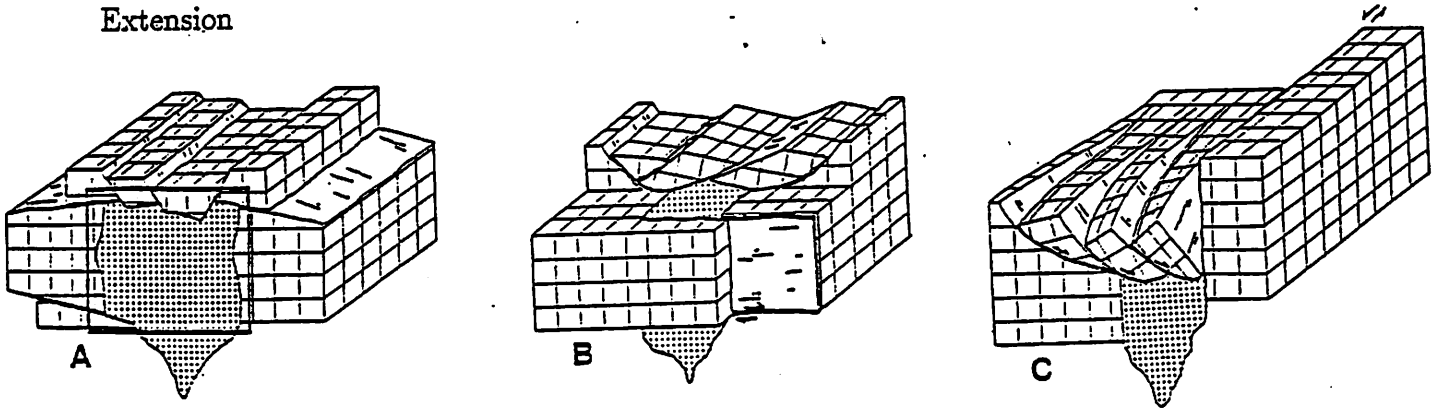

Paterson and Fowler 1993b

Problems:

– Can't open and maintain large voids except very near to the Earth's surface where the lithostatic pressure is less than the strength of the wall rock.

– Extension is slow. This may be conducive to the formation of sheeted plutons by numerous small injection of magma, but makes it very difficult to create large homogeneous plutons.

– Extension will lead to significant faulting of the overlying and underlying wall rocks which needs to be concurrent with the magma emplacement. This is not always observed.

Ductile shortening of surrounding wall-rocks

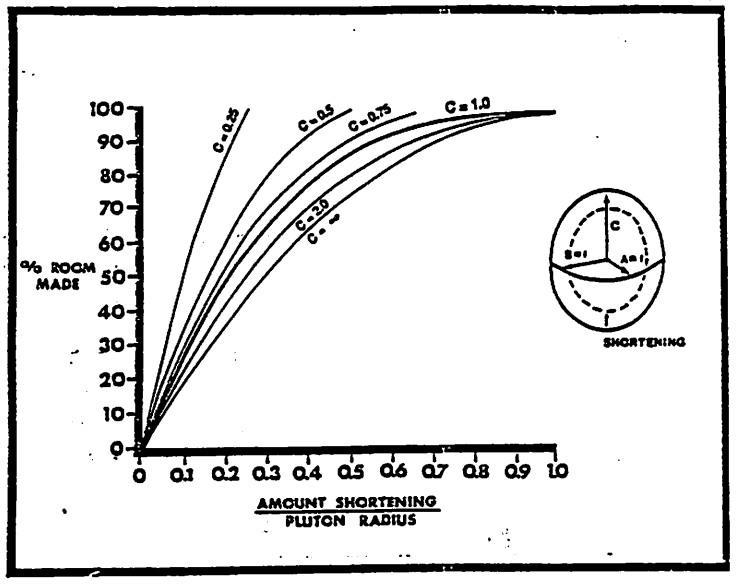

Paterson and Fowler 1993a

Fig. 3. Plot of percent room made vs bulk wall-rock shortening normalized to pluton radius assuming a three-dimensional spherical (thick line) or elliptical (thin lines) shape for the pluton. C = radius of third axis of pluton as shown in inset. $C = 0.25$ means pluton is tabular sheet. $C = 2.0$ means pluton is rod-shaped body.

Problem:

– Some space created, but not enough. Need other mechanisms, too.

Paterson and Fowler consider emplacement on two scales:

Near-field material transfer processes: These operate within the structural aureole of the pluton and provide a means of moving material away from the path of the magma. Examples include: ductile flow of wall rock, assimilation, stoping, roof lifting, elastic strain, volume loss.

Far-field material transfer processes: These transfer material from the immediate region towards the surface of the Earth or back towards the region of magma generation. This is where regional extension fits in.

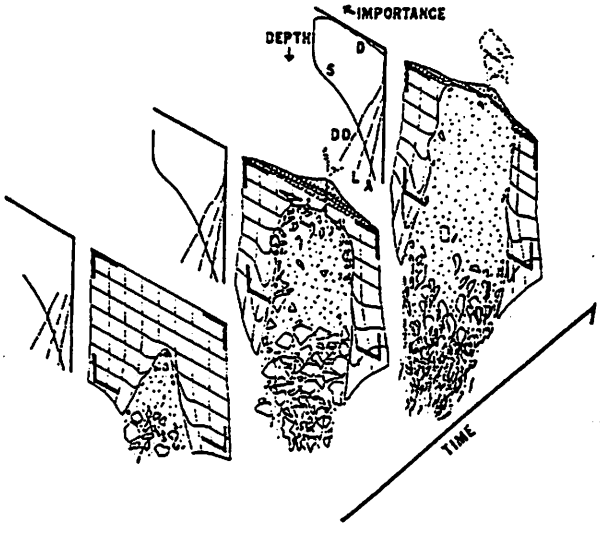

Paterson and Fowler 1993a.

Fig. 12. Diagram showing one possible scenario of changing near- and far-field MTPs with time during pluton emplacement. Each section is areally balanced in a region outlined by the thick black corners. Material displaced during emplacement of the pluton is shown outside these corners. Diagrams to left show relative importance of different MTPs. D = doming of roof rocks. S = stoping. DD = ductile shortening. L = rigid translation of wall-rock. A = assimilation. Note that the relative importance of MTPs change with depth, time and distance from pluton.

The space problem may be solved by incorporating a number of varied processes acting together on different time and distance scales.

References

Hutton, D.H.W., Granite emplacement mechanisms and tectonic controls: inferences from deformation studies. *Transactions of the Royal Society of Edinburgh: Earth Sciences,* **79**, pp. 245-255, 1988

Paterson, S.R. and Fowler, T.K., Jr., Re-examining pluton emplacement processes. *Journal of Structural Geology,* **15**, pp. 191-206, 1993a.

Paterson, S.R. and Fowler, T.K., Jr., Extensional pluton-emplacement models: Do they work for large plutonic complexes? *Geology,* **21**, pp. 781-784, 1993b.

PRECAMBRIAN GEOLOGY OF THE TRANSITION ZONE

Janet McLarty

THE CENTRAL HIGHLANDS

The Central Highlands lie on a diagonal stretch of land between the SW Basin and Range deserts and the Northern Colorado Plateau. This stretch is often called the *Transition Zone.* (see FIG 1)

The Highlands underwent several periods of uplift involving both folding and faulting. At the end of these periods, they were higher than the desert to the south and the plateau to the North. Erosion has since stripped them of most of their Paleozoic and Mesozoic rocks, leaving the hard igneous and metamorphic Precambrian core (1-2 Ga).

A string of basins and valleys run lengthwise through the Transition Zone, many of which have developed terraces.

Desert weathering processes have reduced near-surface granite, gneiss, and diabase (a dark intrusive rock) to rounded boulders surrounded by coarse sand or grus (tan for granite, dark brown for gneiss and diabase). They are rounded due to exfoliation due to heating and cooling.

HISTORY

Older Precambrian Sequence

1820-1750 Ma	Volcanic rocks accumulating across Arizona. Thousands of vertical feet of lava flows, welded tuffs, volcanic breccia. Violent volcanism.
1750-1830 Ma	Accumulation of sandstone and shale that formed the Mazatzal Quartzite
1730-1650 Ma	Arizona region drifts SE against another crustal plate. Plates buckle and crumple causing a mountain-building event known as the Mazatzal Revolution. A mountain range possibly on the scale of the Himalayas rose on a SE-NW extension beyond today's limits for AZ. Intrusion of vast granite batholiths on same trend (still revealed in bands).

Younger Precambrian Sequence

(sequence of events)

Layers of sedimentary rocks deposited. (sediments = sand, silt, clay, limy mud)
The sedimentary layers alternated with volcanic ash and lava flows.
Dark diabase magma forced its way up into the granite and metamorphic rocks, and squeezed between sedimentary layers, which have hardened into sills.
Erosion until the end of the Precambrian period.

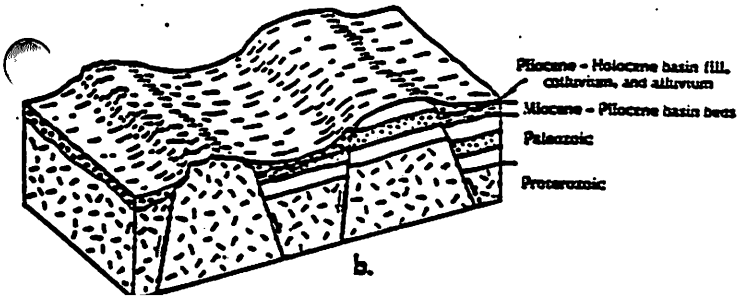

b) Typical structure of the Transition Zone, showing fault-controlled basins and intervening ranges, similar to those of the Basin and Range terrane but less well developed.

THE ROUTE (South to North on AZ 87) (See FIG 2)

Mile 203	gravel veneered pediment sloping towards the Phoenix Basin to the south. Can see the Four Peaks (preserved as roof pendants, see figure), granite hills, and Superstition Mountains.
Mile 206	Exposed Mazatzal Quartzite, Four Peaks to the east.
Mile 224-229	Faults, Tertiary gravel over Precambrian rocks Mercury mining district around Ord Dark red conglomerates, slaty shale, quartzite, purple mica schist cut by dikes and veinlets.
South of 188 Jn	Mazatzal mountains intersection. Precambrian schist, volcanic rocks and granite. Whitish lake beds.
N of 188 Jn	Tonto Basin
S of Payson	Precambrian metavolcanic rocks (i.e. greenstone).

REFERENCES

Chronic, Halka.
Roadside Geology of Arizona. Mountain Press Publishing Co: 1983.

Davis, George and VandenHolder, Evelyn
Geologic Diversity of Arizona and Its Margins: Excursions to Choice Areas. Az Bureau of Geology and Mineral Technology, Special paper 5, 1987.
Article:
Geomorphology and Structure of the Colorado Plateau/Basin Range Transition Zone, Arizona, by R. Young, H.W. Peirce, and J Faulds.

Lucchitta, Ivo
Overflight of the Tectonic Boundary Between the Colorado Plateau and the Basin Range Provinces. Field Trip guidebook. 1989 AGU, 1989.

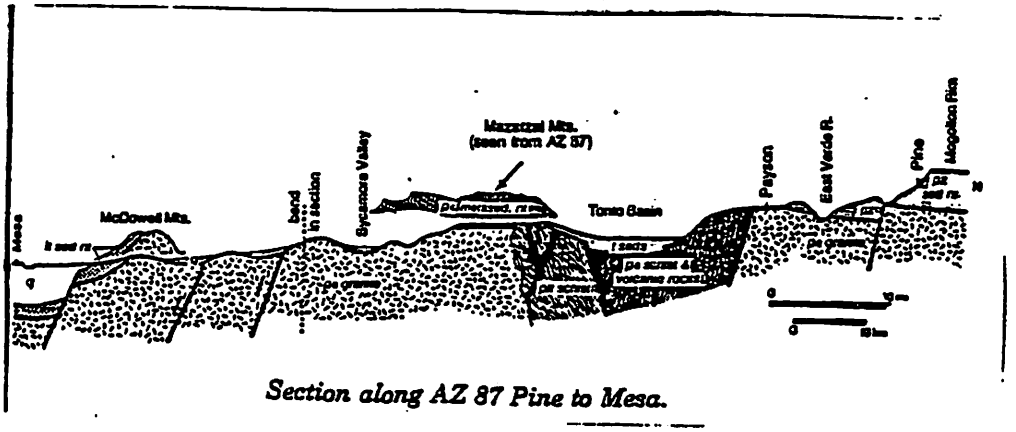

Section along AZ 87 Pine to Mesa.

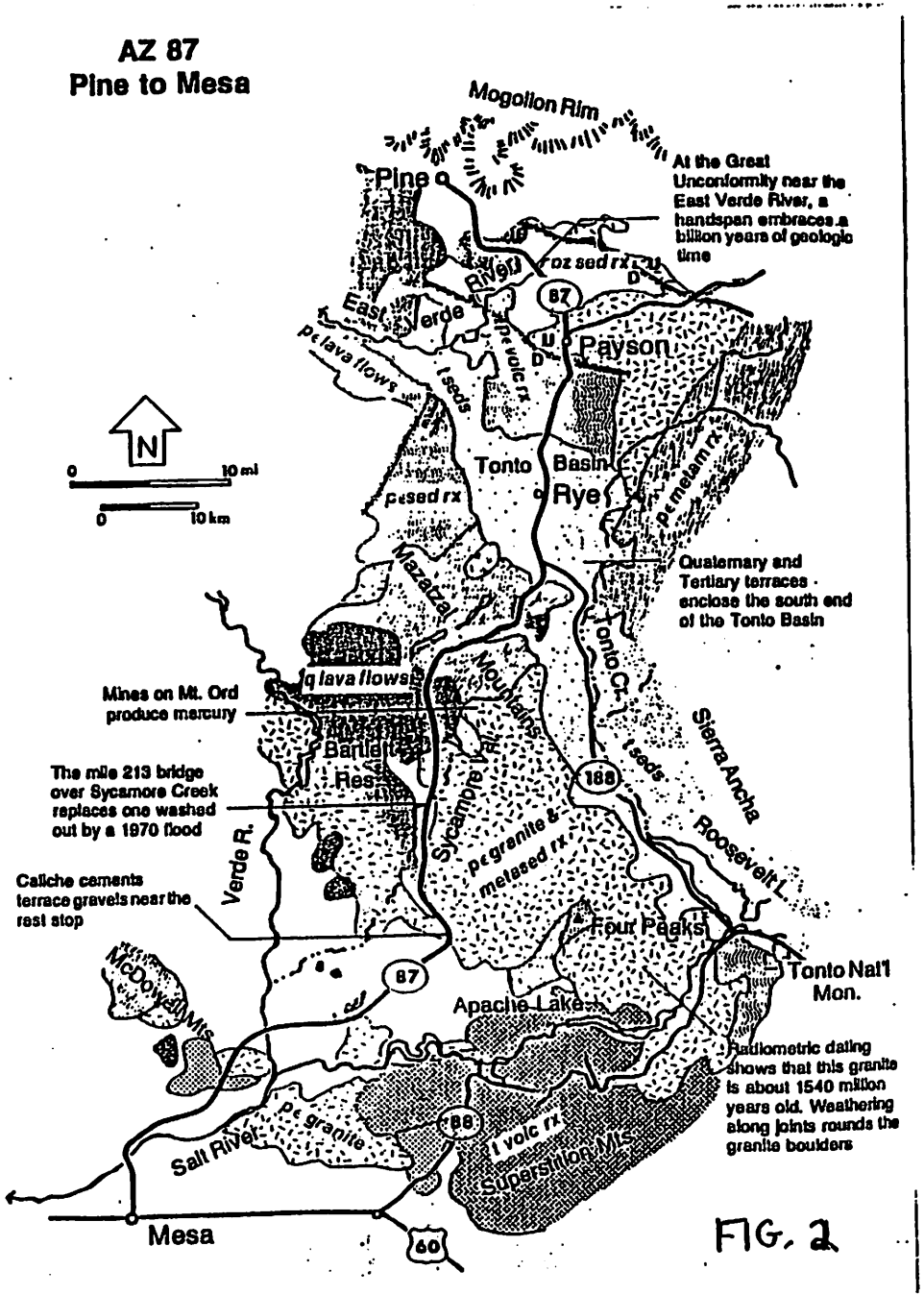

FIG. 2

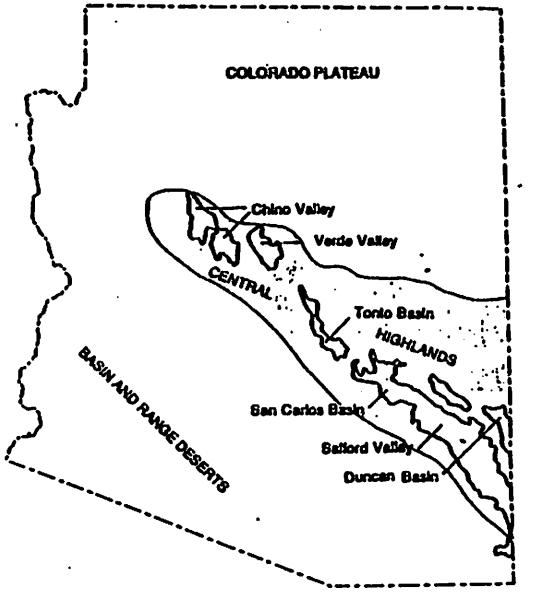

A chain of valleys divides the Central Highlands (shaded) or separates them from the Colorado Plateau to the north.

FIG 1

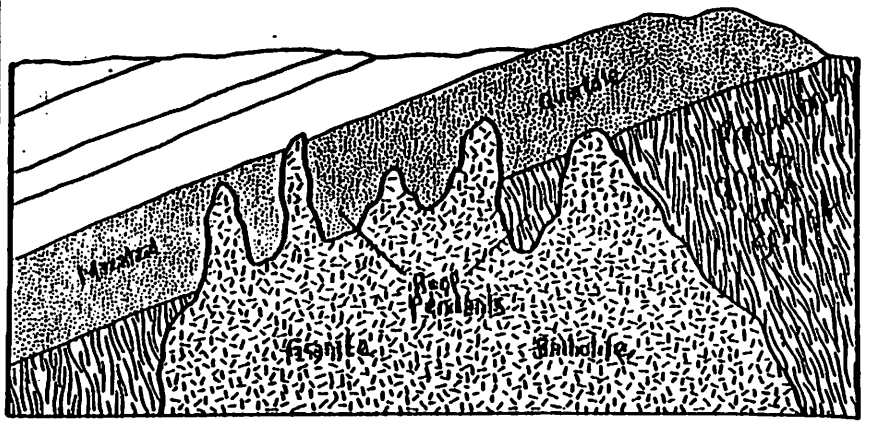

Hanging down into a molten batholith, quartzite roof pendants were preserved as the granite crystallized. Today they form the Four Peaks.

The Payson Ophiolite

with your hypabyssal hosts, Andy Rivkin and Will Grundy

References: Dann, Jesee C. (1991) "Early Proterozoic ophiolite, central Arizona" *Geology* **19** p. 590-593; Karlstrom et al. (1991) "Juxtaposition of Proterozoic Crustal Blocks" in Geologic Excursions Through the Sonoran Desert Region. Arizona and Sonora, AGS Special Paper #7; Wessels, Rick L. "Nuclear" (1990) "Re-evaluation of the Slate Creek Shear Zone: Structure of Early Proterozoic Rocks Northern Sierra Anchas, Gila County, Arizona" Masters Thesis, NAU; Wessels, Rick L. "Nuclear" and Karl E. Karlstrom (1991) "Evaluation of the Tectonic Significance of the Proterozoic Slate Creek Shear Zone in the Tonto Basin Area" in Proterozoic Geology and Ore Deposits of Arizona, AGS Digest 19, p 193-209

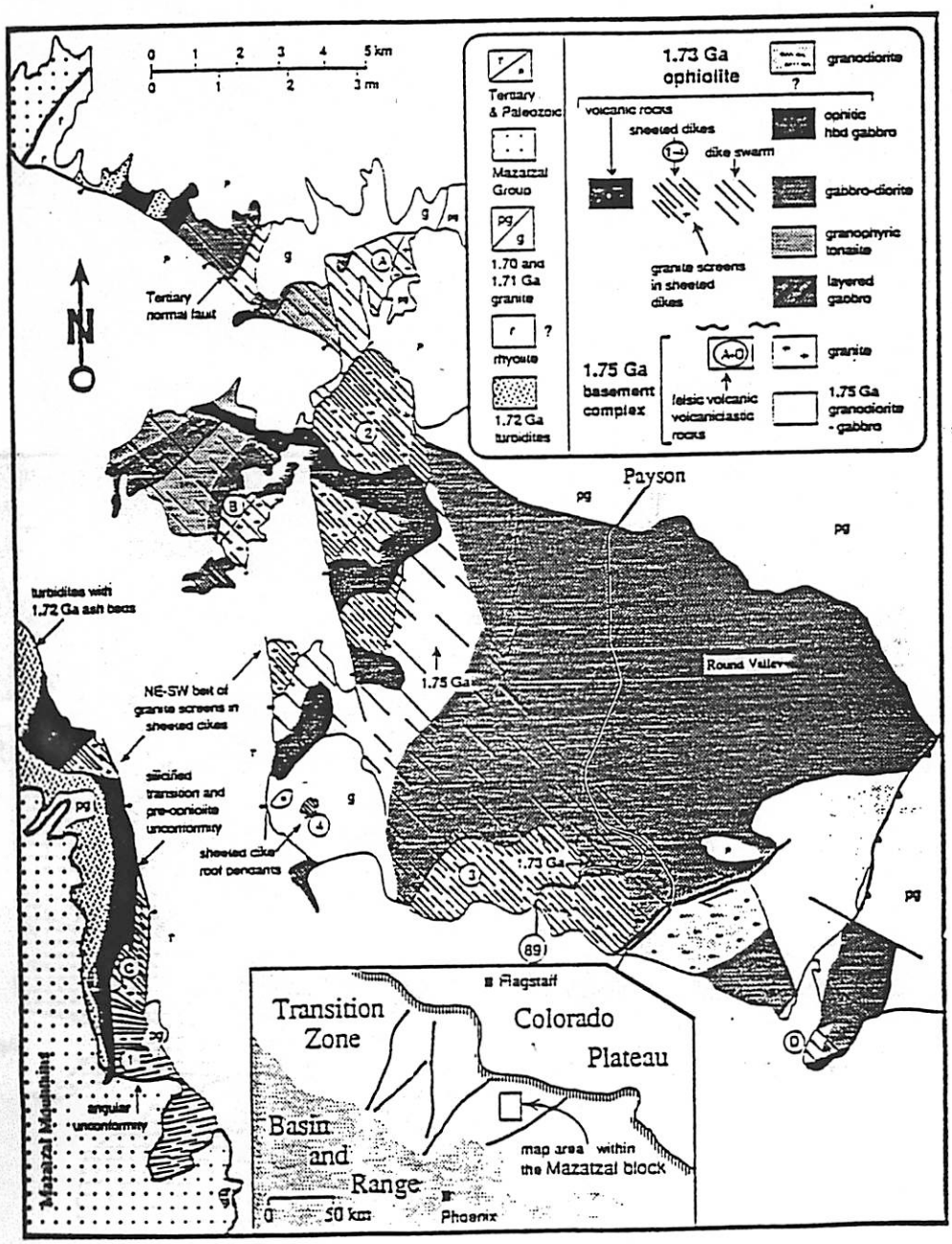

Figure 1. Geologic map of Payson ophiolite. Map area is within Mazatzal block (lower inset). Tertiary, Cambrian, and Mazatzal group contacts from Wrucke and Conway (1987).

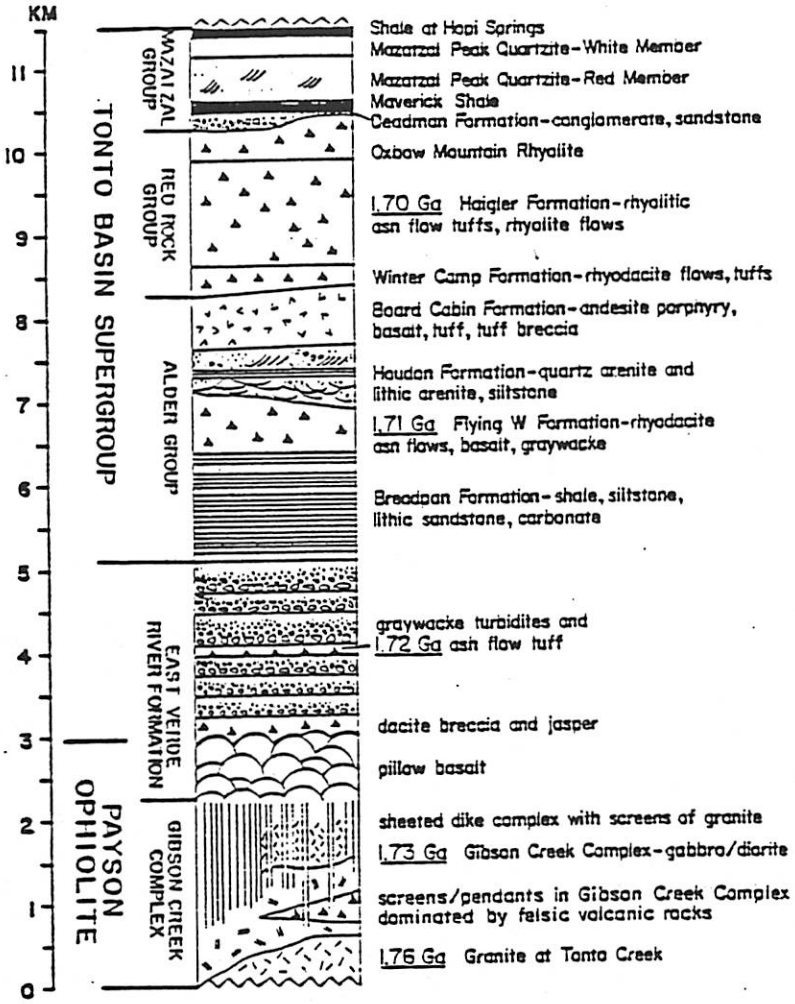

Figure 2. Summary of stratigraphic units in the Mazatzal block.

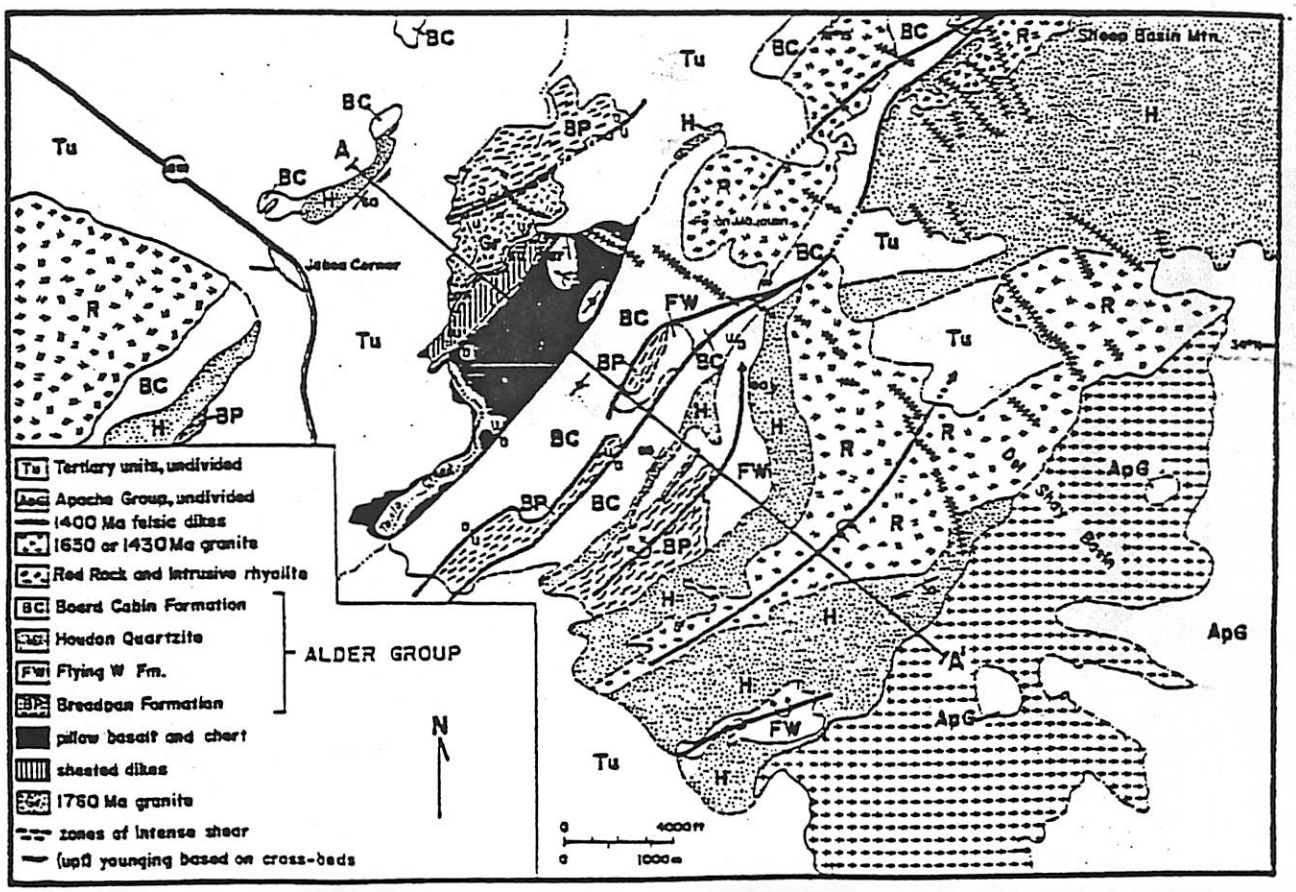

What is an ophiolite, anyway?

1820's - Alexandre Brogniart first coined the term (from the Greek *ophis*, meaning snake, and the suffix *-ite* meaning rock) to describe sepentinites and serpentinized peridotites.

1906-1927 - Gustav Steinmann emphasized the connection between some sepentinized rocks, certain mafic igneous rocks, and radiolarite (a deep sea sediment composed of the silicious remains of planktonic radiolaria). The use of the term *ophiolite* came to refer to associations of these 3 rock types, also known as the Steinmann Trinity. They were thought to form in geosynclines.

mid 1960's - With the advent of the theory of global plate-tectonics, Nikolas Christensen, Matthew Salisbury, and others showed that ophiolites are samples of oceanic crust, produced at mid-ocean ridge spreading centers. This is the current meaning of the term.

Map showing global distribution of ophiolites (ages < 1.2 Ga).

Oceanic rock profile, mantle to sea floor:

below 70km - lherzolite, mantle rocks, metamorphosed by solid state mantle convection.
- harzburgite, mantle rocks Ca and Al depleted by removal of basaltic melt, metamorphosed.

5-8 km deep - Mohorovičić seismic discontinuity ("Moho").
~1 km thick - layered gabbros - solidified, vertically zoned magma chambers.
~2 km thick - tholeitic basalt and diabase sheeted dikes.
~1 km thick - basalt pillow lavas and sheet flows.
<1 km thick - ocean floor sediments, including radiolarite, red clay, and ribbon chert.

Cartoon showing formation of oceanic crust at a spreading center.

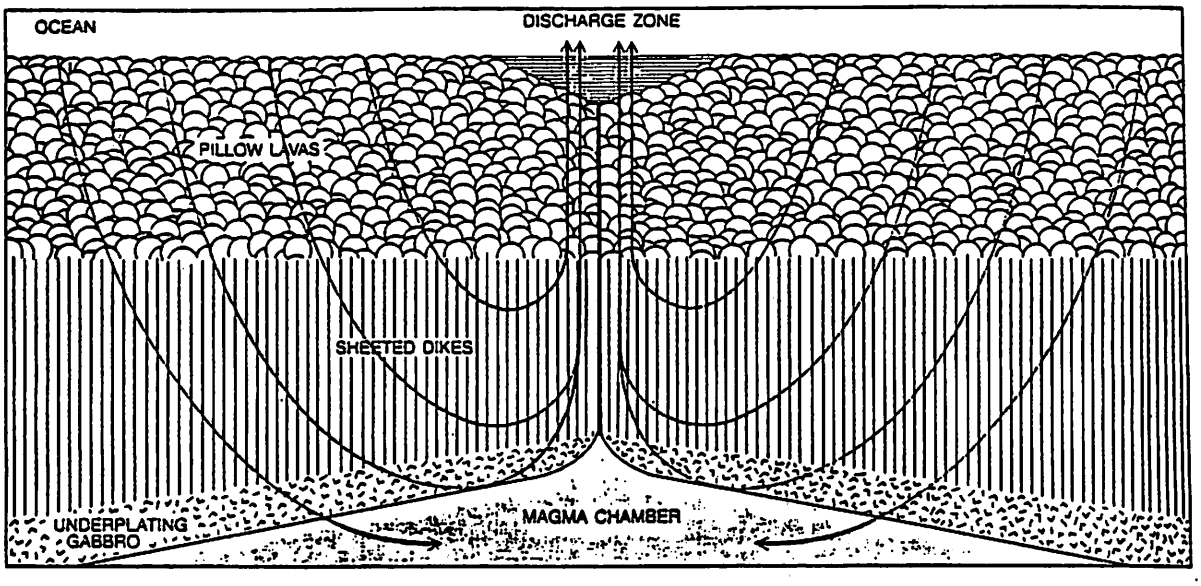

Hydrothermal circulation around a spreading center leads to considerable alteration, serpentinization of the basaltic rocks and precipitation of metals and sulfides at "black smokers". Consequently ophiolites can have economic value as a source of ores.

Ophiolite structure tends to be more messy, due to damage sustained as a result of being hoisted above sea level, in order to be exposed for human inspection.

Fall 93'- Plty. Geologic Field Trip
Superstition Mountains

Cenozoic Sequence
Tonto Basin, AZ

Guides; R. Casavant, K. Yanow

STRATIGRAPHY

TONTO BASIN

- Basin fill sediments
  - sandstones, siltstones, claystones, conglomerates, marls, limestones, gypsum, diatomite, caliche, misc. volcanic ash/ basalts
  - deposited in rivers, lakes, alluvial fans, talus
  - thickness estimated; ~ 1000 ft. exposed by erosion, 2000 ft. exploratory wells, thus est. 4000 ft.
  - age not precise--fossils rare; camel, dog, horse = M-Pliocene
  - deposition . 18.6 Ma

- Associated with Basin & Range extension
  - *Pre-extension* = Whitetail Conglomerate(SE part of basin w/ interbedded basalts), 23.6-32 Ma; and Apache Leap Tuff(ash, dacite clasts from Mazatzal Mtns.), 19-20 Ma: Mio-Pliocene
  - *Syn-extension* = Gila Conglomerate
  - *Post-extension* = Tonto Basin Fm (mudstones, conglomerates)

- Tonto Basin Fm
  - mudstone - massive bedded, red-brown, silty, gypsiferous, , 280m, grades into ss & congl. along basin margins; minor bedded carbonates, gypsum occur in mudstone in northern part of basin near Punkin Center
  - conglomerates/ss - especially in northern part of basin; along flanks of asymmetrical basin w/ NW-SE trending western axis, large-scale x-bedding, clast imbrication, good sorting = braided stream w/ sustained flow; arkosic from K-feld in granites
  - sediments and facies changes = internally-drained basin

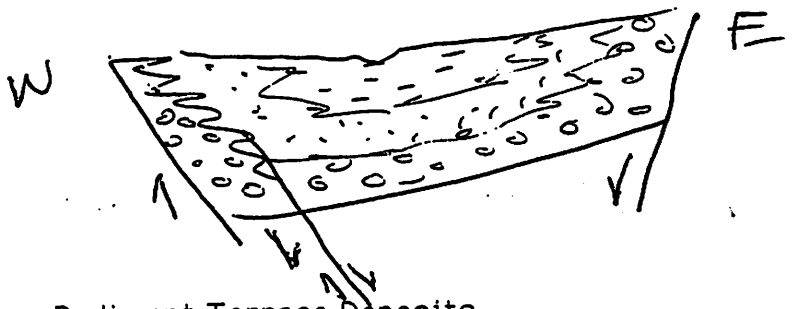

- Pediment Terrace Deposits

  - deposited as pediment benches on erosional surfaces that truncate fault and fold structures in softer Tertiary basin fill sediments
  - downcutting by main stream and tributaries leaving old floodplains elevated
  - not necessarily related to present drainage
  - very extensive, flat fan-like(?) features from mtn. fronts to Tonto Creek
  - 7 to 0.5 degree dips from mtns. towards creek
  - 5-10 widespread pediment terraces in Tonto Basin
  - 2-3 m thick, some very thin;
  - clast lithology influenced strongly by local rock types(1-2 lithos dominate); cobbles, boulders in ss. matrix

- River Terrace Deposits

  - erosional benches related to present drainage
  - slope about same dip as stream(down-valley)
  - lower terraces on Salt River now under the lake
  - 3-10 m thick
  - well-rounded cobbles, boulders, ss matrix
  - 7-11 terrace deposits mapped parallel to Tonto Creek/Salt River

- Alluvial Fan Deposits

  - fan morphology
  - variable thicknesses 1-20 m
  - traced to present-day drainage
  - like the ped. terraces they slope to basin, but have steeper gradients
  - 9 alluvial fans in Tonto Basin

- Ages/Downcutting rates
  - Terraces dated and downcutting rates determined from intruded basalts; terraces = Pliocene(?) to Quaternary alluvium
  - Pediment terraces = pre-Quaternary age; oldest ped. terrace = 3.6 Ma
  - 3.6 Ma to 1.0 Ma = 20 m / Ma
    1.0 Ma to present = 71 m / Ma

- Terrace development
  - models for periodic regional uplift, and/or climatic changes = changes in discharge, slope stability

  - currently, climatic model favored - changes tied to separate erosional/ more humid climatic processes associated w/ Pleistocene glaciation;

  - Ped. terraces function of discharge rates(water availability)
    - interglacial periods (interpluvial) = pediment terraces
    - glacial periods (pluvial) = river terraces

SAFFORD BASIN
- 300 km long, Globe,AZ to Mexico
- San Carlo, Bylas, & 111 Ranch subbasins; asymmetrical
- 2590 m fluvial and lacustrine basin fill seds.- deeper axis than Tonto
- gypsiferous mudstones, gypsum, halite, scarce chert and dolomite = lake(lacustrine) deposits; Lake Grahm; low Si NA-SO4-CL evaporites(Hardie and others, 1978)
- greenish-grey, pale brown, calcareous, poorly-mod. cemented, lam. claystones, ss. partings(mica, qtz, felds, abund. heavy minerals)
- deep water, below wave-base; thickest on SW side(basin axis)

<u>STRUCTURE</u>

TONTO BASIN
- One of several en echelon(?) asymmetric graben basins within Transition Zone
  - Transition Zone separates Colorado Plateau from Basin and Range Province

- slightly accurate; 609 km long, 10-15 km wide; bounded by normal faulted PreCambrian igneous rocks
  - Sierra Ancha Mts (east)--Armer Mtn. fault at base
  - Mazatzal Mtn (west)--fault west of Punkin Center
  - Two-Bar Ridge (south) - Tert. volcanics in Salt River Mtns.
  - ridge of PreC. rocks (north)

- Faulting
  - episodic faulting has occurred through Cenozoic, although very little evidence preserved
  - great cumulative displacement of alluvial geomorphological surfaces with age (terraces thicknesses-frequency; juxtaposed sed. deposits and soil development, triangular facets, alluvial fans)
  - little movement through Quaternary(?); very scarce historical seismicity
  - most high-angle, normal faults postdate TB Fm. mudstone facies; However, some faults truncated by erosion and overlain by fine-grn. basin-fill sediments show some of the smaller faults had ceased
  - throws 900 feet common

REFERENCES

Piety, L. and Anderson, L. W., Distribution, Characteristics, and Estimated Ages of Quaternary(?) Deposits in the Tonto Basin, Central Arizona: in the Field Trip GuideBook to the Tonto Basin, Friends of the Pleistocene, Rocky Mtn. Cell, 1988.

Royse et al., Geologic Guidebook #4--Hwys. of Arizona-87,88,188: in Ariz. Bur. of Mines Bull. 184, 1971.

Houser, B., Anderson, L.W., et al., Late Cenozoic Stratigraphy and Tectonics of the Safford, Tonto, and Payson Basins, Southeastern and Central Arizona: in Geologic Excursions Through the Sonoran Desert Region, Arizona and Sonora, Gehrels, G. and Spencer, J., eds., Ariz. Geol. Surv. Special Paper 7, 1990.

U.S.G.S.
MESA QUAD TOPO.
1978

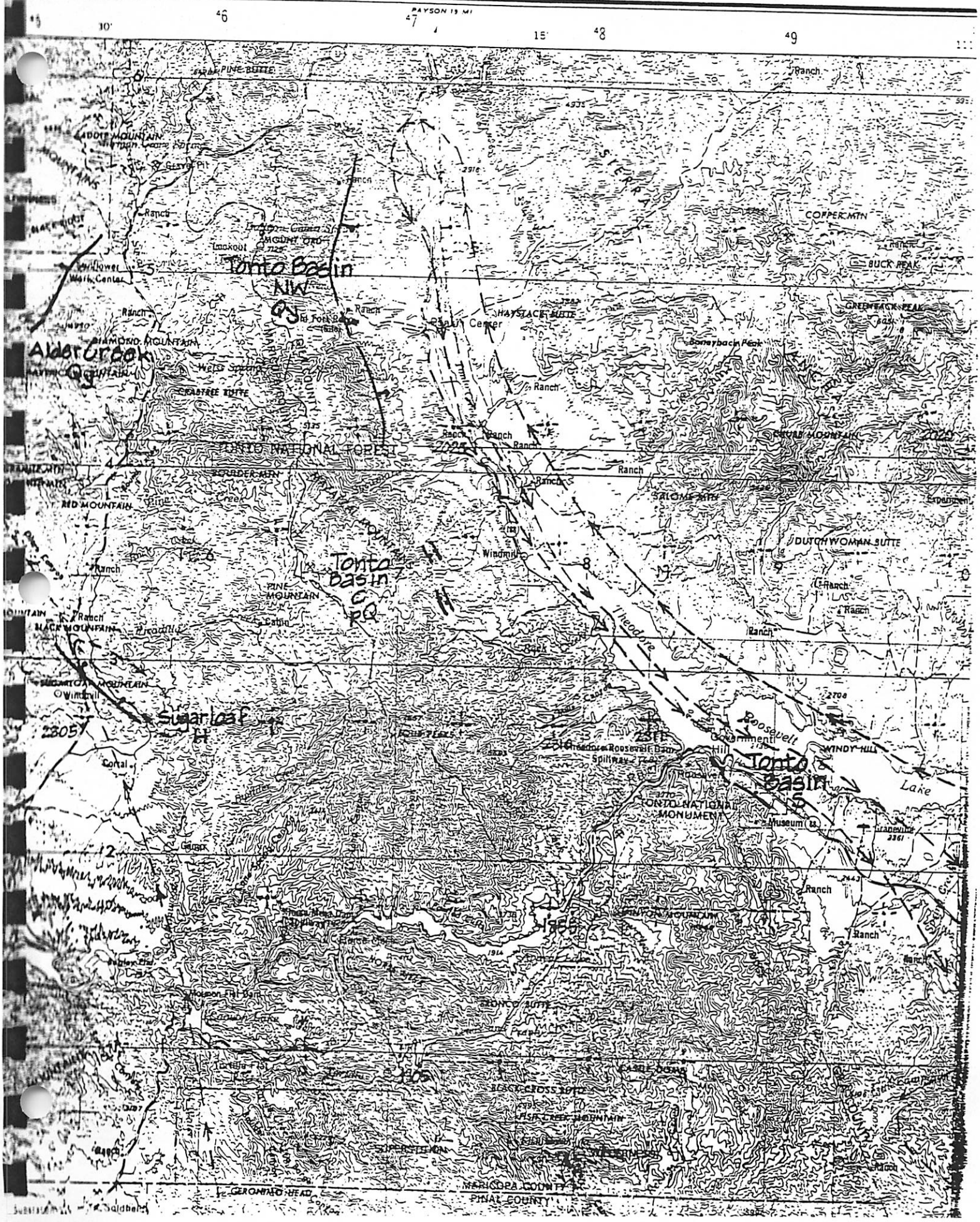

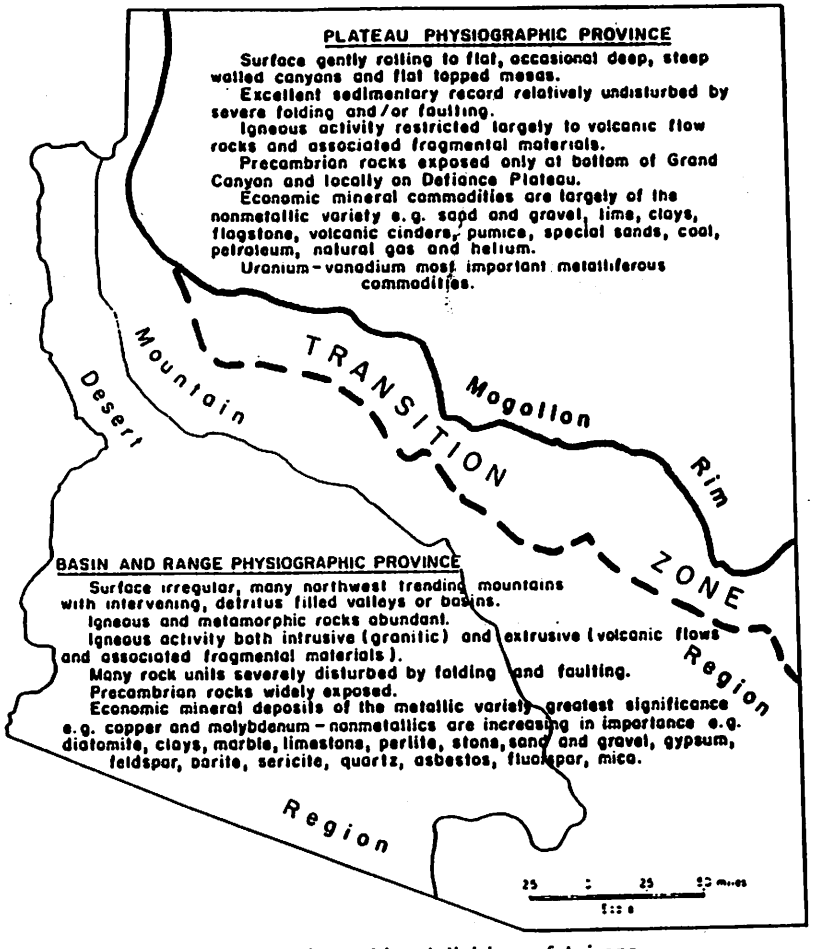

Figure 2. Physiographic subdivisions of Arizona.

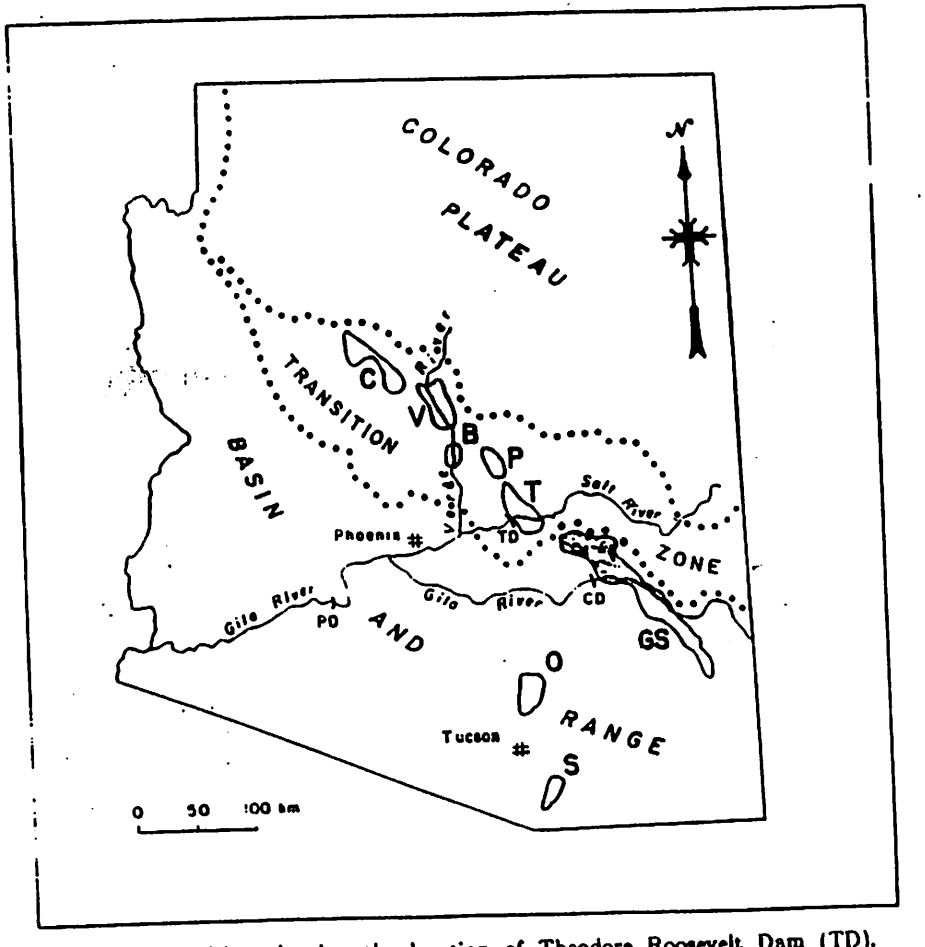

Figure 1. Map showing the location of Theodore Roosevelt Dam (TD), Coolidge Dam (CD), and Painted Rock Dam (PD) with repsect to major late Cenozoic basins within and adjacent to the Transition Zone. The basins are B. Bloody; C. Chino; GS. Gila-Safford; O. Canada del Oro; P. Payson; S. Sonoita Creek; T. Tonto; V. Verde.

Royce et al., 1971

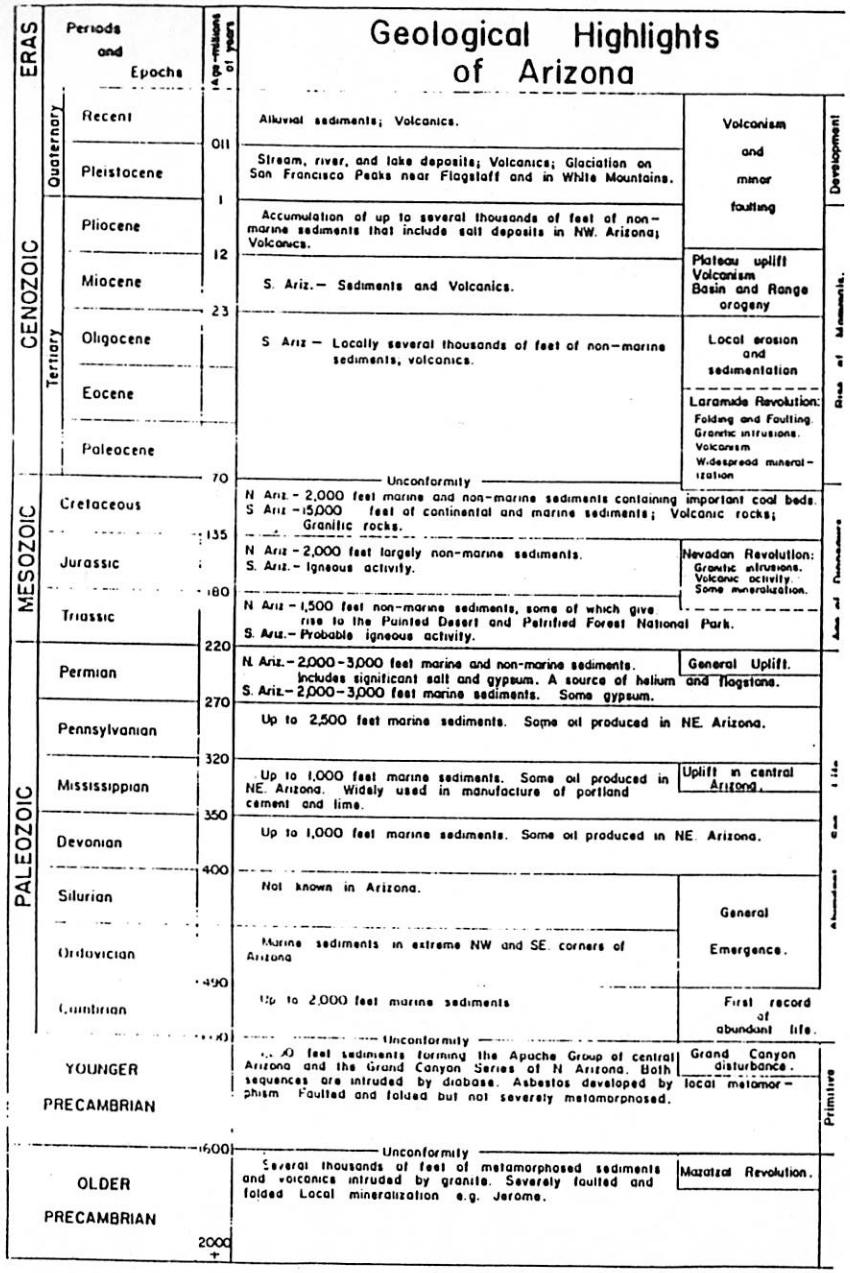

Figure 4. Geologic time scale.

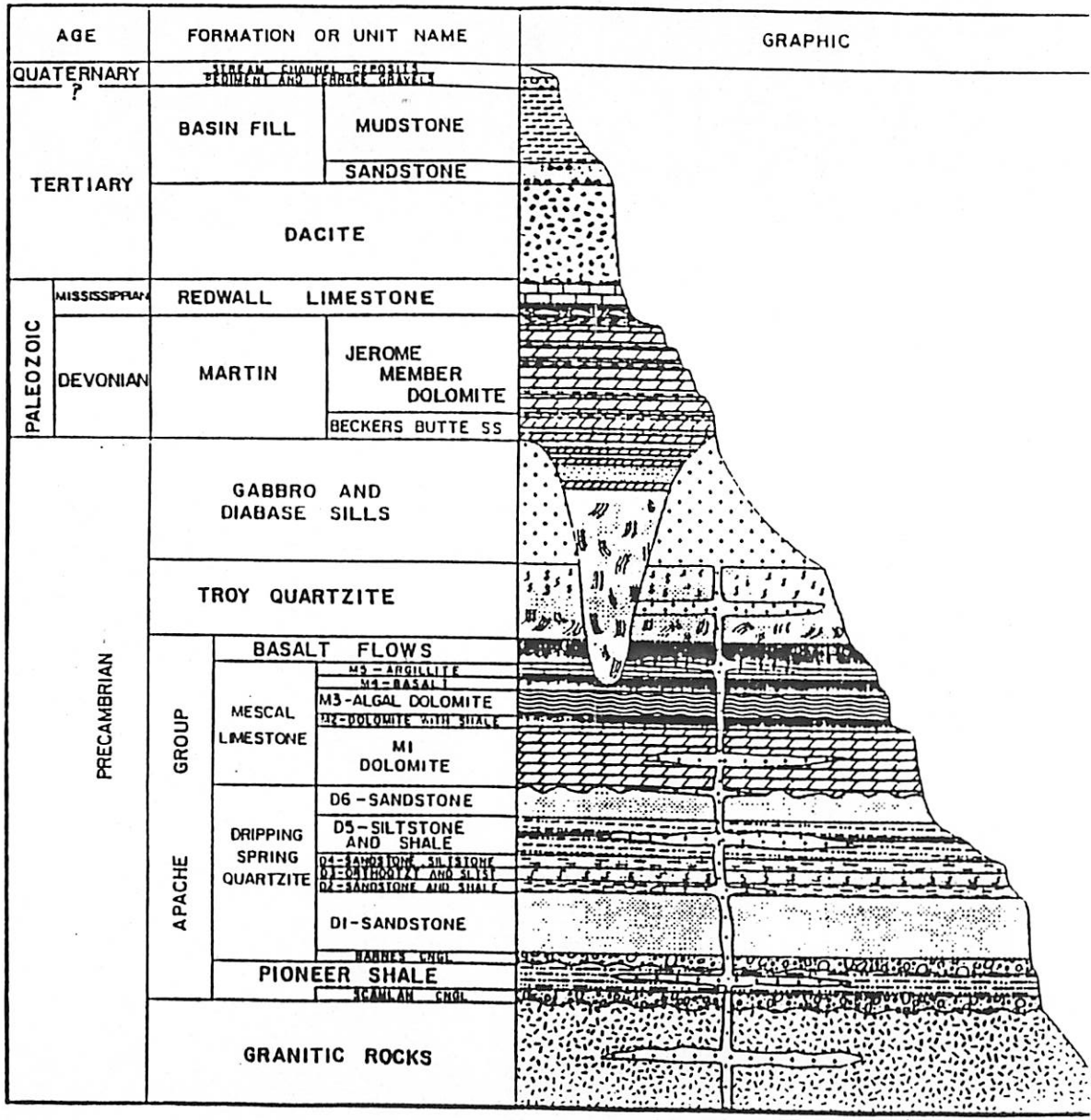

Picty + Anderson, 1988

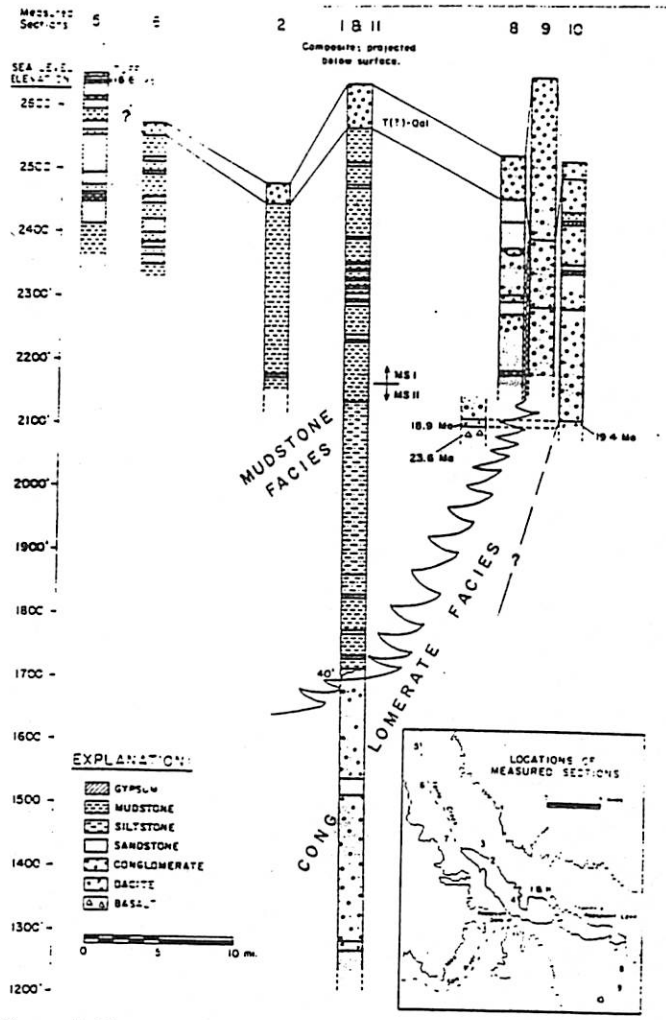

Figure 8: Cross-section and facies of Tonto Basin formation, with K-Ar dates. (modified from Nations, 1988).

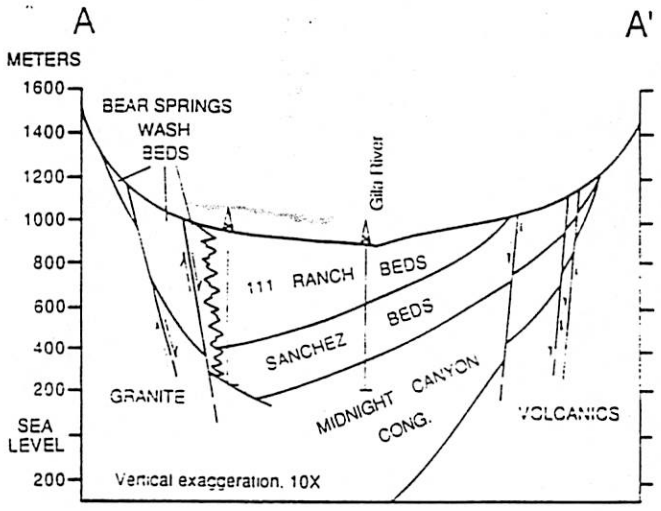

Figure 3: Schematic cross section of 111 Ranch subbasin showing facies relationships of basin-fill units. Approximate line of section shown on Figure 2.

Houser, B. et al., 1990

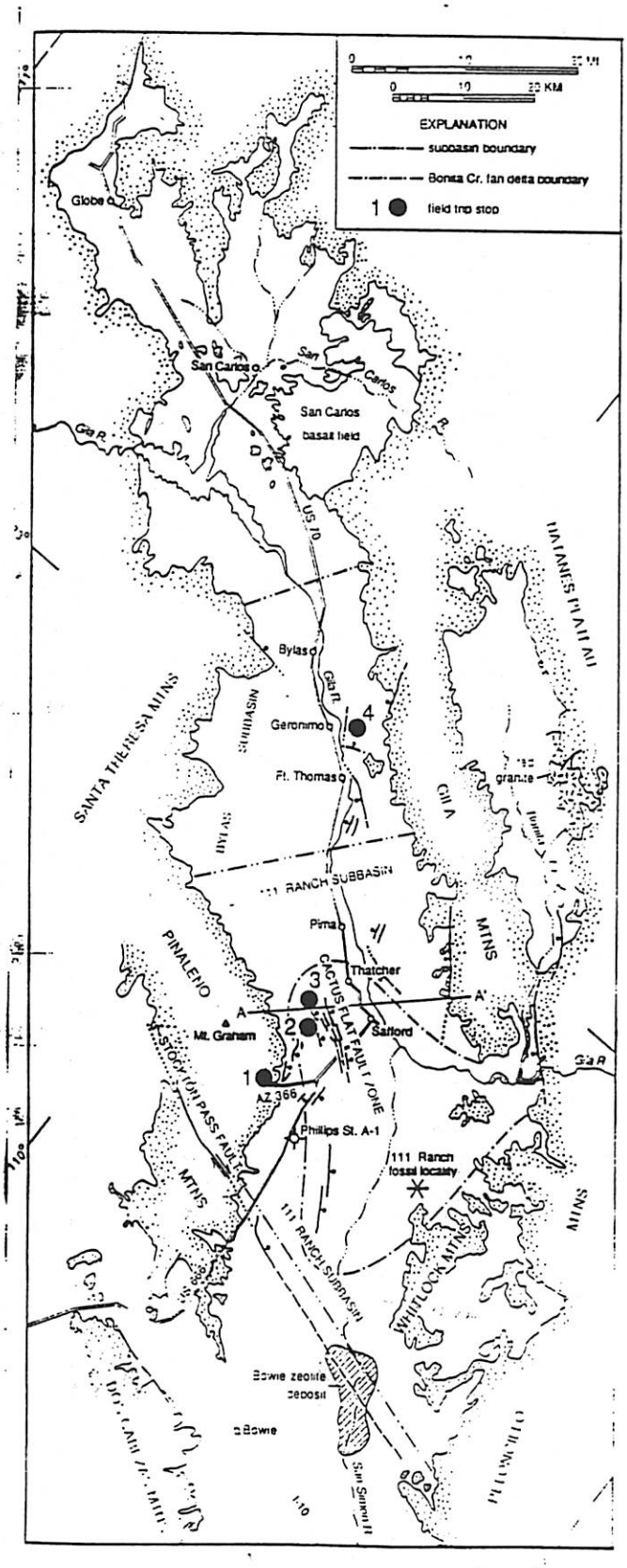

Figure 2: Map of Safford basin showing location of stops, and geologic and geographic features

Houser, B. et al 1990

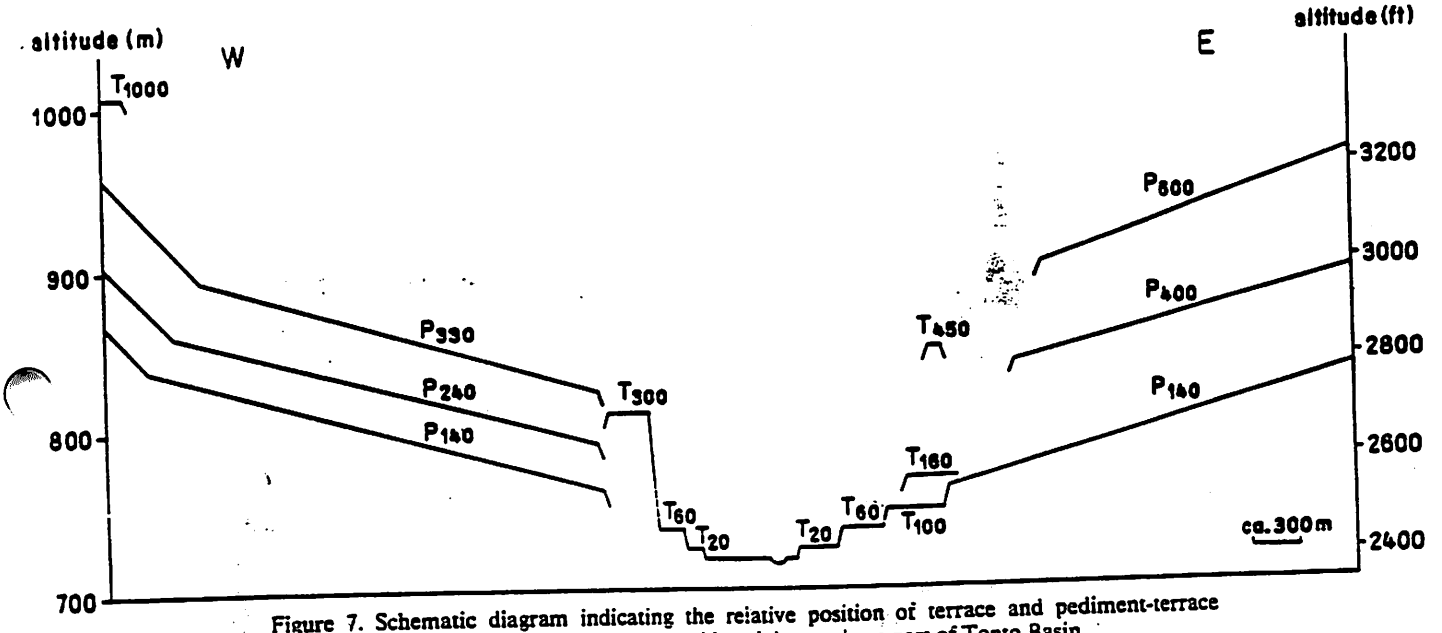

Figure 7. Schematic diagram indicating the relative position of terrace and pediment-terrace surfaces on the east and west sides of the northern part of Tonto Basin (after Barsch and Royse, 1971).

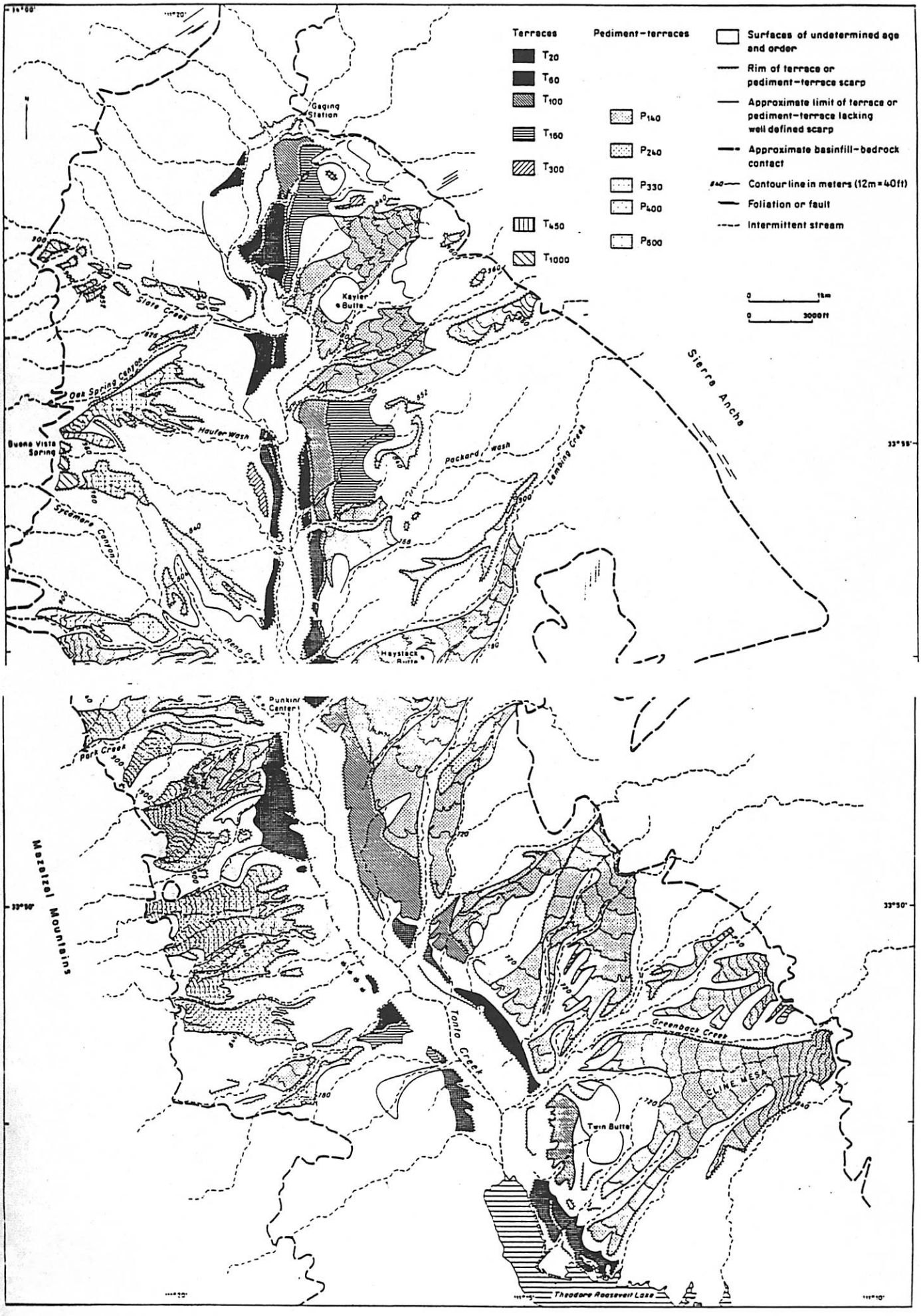

Figure 6. Map indicating the distribution of terraces and pediment-terraces in the northern part of the Tonto Basin (from Barsch and Royse, 1971).

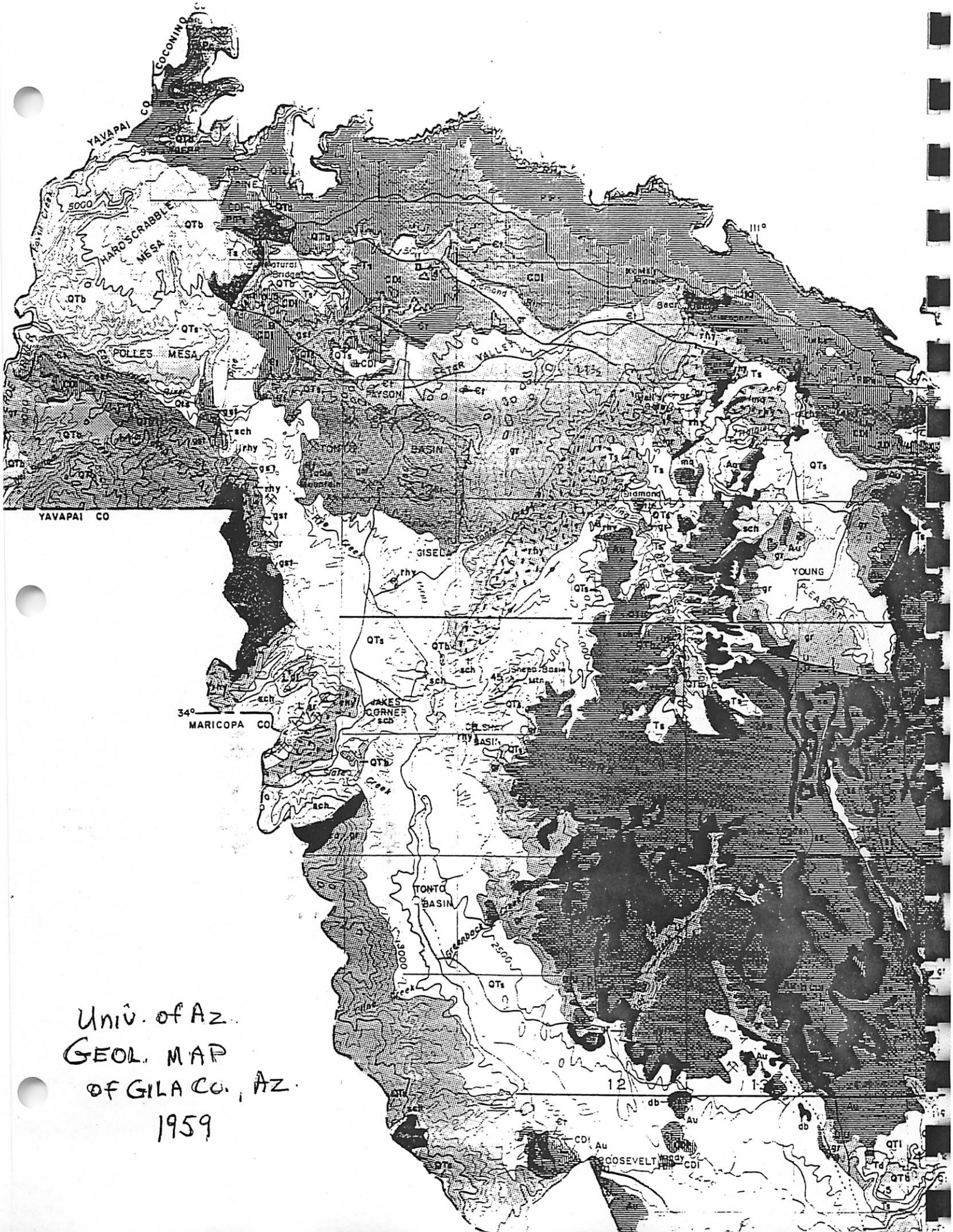

Univ. of Az.
GEOL. MAP
of GILA Co., Az.
1959

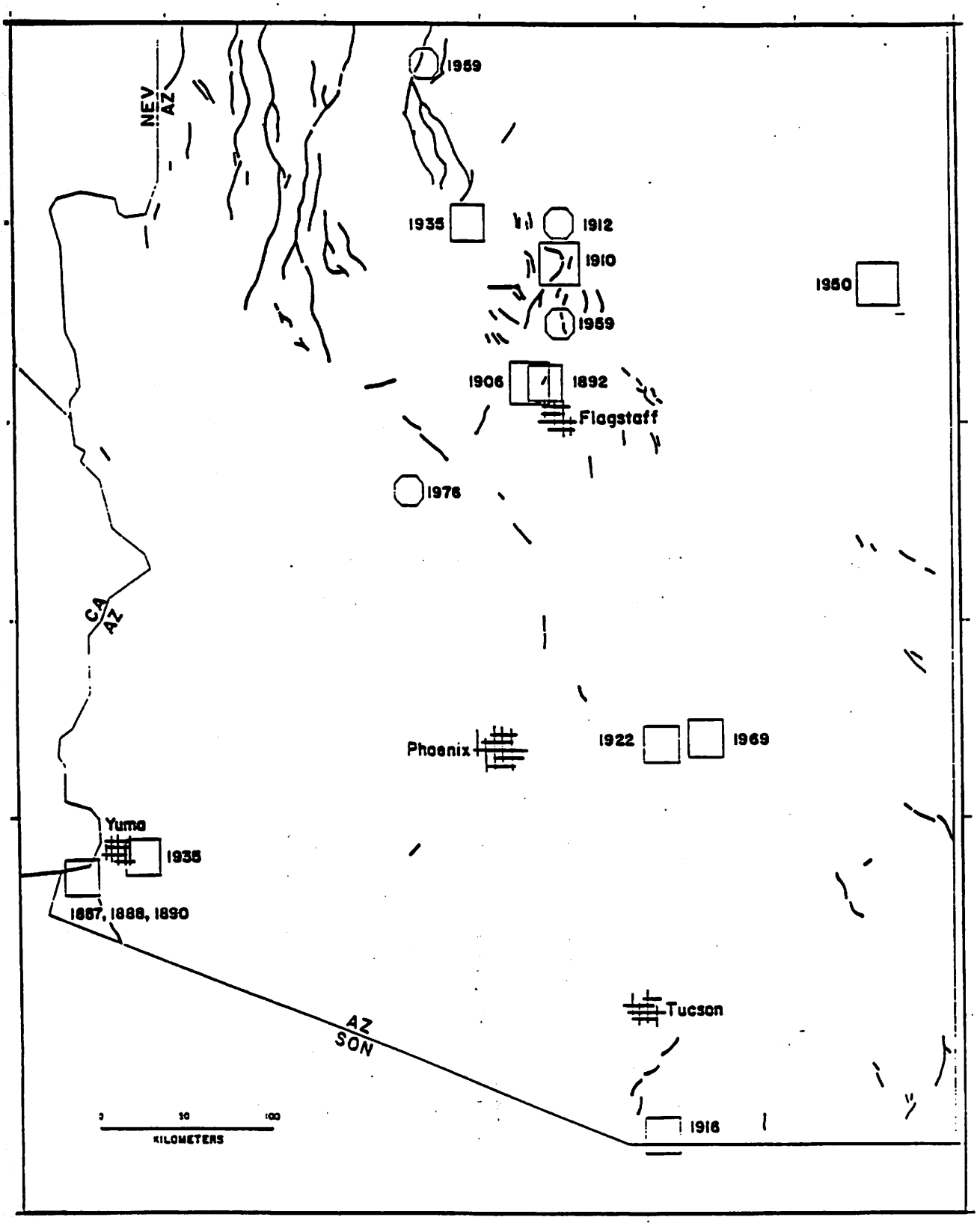

Figure 2. Arizona seismicity, magnitude 5 or Modified Mercalli Intensity VI and larger. Data sources are DuBois and others (1982) and Stover and others (1986). Known and suspected Quaternary faults modified from Pearthree and others (1983).

Piety + Anderson, 1988

Fall 93'- Plty. Geologic Field Trip
Superstition Mountains

PreCambrian Sequence
Tonto Basin, AZ

Guides; R. Casavant, K. Yanow

STRATIGRAPHY

- Folded sedimentary and volcanic strata of Alder, Haigler, Mazatzal Groups

- lower stratigraphy =volcanic rich = eugeosyclinal
  middle stratigraphy = sedimentary = miogeosyclinal
  2 km thick rhyolite
  1 km thick quartzite

- NE-SW belts flanked on NW and SE by large granitic plutons = Payson and Young Granites.
  Young Granite(SE) intruded into Alder Group
  Payson Granite(NW) gradational through granophyre/intrusive rhyolite into contemporaneous extrusive rhyolite
  granites thought to be from same widespread batholith!

- 1165-1715 + 15ma (U-Pb zircon dating)

- sills widespread in U. Payson Granite; all mafic porphories ~ single intrusive event

- Intrusive contact between Payson Granite and overlying stratigraphic rocks favored over basement thrust contact model

- Payson Granite and Gibson Complex part of a great silica alkali magmatic event in Tonto Basin; between age of Haigler Rhyolite and felsic hypabyssal sills
  * regional implication is that latest plutonism in northern province overlapped earliest volcanism in southern province

- Haigler rhyolite, rhyolite, granophyre, & alaskite sills are all silicic alkali rocks of distinct but similar chem. compositions. Some hydrothermal alteration

- Enormous volumes of silicic rocks; almost no intermediate rocks; argument against origin by differentiation and suggest magmas formed by partial melting

- Magmas extruded as ash-flow tuffs, coarse sill rocks(ash-flow tuff caldera complex; similar in chem. composition to Yellowstone rhyolite plateau, WO

STRUCTURE

- All PC units folded and faulted--primary textures in ig./volc. rocks unmodified

- Tectonic history = 1) large scale folding; NE-SW axis w/ shallow plunges, 2) thrusting/reverse faulting towards NW under same NW-SE compression, 3) disruption NE-SW to N-S faults by left-lateral strike-slip(east downthrown)

  Suggests Tonto Basin was site of foreland folding, thrusting as southern basin crustal block moved NW upon older proto-craton. Stresses gave rise to left-lateral couple w/ strike-slip developing along/near the Transition Zone(2-boundary province = Colo. Plateau/ Mogollan Rim (north) and Basin and Range(south); Basin and Range divided into mtns. and desert

REFERENCES

Conway, C. M., Petrology, Structure and Evolution of PreCambrian Volcanics and Plutonic Complex, Tonto Basin, Gila Co., Arizona, CAL Tech. PH. D. Thesis, 1976

TABLE 2
GENERALIZED PRECAMBRIAN STRATIGRAPHY
UPPER TONTO BASIN, GILA COUNTY, ARIZONA

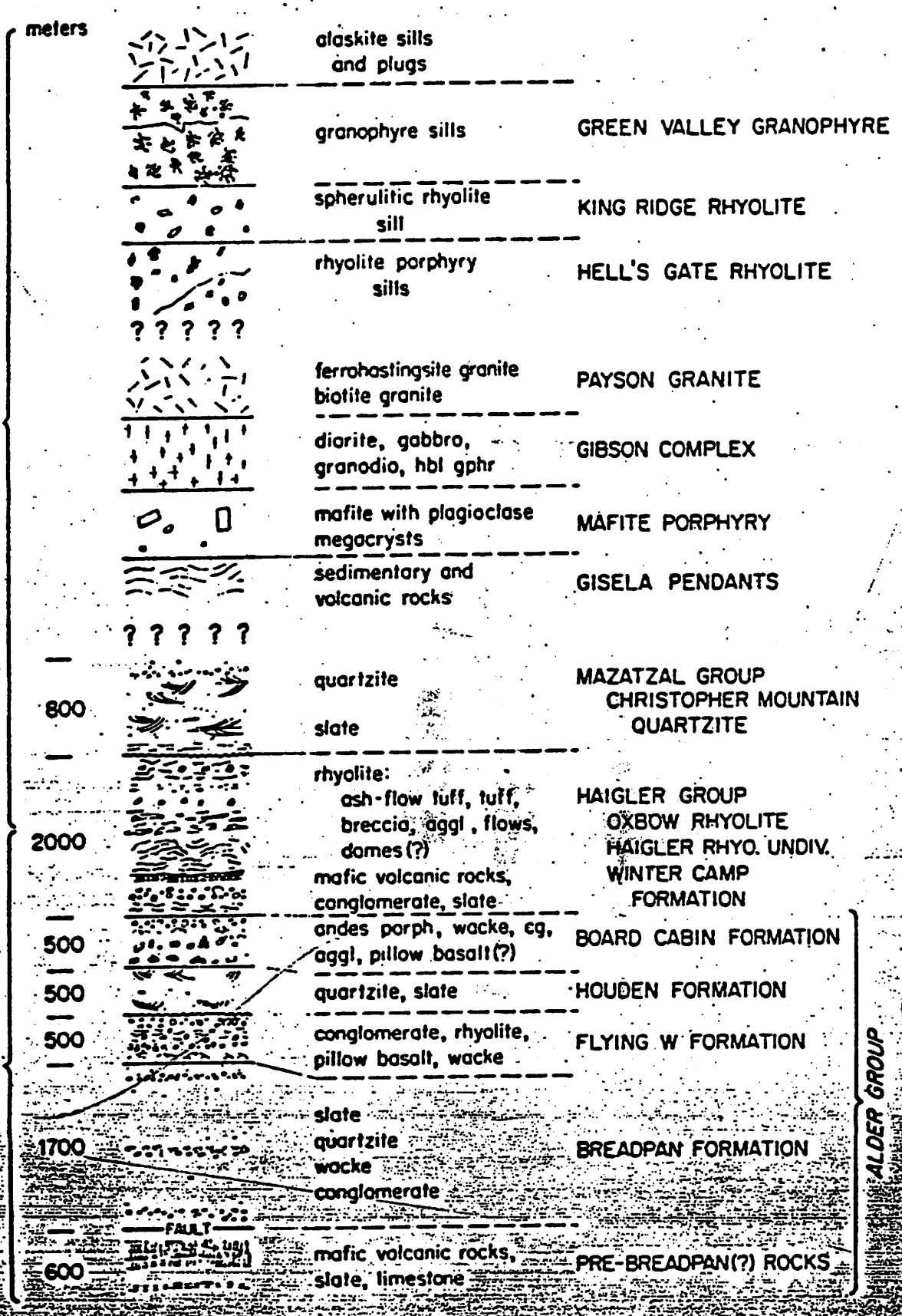

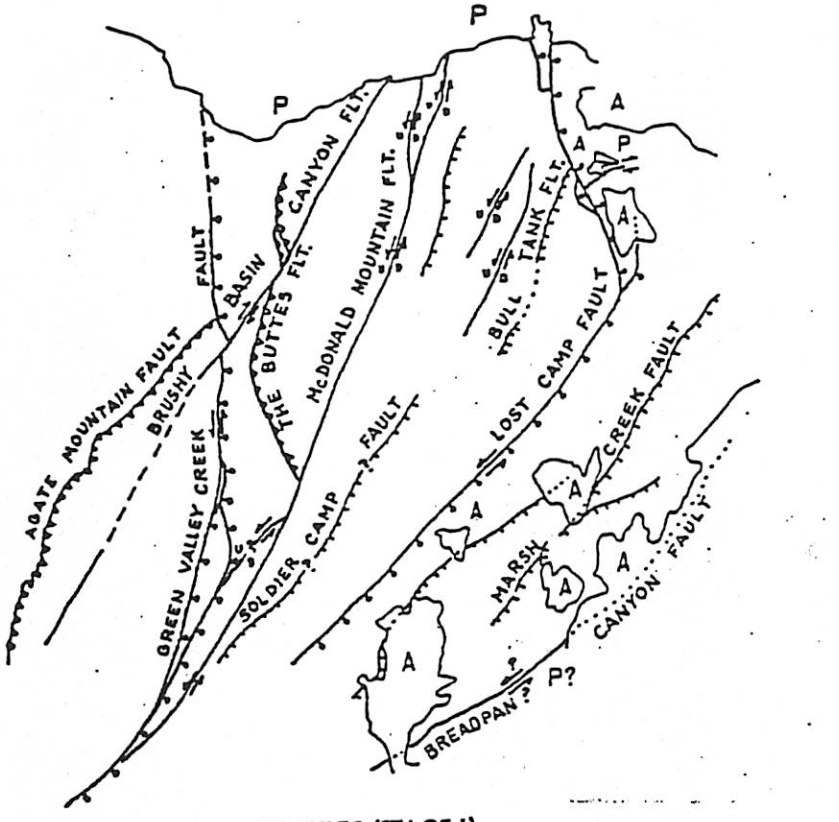

Figure 7. Major Precambrian faults in Tonto Basin.

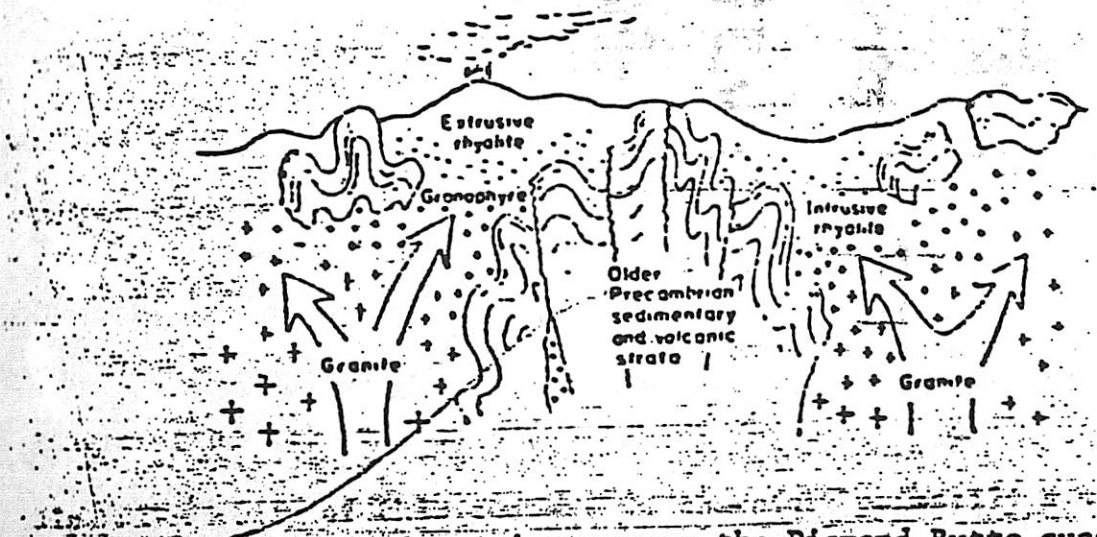

Figure 5. Hypothetical section across the Diamond Butte quadrangle at the time of granitic intrusion (from Gastil, 1958, Fig. 5). Relation as visualized by Gastil between older stratified rocks and major igneous masses conveying his hypothesis of gradation from granite through granophyre into intrusive and extrusive rhyolite.

Some Things to Think About

As you view the Tonto Basin and its surrounding terrace's, picture the sky as pink rather than blue (or pinkish overcast rather than gray overcast). You're now on the surface of Mars. As you can see, nothing has changed all too much. Next, transform the background sky from the pinkish atmosphere of Mars to the blackness of space. Welcome to the Moon. Again, as you are my witness, nothing has changed all too much.

The basin we are looking at is an artifact of tectonic activity resulting from, most likely, either a strike-slip or a graben fault. If we look to Mars and the Moon (as we've just done) we'll be certain to find similar structures. The Tharis plateau region on Mars, for example, reveals comparable characteristic tectonic activity which presumably lead to the formation of the Tonto Basin.

The terraces and pediment-terraces that you see are perhaps either products of climatic change or increased tectonic activity. The pediment-terraces are alluvial fan-like surfaces across which sediment was transported from the mountain fronts to the axis basin, eventually to be removed by the Tonto Creek. Similarly on Mars, the Argyre Basin, a channel which cuts through the surrounding mountains, has probably transported sediment onto the Argyre Planitia leaving similar alluvial structures. Mars has most likely endured several bouts of climatic surface variations over its lifetime. Glacier movement (a possible explanation for the terrace structure) on Mars would not be too different from glacier movement on the Earth--conceivably, transporting sediment and altering the surface features on both planets in similar fashions.

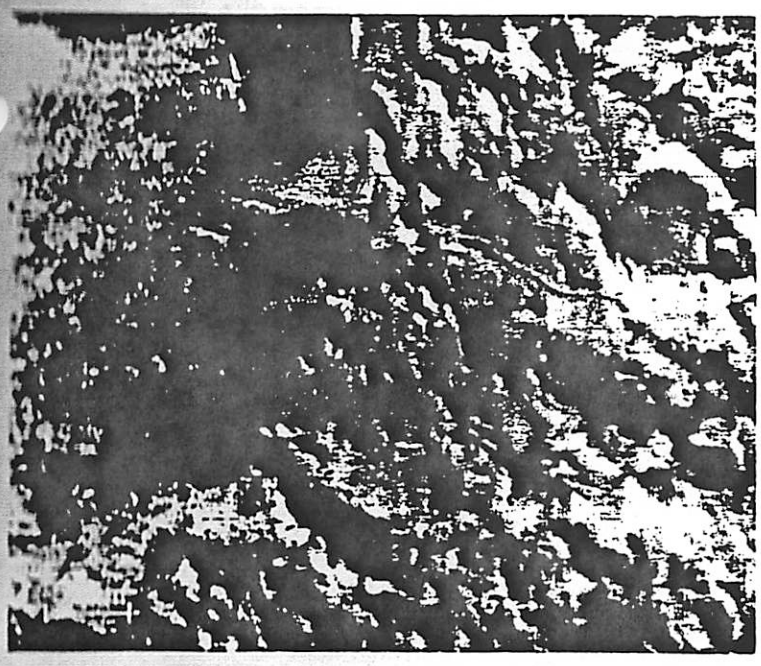

Figure 8.35. The edge of the Argyre basin. A channel cuts through the surrounding mountains. Bright and dark patches on Argyre Planitia (arrows) may be caused by sediment carried down the channel and deposited on the flat plains. (DAS No. 06497928, rev. 137, A camera, center at 48°W, 56°S.)

Figure 8.36. Stubby channels, in the fretted terrain. Parts of the channels appear to form by coalescence of circular depressions. The bright "alluvial fans" which occur where channels debouch on the plains are an artifact of picture enhancement. (DAS No. 09378189, rev. 217, B camera, center at 344°W, 37°S.)

Figure 8.37. Oblique view to the northwest, across the cratered plains of Lunae Planum. Compare with figure 8.38. (DAS No. 08873804, rev. 203, A camera, center at 72°W, 19°N.)

Figure 8.38. Headward tributaries of Kasei Vallis. Channels are formed by erosional enlargement of several sets of intersecting fractures. The large crater is surrounded by a ring of ejecta which has resisted erosion. Position of photomosaic is shown on figure 8.39. (DAS No. 13313735, rev. 667, B camera, center at 75°W, 18°N; DAS No. 13313805, rev. 667, B camera, center at 73°W, 22°N.)

1973b; Carr, 1974b) that Mars is at an evolutionary stage where regional doming has occurred and horizontal plate movement is just beginning. Based on crater densities of affected surfaces, Carr (1974b) estimates that the doming occurred at least 1 b.y. ago.

The cratered plains to the east of the Tharsis Plateau of Mars contain linear ridges reminiscent of those on the lunar maria (fig. 3.13). Such features on the moon are widely believed to be structural in origin (e.g., Baldwin, 1963; Bryan, 1973) resulting from isostatic settling of the lunar maria and consequent crustal shortening. The distribution of the ridges on Mars, concentric to the Tharsis Plateau, is also consistent with this structural interpretation. Thus we see two types of structures on the plateau. The earlier graben formed during uplift and the ridges formed on older volcanic plains surfaces during the later period of relaxation of the Tharsis uplift. However, as on the moon, one may also argue for a volcanic origin for these features. At one place where a ridge intersects the canyon wall, there is evidence that the ridge is not solely a surface feature (fig. 5.48). The ridge appears to be the trace of a subsurface planar body resistant to the erosion that has resulted in scarp recession along the canyon. This feature is most easily explained as an igneous dike.

In the region to the south and west of the Tharsis Plateau are a number of irregular scarps approximately perpendicular to the trends of the radiating graben (fig. 6.31). Those scarps generally face the

Figure 6.31. Irregular en echelon ridges of possible compressional origin, indicated by arrows. Graben transect some of the ridges. Youngest geologic units are plains materials that partly cover graben. (DAS No. 06894548, rev. 148, A camera, center at 147°W, 21°S; DAS No. 06894618, rev. 148, A camera, center at 145°W, 16°S; DAS No. 08297424, rev. 187, A camera, center at 151°W, 18°S; DAS No. 08297494, rev. 187, A camera, center at 149°W, 13°S.)